AD-A060 073 NORTHERN RESEARCH AND ENGINEERING CORP CAMBRIDGE MASS F/G 21/2
FLAMEHOLDER COMBUSTION INSTABILITY STUDY. VOLUME I. ANALYTICAL --ETC(U)
MAY 78 W JANSEN, M PLATT, G E SMITH F33615-76-C-2112
UNCLASSIFIED NREC-1294-1 AFAPL-TR-78-27-VOL-1 NL

1 OF 2
AD
A060073


F
0073

AFAPL-TR-78-27, VOL-1

LEVEL II

P059847

FLAMEHOLDER COMBUSTION INSTABILITY STUDY

VOLUME I, ANALYTICAL CONSIDERATIONS

W. Jansen, M. Platt, and G. E. Smith

Northern Research and Engineering Corporation
219 Vassar Street
Cambridge, Massachusetts 02139

MAY 1978

190 p.

NREC-1294-1

Final Report, May 1976 — January 1978,

F33615-76-C-2112

3966

95

AIR FORCE AERO PROPULSION LABORATORY
AIR FORCE SYSTEMS COMMAND
WRIGHT-PATTERSON AIR FORCE BASE, OHIO 45433

NOTICE

When Government drawings, specifications, or other data are used for any purpose other than in connection with a definitely related Government procurement operation, the United States Government thereby incurs no responsibility nor any obligation whatsoever; and the fact that the government may have formulated, furnished, or in any way supplied the said drawings, specifications, or other data, is not to be regarded by implication or otherwise as in any manner licensing the holder or any other person or corporation, or conveying any rights or permission to manufacture, use, or sell any patented invention that may in any way be related thereto.

This report has been reviewed by the Information Office (OI) and is releasable to the National Technical Information Service (NTIS). At NTIS, it will be available to the general public, including foreign nations.

This technical report has been reviewed and is approved for publication.

F. N. UNDERWOOD, Captain, USAF
Project Engineer

JOSEPH C. HURST, Major, USAF
Chief, Components Branch

FOR THE COMMANDER

ERNEST C. SIMPSON
Director, Turbine Engine Division

"If your address has changed, if you wish to be removed from our mailing list, or if the addressee is no longer employed by your organization please notify AFAPL/TBC, W-PAFB, OH 45433 to help us maintain a current mailing list".

Copies of this report should not be returned unless return is required by security considerations, contractual obligations, or notice on a specific document.

UNCLASSIFIED

SECURITY CLASSIFICATION OF THIS PAGE *(When Data Entered)*

REPORT DOCUMENTATION PAGE

READ INSTRUCTIONS BEFORE COMPLETING FORM

1. REPORT NUMBER: AFAPL-TR-78-27 VOL I
2. GOVT ACCESSION NO.:
3. RECIPIENT'S CATALOG NUMBER:

4. TITLE *(and Subtitle)*: FLAMEHOLDER COMBUSTION INSTABILITY STUDY VOLUME I - ANALYTICAL CONSIDERATIONS

5. TYPE OF REPORT & PERIOD COVERED: Technical - Final 1 May 1976 - 1 January 1978

6. PERFORMING ORG. REPORT NUMBER: 1294-1

7. AUTHOR(s): W. Jansen, M. Platt, G. E. Smith

8. CONTRACT OR GRANT NUMBER(s): F33615-76-C-2112

9. PERFORMING ORGANIZATION NAME AND ADDRESS: Northern Research & Engineering Corp. (NREC), 219 Vassar Street, Cambridge MA 02139

10. PROGRAM ELEMENT, PROJECT, TASK AREA & WORK UNIT NUMBERS: 3066-05-38

11. CONTROLLING OFFICE NAME AND ADDRESS: Air Force Aero Propulsion Laboratory (TBC), Wright-Patterson AFB OH 45433

12. REPORT DATE: May 1978

13. NUMBER OF PAGES: 184

14. MONITORING AGENCY NAME & ADDRESS *(if different from Controlling Office)*:

15. SECURITY CLASS. *(of this report)*: UNCLASSIFIED

15a. DECLASSIFICATION/DOWNGRADING SCHEDULE:

16. DISTRIBUTION STATEMENT *(of this Report)*

Approved for public release; distribution unlimited.

17. DISTRIBUTION STATEMENT *(of the abstract entered in Block 20, if different from Report)*

18. SUPPLEMENTARY NOTES

19. KEY WORDS *(Continue on reverse side if necessary and identify by block number)*

Flameholder	Afterburner	Combustion
Combustion Stability	Turbofan	Combustion Response
Augmentor	Flame Stability	Rumble

20. ABSTRACT *(Continue on reverse side if necessary and identify by block number)*

Rumble is characterized as a combination of stable and unstable longitudinal acoustic modes that interact with each other while exchanging energy. The final result is a system oscillation of finite amplitude with a frequency that bears no relation to the acoustic frequency, but occurs at a level somewhere among those of the modes under consideration. The present work involves a non-linear theory which allows for the inclusion of rumble-related phenomena that a linear theory cannot handle while using

DD FORM 1 JAN 73 1473 EDITION OF 1 NOV 65 IS OBSOLETE

UNCLASSIFIED

SECURITY CLASSIFICATION OF THIS PAGE *(When Data Entered)*

a combustion model previously derived in linear stability work. The final equations have been programmed for use in a digital computer. The use of the computer program is explained in this document, and illustrations with sample input and output are given.

FOREWORD

This document presents the results of the analytical effort in the flameholder combustion instability study. The work was carried out in accordance with the plan outlined in an NREC Proposal No. 959-161, entitled "Flameholder Combustion Instability Study".

This report is the first of two volumes. It contains the method of approach, the computer program and the results of some actual cases. Derivations of equations and program listings are delegated to appendices. Also included in an appendix is a computer program, previously developed by NREC, which is necessary for the preparation of input data. The second volume contains the results of the experimental work.

The work was carried out at Northern Research and Engineering Corporation under the technical direction of Dr. W. Jansen, with Mr. E. R. Norster assuming project responsibility. Other major participants in the program include Messrs. G. E. Smith, A. E. Sotak, M. Platt, and J. A. Given.

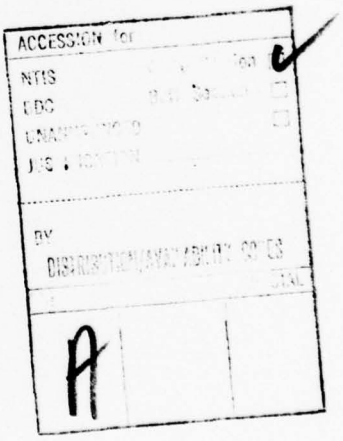

TABLE OF CONTENTS

LIST OF ILLUSTRATIONS

INTRODUCTION

BACKGROUND

This report describes the effort conducted under Contract No. F33615-76-C-2112; Project No. 3066 Item No. 0001, Sequence Nos. 1 and 2, entitled "Flameholder Combustion Instability Study". The program consists of an analytical and an experimental part. The intent of these two parts was as follows:

1. Analytical - The analysis attempts to produce an engineering tool to simulate afterburner rumble. Previous NREC combustion instability programs (see Refs 1 and 2) are used as a basis, but are expanded to include non-linear terms that represent the effects of rather large fluid fluctuations that exist in rumble. The method of solution follows that proposed by Culick, Reference 3, which was successfully used to explain rocket motor instabilities.

2. Experimental - The experimental effort attempts to evaluate the physical mechanisms that are important to trigger rumble. Tests that assess the effects of fuel to air ratio, flameholder shape, pressure disturbances in terms of amplitude and duration, and fuel type (gas, liquid) have been performed.

The report is written in two volumes. The first volume describes the analytical results, while the second describes the experimental results.

THE PHENOMENON OF RUMBLE

Rumble is a special type of combustion instability that occurs in certain turbofan engine augmentors operating at high altitude, low Mach number conditions. It is characterized by sustained, low frequency pressure waves that propagate from the flame region longitudinally upstream toward the fan and downstream toward the nozzle. What distinguishes it from the classical type of combustion instability in augmentors is its characteristically low frequency and its propagating, in contrast to standing, wave pattern. Typically, observed rumble frequencies have

been between 30 and 100 Hz (although there have been reports of rumble at somewhat higher frequencies). Also, rumble exhibits some anomalous features. For example, sustained rumble oscillations have been found to shift from one frequency to another abruptly and for no apparent reason -- e.g. from 62 Hz to 42 Hz.

The high altitude, low Mach number flight conditions which are conducive to rumble merit some comment. They are, of course, conditions under which fuel droplet vaporization and flameholder flame stabilization are poor. They are also conditions which are difficult to test during the early stages of an engine development program. Because of this, rumble can be a costly factor in engine development. The danger is that rumble may first be encountered during simulated high altitude engine tests or during actual flight testing. This can force a renewed component development effort, delaying engine qualification and maybe necessitating changes to other components. This danger is exacerbated by the lack of a standard approach for eliminating rumble, once encountered. Unlike classical augmentor instability, rumble occurs at frequencies too low for acoustic linear suppression. Some cases of rumble have been corrected by changing the flameholders, and others by changing the injectors. But the state-of-the art solution remains one of cut-and-try.

The main reason for the present inability to eliminate rumble during design or early component development, and also the reason for the prevalence of cut-and-try strategies, is that the phenomenon has not been understood. A review of the physics of combustion instability is necessary to appreciate the difficulty.

COMBUSTION INSTABILITIES

Combustion instability in augmentors is characterized by sustained pressure oscillations for which the major energy input is supplied by the combustion process. Two types of augmentor instability have proved troublesome. The classical type involves combustion driving of a natural acoustic mode of the augmentor duct. Rumble, the second type, involves combustion driving of low frequency pressure waves propagating from the

flame region upstream toward the turbine and fan and downstream toward the nozzle. The pressure oscillation amplitudes produced by combustion instability are substantial. Amplitudes in excess of ±20 per cent of the mean augmentor pressure level have been common. Combustion instability has caused hardware failures in augmentors and in augmented turbofans the pressure oscillations impinging on the fan can contribute to fan stall. Accordingly, the basic engineering problem posed by combustion instability in augmentors is to keep the pressure oscillation amplitudes at safe levels. An allied problem is to assure that any augmentor instabilities will be detected and eliminated early in a development program, prior to simulated or actual flight testing.

For many years the engineering problem was solved by using acoustically treated liners to suppress augmentor instabilities. However, the trend to larger engines, higher volumetric heat release rates, lower augmentor pressures, and augmentation of turbofan engines has reduced the effectiveness of acoustic liners. Some instabilities in recent engines could not be adequately suppressed by any practical acoustic liners. An alternative strategy for handling augmentor instabilities thus became necessary. A significant recent advance has been an analytical model of the classical type of instability. The model was devised by NREC and subsequently validated and refined by General Electric Company. The evidence to date indicates that the model will permit systematic engineering of classical augmentor instability. It can be used during the design phase to reduce the likelihood of encountering acoustic instabilities -- particularly the likelihood of encountering them first during flight tests. It can also be used during development to explain instabilities, once they are encountered, and to identify the best strategies for eliminating them. Furthermore, the model lends itself to further development. As more is learned about the basic mechanisms governing the unsteady combustion process, the model promises to become an increasingly effective tool for handling this type of instability.

CLASSICAL COMBUSTION INSTABILITY

Combustion instability in general is best viewed as a five step process, superposed on the steady combustion process. The five steps are shown in the following sketch.

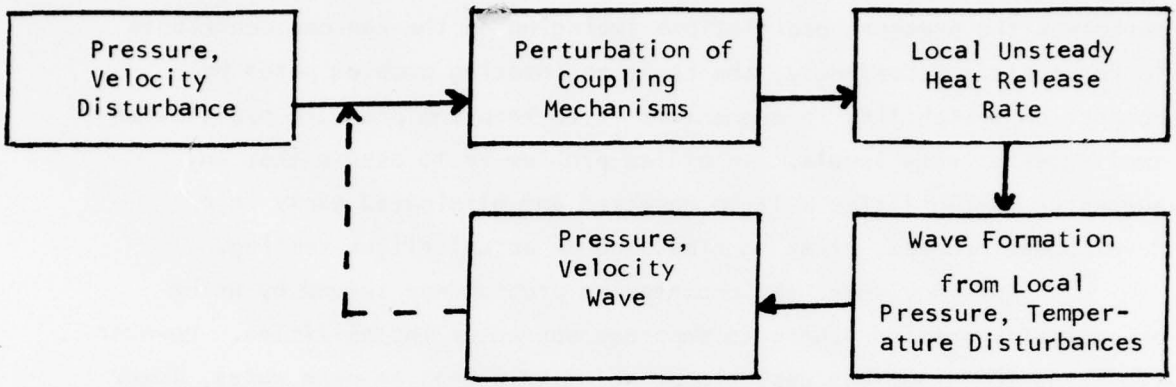

The process is initiated by a pressure or velocity disturbance in the augmentor. This affects the basic combustion mechanisms that govern the overall combustion process -- e.g. droplet vaporization, turbulent mixing, and flame stabilization. These mechanisms are usually called coupling mechanisms because they couple the combustion process to flow conditions. Perturbations of the coupling mechanisms produce perturbations of the local heat release rates throughout the augmentor. These in turn produce perturbations of the local pressures and temperatures. One of two things can now happen. The local pressure and temperature disturbances can cancel one another out, thereby effecting a damping of the original flow disturbance. In this case the energy of the initial flow disturbance is in effect absorbed by the mean combustion process. Alternatively, the local pressure and temperature disturbances can reinforce one another to form a pressure wave. In this case the initial flow disturbance is amplified by energy extracted from the heat release process. Which of these two happens depends on the specifics of the spatial and temporal distribution of the perturbed heat release process.

If a pressure wave is generated, it may become a new initiating disturbance, starting the process all over. That is, the unsteady combustion process may form a closed feedback loop, as indicated by the

broken line in the diagram. If it does, it yields a sustained, self-exciting resonant oscillation, the energy for which comes from the augmentor heat release process. This does happen in classical augmentor instability, but the closing of the feedback loop is not necessary for combustion instability to occur. Sustained, combustion-driven pressure oscillations can also occur if there is an independent mechanism which continually introduces flow disturbances into the flame region and if the augmentation process amplifies these disturbances. Vortex shedding from the flameholders might be such an independent source of flow disturbances. This type of combustion instability would be a forced oscillation, in which the augmentor combustion process acts only as an amplifier. In sum, what is crucial for augmentor instability is that the augmentor heat release (positive or negative) process add significant energy to flow disturbances.

To under stand a particular type of combustion instability involves knowledge of four distinct things:

1) Which coupling mechanisms are significantly implicated in that type of instability.
2) What fluctuations these mechanisms produce in the local heat release rates as a result of fluctuations in the flow -- i.e., the unsteady combustion response.
3) How the fluctuations in the local heat release rates do or do not lead to the formation of pressure waves -- i.e., the wave formation process.
4) What causes the oscillation to become sustained -- i.e., the sustaining mechanism (either a feedback loop or an independent source of excitation).

In the case of classical augmentor instability three of these four are now well-understood, and the fourth is understood sufficiently to permit a practical engineering model of the overall process. In particular, classical instability is known to involve a feedback loop, in which the

pressure wave formed is a standing acoustic wave that corresponds to one of the natural acoustic modes of the augmentor duct. The principal coupling mechanisms implicated are the various evaporation droplet mechanisms and turbulent mixing in the flame zone.

None of these four things is well-understood in the case of rumble. Which among the various possible coupling mechanisms govern rumble is not known. Nor has the characteristic spatial and temporal distribution of the unsteady heat release rate been identified. Since rumble involves propagating rather than standing waves, the wave formation process appears not to be one of simple energy addition to a natural acoustic mode. Finally, it is not clear whether rumble is sustained by a feedback loop or by an independent source of sustained excitation. That is, it is not known whether rumble is a self-exciting resonance or a forced vibration. Hence, an applied research program investigating the physics of rumble is appropriate.

REQUIREMENTS OF THE ANALYTICAL PROGRAM

The general requirement of the analytical effort is to characterize the pressure waves resulting from flow disturbances in the flame region. Such a characterization requires an overall analytical model consisting of three distinct parts:

1) Submodels corresponding to each salient coupling mechanism implicated in rumble.
2) A model of the spatial and temporal variation of the heat release rate.
3) A model of the process by which pressure waves are formed by fluctuations in the local heat release rates.

As discussed in the first section of this chapter, all of these distinct parts are required specifically because of the complexity of the combustion instability process.

The overall model must determine the amplitude, phase, and harmonic composition of the pressure wave produced by the flame region, given the amplitude and the duration of the initiating flow disturbance.

The current approach to constructing such a model relied heavily on our past experience with a comparable model for classical augmentor instability. (We refer here specifically to that portion of NREC's REFINE model, Refs 1 and 2, that deals with the energy added to pressure waves by unsteady combustion.) Many parts of the model are direct extensions of the corresponding parts of the earlier model. For example, the local heat release rate model is virtually the same as our earlier model for ω_c. The pressure wave formation model is a straightforward mathematical generalization of the so-called equations of motion and energy. The generalization in question is required to enable calculation of propagating as well as standing waves. The coupling mechanism model is largely original in the new model.

Heat Release Rate Model

The quantity which must be determined by this model is the heat release rate, ω_c, defined as a function of location and time. As explained at the beginning of the chapter, this quantity is crucial because it is the detailed spatial and temporal variation of ω_c that determines whether the combustion process amplifies or dampens the flow disturbance. A comparatively complex model is required to determine this quantity. The difficulty is that the heat release process is cumulative along the length of the burning region. That is, the heat release rate near the flameholders affects the rate further downstream. For example, if the rate becomes very high near the flameholders, the rate downstream must become low since combustion of the fluid particles in question will be largely completed before they reach the downstream region. Consequently, the model determining ω_c must trace the history of the chemical reaction of fluid particles entering the flame region. Any model which fails to do this, will fail to determine local values of ω_c versus time, and hence will fail to distinguish accurately those cases in which the combustion process amplifies from those in which it dampens. The basic model employs a time-unsteady version of the plug-flow

reactor concept. It is formulated in terms of flow variables and two combustion related parameters, $\tilde{\tau}$, the characteristic time of combustion, and E, the energy content of the fuel. To describe the unsteady heat release, ω_c', decaying with distance from the flameholder, a simple exponential form is used.

$$\omega_{c_1}'(z,t) = \frac{\bar{\rho}\bar{E}}{\bar{\tau}} \cdot e^{-\frac{z}{\bar{v}\bar{\tau}}} \cdot \left\{ \frac{\rho'}{\bar{\rho}} + \frac{E'}{\bar{E}} - \frac{\tau'}{\bar{\tau}} \right\}$$

where z is the distance downstream of the flameholder. This heat release is the instantaneous or non-cumulative heat release. However, there are other heat releases that are associated with the fluid fluctuations and should be integrated over the entire length, downstream of the flameholder.

$$\omega_{c_2}'(z,t) = \frac{\bar{\rho}\bar{E}}{\bar{\tau}} \cdot e^{-\frac{z}{\bar{v}\bar{\tau}}} \cdot \int_0^z \frac{\tau'}{\bar{\tau}} \cdot e^{i\left(\omega \cdot \frac{z-y}{\bar{v}}\right)} \frac{dy}{\bar{v}\bar{\tau}}$$

The value of $\tilde{\tau}$ is of course a function of many variables. In Reference 1, it was expressed as

$$\frac{\tau'}{\bar{\tau}} = C_1 \cdot \frac{p'}{\bar{p}} + C_2 \frac{u'}{\bar{u}} e^{i\frac{\omega z}{\bar{v}}}$$

This model for ω_c provides precisely what is needed to evaluate the energy added to or removed from a flow disturbance by the combustion process. That is, it determines ω_c as a function of location and time, and it expressly takes into account the cumulative character of the combustion process. The model is known to work for higher frequency, shorter wave length instability. Hence it was suspected to describe the heat release process in sufficient detail for the lower frequency, longer wave length oscillations typical of rumble.

METHOD OF APPROACH

GENERAL

As has been pointed out, the phenomenon of rumble is a large-amplitude flow oscillation that takes place due to interactions between flow and combustion processes. Previous analyses have considered the stability of the combined process from a small perturbation and linear point of view. However, these analyses did not lead to reasonable results and nonlinear effect must be introduced to resolve the problem of rumble.

However, solving the nonlinear equation of motion is a formidable task, which has no precedent. For this reason, the selected analysis follows an approach that has been initiated by Culick (Ref 3). In essence, the approach is to use the acoustic solutions and insert these into a forcing function, F, that contains the nonlinear terms that will modify the acoustic solutions. This modification consists of allowing the constants of integration that exist in the acoustic solution to vary slowly in time, at a rate dictated by the nonlinear terms. In its elementary form this would mean that a sine wave of form $p = A \sin \omega t$ now has an additional variable in time, which is $A = A(t)$. Thus if the value of A can be calculated as a function of time, it can be established whether p is decaying or growing (see sketch below).

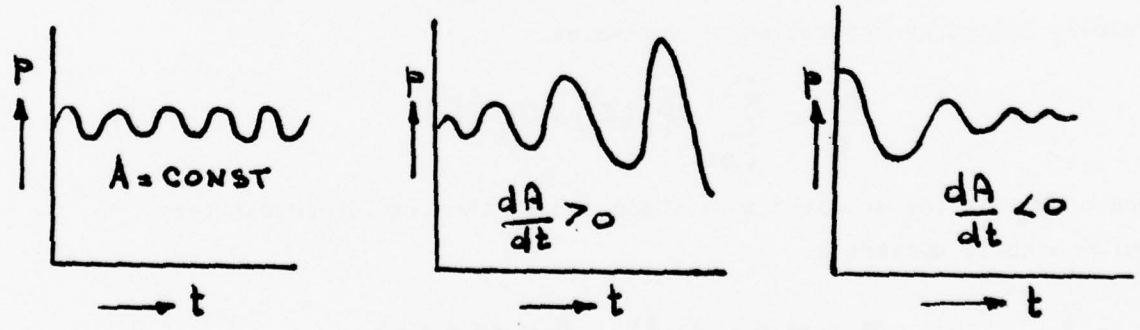

A growing value of $A \left(\frac{dA}{dt} > 0\right)$ indicates that rumble can be sustained.

EQUATIONS OF MOTION

The starting points of the analysis are the equations of motion that express conservation of energy and momentum for an infinitesimal one-dimensional state of nonviscous fluid. These are

$$\rho \frac{\partial u}{\partial t} + \rho u \frac{\partial u}{\partial z} + \frac{\partial p}{\partial z} = 0 \tag{1}$$

$$\frac{\partial p}{\partial t} + u \frac{\partial p}{\partial z} + \gamma p \frac{\partial u}{\partial z} = (\gamma - 1)\omega_c \tag{2}$$

where ω_c defines the heat addition per unit fluid mass due to combustion. writing the variables in terms of steady and fluctuating quantities ($p = \bar{p} + p'$) and retaining terms of equal order of magnitude results in a single second-order wave equation:

$$\frac{\partial^2 p'/\bar{p}}{\partial t^2} - c^2 \frac{\partial^2 p'/\bar{p}}{\partial z^2} = F(z,t) \tag{3}$$

where the function, F , includes all effects not incorporated in the pure acoustic analysis.

In the acoustic analysis where $F = 0$, Equation 3 can be readily solved by separation of variables

$$\frac{p'}{\bar{p}} = \sum_{i=1}^{n} \psi_i(z) \cdot \eta_i(t) \tag{4}$$

where ψ_i is the acoustic mode shape and η the time dependent term which usually appears as

$$\eta = \alpha \sin(\omega t) + \beta \cos(\omega t) \tag{5}$$

with α and β constants of integration, determined by the boundary conditions.

In its previous programs on combustion instability (see again Refs 1 and 2), NREC developed a computer program to calculate the acoustic frequencies, ω_i, and their corresponding mode shapes, ψ_i . A user's guide for this program, HLMHLT, has been reproduced here in Appendix C.

The acoustic solution is used in Equation 3 to resolve the forcing function, F . Subsequently, the spatial (Z-coordinate) dependence of this equation is then eliminated using the Galerkin method, whereby the equation is averaged through integration over the combustor volume and Green's theorem applied. The equation then reduces from a partial to an ordinary differential equation, and may be written as

$$\ddot{\eta}_k + \omega_k^2 \eta_k = F_k \tag{6}$$

where F_k has the form:

$$F_k = \sum_{i=1}^{n} \left(D_{ki} \dot{\eta}_i + E_{ki} \eta_i \right) + \sum_{i=1}^{n} \sum_{j=1}^{m} \left(A_{kij} \eta_i \eta_j + B_{kij} \dot{\eta}_i \dot{\eta}_j \right) \tag{7}$$

NONLINEAR EFFECTS

In the pure acoustic case with the forcing function $F_k = 0$ the value of η_k would be of a sinusoidal form as follows:

$$\eta_k = \alpha_k \sin(\omega_k t) + \beta_k \cos(\omega_k t) \tag{8}$$

where α_k and β_k are constants of integration.

However, with F_k being finite we assume that η_k has the form of Equation 8, but α_k and β_k are time dependent and vary slowly over the fundamental period, $2\pi/\omega_k$. The next step then would be to insert Equation 8 into Equations 6 and 7. However, the mathematical obstacles are considerable when numerical solutions are attempted and, following Culick, (Ref 3) a time averaging process is instituted that reduces the

second order equations to first order equations. In fact it is shown that α_k and β_k can be expressed as

$$\frac{d\alpha_k}{dt} = \frac{1}{\omega_k \tau} \int_t^{t+\tau} F_k(t) \cos(\omega_k t)\, dt \tag{9}$$

$$\frac{d\beta_k}{dt} = \frac{1}{\omega_k \tau} \int_t^{t+\tau} F_k(t) \sin(\omega_k t)\, dt \tag{10}$$

for values of $\tau = 2\pi/\omega_k$

In this project the first five terms of k are carried and the result is a set of ten simultaneous differential equations that can be solved exactly.

The values of α and β determine the stability of the system in the manner indicated at the beginning of this section; i.e., stability is achieved when $\dot{\alpha}$ and $\dot{\beta}$ are negative. Since α_k and β_k are terms of a series the usual manner in which stability is determined is by observing the value of η which consists of the summation of α's and β's as follows: $\eta = \sum_{k=1}^{n} \eta_k(\alpha_k, \beta_k, t)$

There are further consequences generated by the nonlinear nature of the solution, which comes about when various modes interact with each other. Modes proven unstable by a linear theory become stabilized; frequencies of certain modes change to a different value due to the influence of other modes. Discussions on this topic can be found in the section on analysis of results.

The appendices at the end of this report provide the theoretical derivations of all equations. A computer program was developed to solve these equations. The results are provided in subsequent chapters of this report.

COMPUTER PROGRAM

The computer program which incorporates the previously described calculation procedure for the nonlinear analysis of combustion instability is presented in this section. Program NØNLIN is a digital computer program written in the Fortran language and developed on the CDC 7600 computing system. Within the limits of accuracy imposed by the assumptions, it can be used to determine the stability of the process by which combustion downstream of augmentor flame holders introduces energy into low frequency, propogating pressure waves. Formally, the program will determine the pressure oscillation amplitude, phase, harmonic structure, and propogating characteristics, given an initiating flow disturbance.

DESCRIPTION OF INPUT DATA

The input data used by Program NØNLIN falls into several categories: combustor dimensions, fluid flow properties, combustion parameters, acoustic mode characteristics, the initiating disturbance, and various other quantities necessary to operate the program. Detailed information concerning the items in these categories is furnished in the table below. This information contains a description of each input item as well as a description of the form in which these items are punched onto input data cards. The units of each item are included in the item's description. For each case to be considered, the input data begins with the item on Card 1.

Card	Location	Input Item	Type of Number*	Fortran Symbol	Description
1	1-72		A	CØMENT	A statement identifying the case (this must not be omitted); write STØP in columns 1-4 if there are no more cases.

* A refers to alphanumeric words, while Int refers to integer values and FP refers to floating-point values.

Card	Location	Input Item	Type of Number	Fortran Symbol	Description
2	1-6		Int	NM	Number of acoustic modes to be considered in the solution; any number up to 5 is allowed (if no value is entered, a default value of 5 is used).
	7-12		Int	NZSTEP	Number of axial locations in the chamber at which the unsteady component of the pressure is printed; any number up to 80 is allowed (if no value is entered, a default value of 40 is used). This number does not effect the accuracy of the results.
	13-18		Int	ITAU	Indicator for τ (see Eqs 9 and 10): ITAU = 0 if the time-averaging interval is based on the fundamental acoustic frequency ITAU = 1 if the interval is based on the acoustic frequency appropriate to the specific modes ITAU = 2 if the interval is based on the fundamental frequency for mode 1, but the second acoustic frequency for the higher modes. Based upon results to date, a value of ITAU = 0 is recommended.
	19-24		Int	NPRINT	Number of time increments of analysis per print-out interval for time dependent quantities.
3	1-12	t_o	FP	TZERO	Initial time of the analysis, sec.
	13-24	t_f	FP	TFIN	Limiting time of the analysis, sec (if a value is entered less than TZERØ, a default value of TZERØ + 1.0 is used).
	25-36	Δt	FP	TSTEP	Time increment of the analysis, sec (if no value is entered, a default value of 0.005 is used). Successive runs must be made for new cases to determine the value of Δt small enough not to affect the accuracy of results.

Card	Location	Input Item	Type of Number	Fortran Symbol	Description
4	1-12	α_k	FP	AFIRST(1)	Amplitude of the sine term for the fundamental component of the traveling wave disturbance at t_o. There are NM values at AFIRST entered in locations 1-12, 13-24, 25-36, 37-48, and 49-60, as required.
5	1-12	β_k	FP	BFIRST(1)	Amplitude of the cosine term for the fundamental component of the traveling wave disturbance at t_o. There are NM values of BFIRST entered in locations 1-12, 13-24, 25-36, 37-48, and 49-60, as required.
6	1-12	γ	FP	GAM	Ratio of specific heats of the gas in the chamber (if no value is entered, a default value of 1.4 is used).
	13-24	c_1	FP	C1	Characteristic sound velocity upstream of the flameholder, ft/sec.
	25-36	c_2	FP	C2	Characteristic sound velocity downstream of the flameholder, ft/sec.
	37-48	ℓ_1	FP	EL1	Length of the chamber to the flameholder, ft.
	49-60	ℓ_2	FP	EL2	Total length of the chamber, ft.
7	1-12	ω_i	FP	W(1)	Acoustic frequency of the fundamental mode, rad/sec.*
	13-24	θ_{1i}	FP	THU(1)	Upstream value of the index of location for the fundamental acoustic mode, rad.*
	25-36	θ_{2i}	FP	THD(1)	Downstream value of the index of location for the fundamental acoustic mode, rad.* There are NM lines of values for ω_i, θ_{1i}, and θ_{2i} entered in the multiple list format, one for each acoustic mode considered, with the last set of values on line N_A.
N_A+1	1-12	ℓ_3	FP	EL3	Length of the chamber to the fuel injector, ft.

*The values of acoustic frequency are obtained from Program HLMHLT (see Appendix C) where the Mach number equals zero and the admittances are purely imaginary, iZ. The values of the index of location are calculated from

$$\theta_{1i} = -\tan^{-1}(Z_{\ell=0})$$

$$\theta_{2i} = -\tan^{-1}(Z_{\ell=\ell_2}) - \omega_i \ell_2 / c_2$$

Card	Location	Input Item	Type of Number	Fortran Symbol	Description
	13-24	a_1	FP	A1	Coefficient in the velocity profile $\bar{U}_1 = a_1 z + b_1$ for the chamber upstream of the flameholder, per sec.
	25-36	a_2	FP	A2	Coefficient in the velocity profile $\bar{U}_2 = a_2 z + b_2$ for the chamber downstream of the flameholder, per sec.
	37-48	b_1	FP	B1	Constant in the velocity profile $\bar{U}_1 = a_1 z + b_1$ for the chamber upstream of the flameholder, fps.
	49-60	b_2	FP	B2	Constant in the velocity profile $\bar{U}_2 = a_2 z + b_2$ for the chamber downstream of the flameholder, fps.
N_A+2	1-12	$\bar{U}_c$	FP	VELC	Mean characteristic velocity of combustion for the system, fps.
	13-24	$\bar{\tau}_c$	FP	TAUB	Mean characteristic time of combustion for the system, sec.
	25-36	$\bar{E}$	FP	EBAR	Mean energy content of the fluid per unit mass, $(\text{fps})^2$.
	37-48	$\hat{C}_1$	FP	CITL	Unsteady combustion coefficient relating $\bar{\tau}_c$ to the pressure oscillation.

DESCRIPTION OF OUTPUT DATA

The output of Program NØNLIN consists entirely of printed data. The printed data is divided into three sections: input data, time-independent calculated values which are required for time integration, and time-dependent values which are printed at regular intervals during that integration. The quantities printed in each section are described below, including their dimensions.

The input data appears for each case considered, as follows:

1) The statement describing the case being considered.
2) Time specifications - initial and terminal time, and computational time increment, all given in seconds, as well as an indication of the time-averaging option chosen.

3) Basic chamber geometry - total length, length to flameholder, and length to injector, all given in feet.

4) Fluid properties - ratio of specific heats, and sound velocity (in fps) both upstream and downstream of the flameholder.

5) Fluid velocity - as specified by the intercept (in fps) and slope (per sec) of a straight line approximation to the velocity profile in each chamber.

6) Combustion characteristics - characteristic combustion velocity (fps) and time (sec), energy content (fps^2), and unsteady coefficient.

7) Acoustic wave specifications for each mode - natural frequency (rad per sec), and index of location both upstream and downstream of the flameholder.

The time-independent output data, appearing for each case, consists of:

1) Again, the statement describing the case.

2) Calculated properties of the acoustic wave-relative amplitude (R_i) for each mode, matrix of the inner product integrated over the chamber (in ft), and the inverse of the inner product matrix (in ft^{-1}).

3) Coefficients in the forcing function F_k - the doubly-subscripted matrices D_{ki} (in fps) and E_{ki} (in ft per sec^2) of the linear terms, and the triply-subscripted matrices A_{kij} (in ft per sec^2) and B_{kij} (in ft) of the nonlinear terms.

The time-dependent output data appears for each case in groups of forty values of time, or until either the terminating time is reached or instability is encountered. The print-out time interval is a factor NPRINT of the time step used in the analysis, as specified in the input data. The output data at each time interval consists of characteristics of the traveling pressure wave as follows:

1) Coefficients of the sine and cosine term, α_k and β_k, respectively, in the expression for the weighting coefficient η_k for each mode.
2) Amplitude of the traveling wave, $\sqrt{\alpha_k^2 + \beta_k^2}$ magnitude of the traveling wave (or, the weighting coefficient as otherwise noted) η_k, and time derivative of the wave magnitude $d\eta_k/dt$ for each mode.
3) Total acoustic energy in the traveling wave (in ft).
4) The normalized unsteady pressure $p'/\bar{p}$ along the length of the chamber, where NZSTEP is specified in the input data.

In addition, if the terminating time is reached in the time integration, the message

* CALCULATIØNS CØMPLETED *

will be printed at the conclusion of the output data for the case. On the other hand, if instability is encountered, the message

* INSTABILITY ENCØUNTERED IN SYSTEM *

will appear at the beginning of the time-dependent output for the case.

OVERALL PROGRAM STRUCTURE AND MISCELLANEOUS OPERATIONAL INFORMATION

Program NØNLIN is composed of a main routine and twelve subroutines; the subroutines are INPUT, ØRTHØG, SIMEQ, PØUR, LINCØF, ABMAT, ØUTPTI, RUNKUT, DERIV, TRISIN, BISIN, and ØUTPT2. Information is transferred within the program through two labeled blocks of CØMMØN and as arguments of certain subroutines.

The logic flow of Program NØNLIN begins at the start of the main routine where Subroutine INPUT is called. Subroutine INPUT reads the input data, sets default values as necessary, and prints the input to the calculations for the case being considered. Next, the main routine calls Subroutines ØRTHØG and SIMEQ, in turn. Subroutine ØRTHØG calculates the elements of the inner product matrix for the acoustic mode shapes ψ_i, while Subroutine SIMEQ inverts that matrix. SIMEQ,

itself, calls Subroutine PØUR as necessary to control overflow and underflow during the inversion procedure. After control is returned to the main routine, Subroutine LINCØF is called. Subroutine LINCØF calculates the elements of the doubly-subscripted coefficient matrices D_{ki} and E_{ki} for the linear terms in the forcing function F_k. Next, Subroutine ABMAT is called to calculate the elements of the triply-subscripted coefficient matrices A_{kij} and B_{kij} for the nonlinear terms in the forcing function. With that subroutine, the time-dependent segment of the calculation procedure concludes and Subroutine ØUTPT1 is called by the main routine to print the output of the calculations.

The logic flow of Program NØNLIN continues in the main routine with the repetitive calculation of time-dependent output. The repetitive calculation begins with a call to Subroutine RUNKUT which performs a Runge-Kutta integration according to the Gill variation (see Ref 4). The integration is from time t to time $t+\Delta t$ of the simultaneous sets of equations for $\dot{\alpha}_k$ and $\dot{\beta}_k$ where α_k and β_k are the coefficients of the sine term and the cosine term, respectively, in the expression for the weighting coefficient η_k. Subroutine RUNKUT, in turn, calls Subroutine DERIV four times to furnish values of $\dot{\alpha}_k$ and $\dot{\beta}_k$ at each stage of the Runge-Kutta solution. DERIV, itself, calls Subroutines TRISIN and BISIN, repetitively. Subroutine TRISIN calculates various triple integrals of trigonometric functions, while Subroutine BISIN calculates various double integrals of trigonometric functions. After the Runge-Kutta integration to time $t+\Delta t$ is complete, control is returned to the main routine where Subroutine DERIV is called again. The derivatives $\dot{\alpha}_k$ and $\dot{\beta}_k$ furnished by DERIV are then used in the main routine to calculate the total acoustic energy in the system at that time. The loop on time then concludes with the calculation of the non-dimensional unsteady pressure at various axial stations in the chamber, and the storage of time-dependent data to be printed in the program output. Next, if the time-dependent calculations have concluded, or data for forty values of time has been stored, Subroutine ØUTPT2 is called by the main routine. Subroutine ØUTPT2 prints the variation with time on an item-by-item basis for the time-dependent output. Once the printout for a case is complete,

control is returned to the start of the main routine to consider a new case.

Program NØNLIN occupies approximately 7500 storage locations on the CDC 7600 computer. System subroutines required for the operation of the program occupy another 2600 storage locations. Compilation time in the standard compile mode is 2.9 CP seconds. Execution time for a typical case can be approximated from

$$\text{CP Seconds} = 0.18 * \left(\frac{\text{TFIN-TZERØ}}{\text{TSTEP}}\right)$$

SAMPLE CASES

Two sample cases are presented on the following pages to illustrate the format used in Program NØNLIN. The first sample case is a hypothetical one which provided a check for the analysis of non-linear lossless acoustics. The remaining sample case models the TF-30 duct burner at sea level. The input data for each of these cases is listed in its entirety, followed by the resulting output.

Lossless Acoustics Sample

A case involving lossless acoustics was analyzed with Program NØNLIN to provide a check which did not involve the entire complexity of the physical problem. Among the techniques checked was the integration of the governing differential equations in time. The case also allowed the energy convection between modes to be investigated.

The input data for the lossless acoustics case is characterized by a zero energy content of the fuel, thus eliminating combustion, and a zero thru-flow velocity. Further, with the elimination of combustion, the sound velocities upstream and downstream of the flameholder are identical. The acoustic frequencies entered are simple multiples of the fundamental mode, as obtained from $\omega_1 = \pi c / l_2$. The initial disturbance is entered as an energy input into the fundamental and second harmonic modes.

The output of this case indicates the absence of dissipative effects in the zero elements of the linear coefficient matrices D_{ki} and E_{ki}, and in the approximately constant value of the total acoustic energy during the elapsed time. Departures from a truly constant total acoustic energy are due to the various approximations in the mathematical solution. It should also be noted that the amplitude of the traveling wave indicates a transference of energy from the lower modes to the higher modes.

The lossless acoustics case was also run on established software that solves sets of nonlinear differential equations, Program MIMIC (Ref 5), to provide an independent check of the time integration technique. The results confirmed those obtained from Program NØNLIN.

NORTHERN RESEARCH AND ENGINEERING CORPORATION

DATA INPUT SHEET

Nonlinear

ENGINEER: M. Platt PROJECT: Combustion Instability PROJECT NO: 1294

TITLE: Lossless Acoustics Sample SHEET: 1 OF 1

LOCATION

1 6	7 12	13 18	19 24	25 30	31 36	37 42	43 48	49 54	55 60	61 66	67 72
NONLINEAR LOSSLESS ACOUSTICS - SAMPLE CASE 1											
	20	0	2								
0.		.02		.0005							
.2		.1			1.0E-6		1.0E-6		1.0E-6		
.2		.1			1.0E-6		1.0E-6		1.0E-6		
1.4		1260.		1260.		2.7		8.3			
476.916		0.		0.							
953.833		0.		0.							
1430.749		0.		0.							
1907.666		0.		0.							
2384.582		0.		0.							
1.7		0.		0.		0.		0.			
1000.		.001		0.		0.					

NREC PROGRAM NONLIN2

NONLINEAR LOSSLESS ACOUSTICS - SAMPLE CASE 1

INPUT DATA

INITIAL TIME, SEC	0.0000
LIMITING TIME, SEC	.0200
COMPUTATIONAL TIME INCREMENT, SEC	.0005
AVERAGING TIME	MODE INDEPENDENT
TOTAL CHAMBER LENGTH, FT	3.300
LENGTH TO FLAMEHOLDER, FT	2.700
LENGTH TO FUEL INJECTOR, FT	1.700
RATIO OF SPECIFIC HEATS	1.400
SOUND VELOCITY UPSTREAM (OF FLAMEHOLDER), FPS	1260.
SOUND VELOCITY DOWNSTREAM (OF FLAMEHOLDER), FPS	1260.
VELOCITY PROFILE UPSTREAM - AXIAL COEF, PER SEC	0.0
CONSTANT, FPS	0.
VELOCITY PROFILE DOWNSTREAM - AXIAL COEF, PER SEC	0.0
CONSTANT, FPS	0.
CHARACTERISTIC COMBUSTION VELOCITY, FPS	1000.
CHARACTERISTIC COMBUSTION TIME, SEC	.001
ENERGY CONTENT, FPS**2	0.
UNSTEADY COMBUSTION COEFFICIENT	0.000000

MODE NUMBER	ACOUSTIC WAVES: NATURAL FREQUENCY, RAD/SEC	ACOUSTIC WAVES: INDEX OF LOCATION, RAD: UPSTREAM	ACOUSTIC WAVES: INDEX OF LOCATION, RAD: DOWNSTREAM	TRAVELING WAVES: INITIAL AMPLITUDE OF: SIN TERM	TRAVELING WAVES: INITIAL AMPLITUDE OF: COS TERM
1	476.916	0.00000	0.00000	.2000000	.2000000
2	953.833	0.00000	0.00000	.1000000	.1000000
3	1430.749	0.00000	0.00000	.0000010	.0000010
4	1907.666	0.00000	0.00000	.0000010	.0000010
5	2384.582	0.00000	0.00000	.0000010	.0000010

NONLINEAR LOSSLESS ACOUSTICS - SAMPLE CASE 1

TIME-INDEPENDENT OUTPUT DATA

		MODE NUMBER				
		1	2	3	4	5
RELATIVE AMPLITUDE OF ACOUSTIC WAVE		.1000E+01	.1000E+01	.1000E+01	.1000E+01	.1000E+01
INNER-PRODUCT MATRIX(I,J)	I / J	1	2	3	4	5
	1	.4150E+01	-.3334E-05	-.1742E-05	-.1017E-05	-.1017E-05
	2	-.3334E-05	.4150E+01	.4788E-05	.4329E-06	.1639E-05
	3	-.1742E-05	.4788E-05	.4150E+01	-.4162E-05	-.4548E-06
	4	-.1017E-05	.4329E-06	-.4162E-05	.4150E+01	.4401E-05
	5	-.1017E-05	.1639E-05	-.4548E-06	.4401E-05	.4150E+01
INVERSE OF IN-PR MATRIX(I,J)	I / J	1	2	3	4	5
	1	.2410E+00	.1936E-06	.1012E-06	.5882E-07	.5907E-07
	2	.1936E-06	.2410E+00	-.2780E-06	-.2514E-07	-.9516E-07
	3	.1012E-06	-.2780E-06	.2410E+00	.2417E-06	.3802E-07
	4	.5882E-07	-.2514E-07	.2417E-06	.2410E+00	-.2556E-06
	5	.5907E-07	-.9516E-07	.3802E-07	-.2556E-06	.2410E+00
LINEAR COEF MATRIX D(I,J)	I / J	1	2	3	4	5
	1	0.	0.	0.	0.	0.
	2	0.	0.	0.	0.	0.
	3	0.	0.	0.	0.	0.
	4	0.	0.	0.	0.	0.
	5	0.	0.	0.	0.	0.
LINEAR COEF MATRIX E(I,J)	I / J	1	2	3	4	5
	1	0.	0.	0.	0.	0.
	2	0.	0.	0.	0.	0.
	3	0.	0.	0.	0.	0.
	4	0.	0.	0.	0.	0.
	5	0.	0.	0.	0.	0.
NON-LIN COEF MATRIX A(K,I,J)	I / J	1	2	3	4	5
K=1	1	-.1556E+00	-.8123E+05	-.1817E+00	-.4343E+00	-.2343E+00
	2	-.8123E+05	-.2590E+00	-.2112E+06	.5336E-01	.7434E-01

	3	-.1817E+00	-.2112E+06	-.7449E+00	-.4062E+06	-.2181E+00
	4	-.4343E+00	.5336E-01	-.4062E+06	-.9647E+00	-.6661E+06
	5	-.2343E+00	.7434E-01	-.2181E+00	-.6661E+06	-.1881E+01
K=2	1	-.3249E+05	-.1136E+00	-.1625E+06	.6949E+00	.2881E+00
	2	-.1136E+00	-.1356E-01	.3130E-08	-.3249E+06	-.1045E+00
	3	-.1625E+06	.3130E-08	.1680E+00	-.6579E+00	-.5526E+06
	4	.6949E+00	-.3249E+06	-.6579E+00	-.1085E+00	-.9376E-01
	5	.2881E+00	-.1045E+00	-.5526E+06	-.9376E-01	.1854E+00
K=3	1	.3518E-01	-.8123E+05	-.3893E+00	-.2762E+06	-.2512E+00
	2	-.8123E+05	-.7728E-01	-.1627E-08	.1096E+00	-.4711E+06
	3	-.3893E+00	-.1627E-08	-.3478E+00	.2557E+00	-.2161E+00
	4	-.2762E+06	.1096E+00	.2557E+00	-.1054E+00	.4690E-01
	5	-.2512E+00	-.4711E+06	-.2161E+00	.4690E-01	-.7165E+00
K=4	1	-.2610E-01	-.2271E-01	-.1625E+06	-.4964E+00	-.4224E+06
	2	-.2271E-01	-.1300E+06	.1469E-08	-.3390E-01	-.1604E+00
	3	-.1625E+06	.1469E-08	.3069E+00	-.2518E+00	.3286E+00
	4	-.4964E+00	-.3390E-01	-.2518E+00	-.1085E+00	-.1390E+00
	5	-.4224E+06	-.1604E+00	.3286E+00	-.1390E+00	.2861E+00
K=5	1	.2741E-02	.1419E-01	.3028E+00	-.2762E+06	-.5196E+00
	2	.1419E-01	-.4095E-01	-.2112E+06	.3436E+00	.3317E-01
	3	.3028E+00	-.2112E+06	-.4518E+00	.9957E-01	-.2691E+00
	4	-.2762E+06	.3436E+00	.9957E-01	.3021E-01	.3027E-01
	5	-.5196E+00	.3317E-01	-.2691E+00	.3027E-01	-.5118E+00

NON-LIN COEF MATRIX B(K,I,J)

I / J	1	2	3	4	5
K=1					
1	.1832E-05	-.3572E-01	-.1957E-05	-.2306E-06	-.4345E-05
2	-.3572E-01	.1296E-05	.8333E-01	.6231E-06	.8336E-06
3	-.1957E-05	.8333E-01	-.2246E-06	.1131E+00	-.5545E-06
4	-.2306E-05	.6231E-06	.1131E+00	.5444E-06	.1250E+00
5	-.4345E-05	.8336E-06	-.5545E-06	.1250E+00	-.3318E-07
K=2					
1	.1571E+01	-.1829E-05	-.3333E+00	.1100E-05	.5790E-05
2	-.1829E-05	-.1341E-06	-.1380E-05	-.3571E-01	-.1212E-05
3	-.3333E+00	-.1380E-05	.7083E-06	.4925E-08	.4762E-01
4	.1100E-05	-.3571E-01	.4925E-08	-.8197E-07	-.2613E-06
5	.5790E-05	-.1212E-05	.4762E-01	-.2613E-06	.4163E-06
K=3					
1	-.5988E-06	.1750E+01	.3325E-05	-.4607E+00	-.1741E-05
2	.1750E+01	.2294E-05	-.1076E-06	.1070E-05	-.1786E+00
3	.3325E-05	-.1076E-06	.1699E-06	-.4350E-06	-.1980E-06
4	-.4607E+00	.1070E-05	-.4350E-06	.5172E-06	-.4928E-07
5	-.1741E-05	-.1786E+00	-.1980E-06	-.4928E-07	-.5775E-07
K=4					
1	.9191E-05	-.2907E-05	.2048E+01	-.2700E-05	-.1000E+01
2	-.2907E-05	.1571E+01	-.1703E-05	.8942E-07	-.1246E-05
3	.2048E+01	-.1703E-05	.1657E-06	-.8688E-07	.6169E-06
4	-.2700E-05	.8942E-07	-.8688E-07	.2881E-07	-.2810E-06
5	-.1000E+01	-.1246E-05	.6169E-06	-.2810E-06	.3808E-06
K=5					
1	.4076E-05	-.5419E-05	-.3304E-05	.2375E+01	.1858E-05
2	-.5419E-05	.3156E-05	.1631E+01	.3733E-06	-.2197E-06
3	-.3304E-05	.1631E+01	.1529E-05	-.6525E-06	.2342E-06
4	.2375E+01	.3733E-06	-.6525E-06	.4509E-06	-.1944E-06
5	.1858E-05	-.2197E-06	.2342E-06	-.1944E-06	.9001E-07

NONLINEAR LOSSLESS ACOUSTICS - SAMPLE CASE 1

TIME-DEPENDENT OUTPUT DATA

TRAVELING WAVE, AMPLITUDE OF SIN TERM

TIME	MODE NUMBER 1	2	3	4	5
.0010	.1958E+00	.9963E-01	-.4361E-03	-.6823E-03	-.5895E-03
.0020	.1913E+00	.9853E-01	-.1726E-02	-.2743E-02	-.2407E-02
.0030	.1867E+00	.9675E-01	-.3806E-02	-.6222E-02	-.5350E-02
.0040	.1818E+00	.9432E-01	-.6579E-02	-.1096E-01	-.1201E-01
.0050	.1767E+00	.9132E-01	-.9912E-02	-.1681E-01	-.1964E-01
.0060	.1715E+00	.8781E-01	-.1365E-01	-.2352E-01	-.2820E-01
.0070	.1661E+00	.8386E-01	-.1764E-01	-.3084E-01	-.4051E-01
.0080	.1606E+00	.7957E-01	-.2169E-01	-.3846E-01	-.5331E-01
.0090	.1550E+00	.7501E-01	-.2565E-01	-.4607E-01	-.6726E-01
.0100	.1494E+00	.7029E-01	-.2936E-01	-.5339E-01	-.8198E-01
.0110	.1438E+00	.6548E-01	-.3270E-01	-.6015E-01	-.9707E-01
.0120	.1382E+00	.6067E-01	-.3556E-01	-.6613E-01	-.1121E+00
.0130	.1327E+00	.5593E-01	-.3787E-01	-.7115E-01	-.1268E+00
.0140	.1273E+00	.5133E-01	-.3957E-01	-.7507E-01	-.1407E+00
.0150	.1220E+00	.4690E-01	-.4064E-01	-.7783E-01	-.1537E+00
.0160	.1169E+00	.4271E-01	-.4107E-01	-.7937E-01	-.1654E+00
.0170	.1120E+00	.3878E-01	-.4087E-01	-.7970E-01	-.1757E+00
.0180	.1072E+00	.3512E-01	-.4006E-01	-.7884E-01	-.1845E+00
.0190	.1026E+00	.3177E-01	-.3867E-01	-.7685E-01	-.1918E+00
.0200	.9828E-01	.2872E-01	-.3674E-01	-.7379E-01	-.1974E+00

TRAVELING WAVE, AMPLITUDE OF COS TERM

TIME	MODE NUMBER 1	2	3	4	5
.0010	.1999E+00	.1078E+00	.1227E-01	.4699E-02	.5102E-03
.0020	.1995E+00	.1147E+00	.2432E-01	.1037E-01	.1954E-02
.0030	.1989E+00	.1207E+00	.3582E-01	.1659E-01	.4146E-02
.0040	.1980E+00	.1258E+00	.4447E-01	.2296E-01	.6834E-02
.0050	.1968E+00	.1298E+00	.5000E-01	.2904E-01	.9725E-02
.0060	.1954E+00	.1328E+00	.5221E-01	.3446E-01	.1251E-01
.0070	.1938E+00	.1347E+00	.5096E-01	.3887E-01	.1498E-01
.0080	.1919E+00	.1356E+00	.4615E-01	.4202E-01	.1657E-01
.0090	.1899E+00	.1356E+00	.3978E-01	.4370E-01	.1735E-01

.0100	.1877E+00	.1348E+00	.8189E-01	.4380E-01	.1707E-01
.0110	.1853E+00	.1331E+00	.8259E-01	.4228E-01	.1542E-01
.0120	.1829E+00	.1309E+00	.8201E-01	.3916E-01	.1394E-01
.0130	.1804E+00	.1281E+00	.8033E-01	.3452E-01	.9132E-02
.0140	.1779E+00	.1250E+00	.7773E-01	.2850E-01	.4192E-02
.0150	.1755E+00	.1217E+00	.7442E-01	.2125E-01	-.1748E-02
.0160	.1732E+00	.1182E+00	.7057E-01	.1295E-01	-.8555E-02
.0170	.1710E+00	.1147E+00	.6636E-01	.3779E-02	-.1408E-01
.0180	.1690E+00	.1113E+00	.6196E-01	-.6078E-02	-.2416E-01
.0190	.1672E+00	.1081E+00	.5752E-01	-.1644E-01	-.3264E-01
.0200	.1657E+00	.1051E+00	.5314E-01	-.2715E-01	-.4137E-01

AMPLITUDE OF TRAVELING WAVE

	MODE NUMBER				
TIME	1	2	3	4	5
.0010	.2798E+00	.1468E+00	.1228E-01	.4768E-02	.7797E-03
.0020	.2766E+00	.1512E+00	.2638E-01	.1073E-01	.3258E-02
.0030	.2727E+00	.1547E+00	.3602E-01	.1772E-01	.7584E-02
.0040	.2688E+00	.1572E+00	.4493E-01	.2544E-01	.1381E-01
.0050	.2645E+00	.1587E+00	.5487E-01	.3355E-01	.2192E-01
.0060	.2606E+00	.1592E+00	.6565E-01	.4172E-01	.3174E-01
.0070	.2552E+00	.1587E+00	.7711E-01	.4962E-01	.4316E-01
.0080	.2503E+00	.1573E+00	.7918E-01	.5696E-01	.5583E-01
.0090	.2452E+00	.1550E+00	.8380E-01	.6350E-01	.6964E-01
.0100	.2399E+00	.1520E+00	.8499E-01	.6906E-01	.8374E-01
.0110	.2346E+00	.1484E+00	.8883E-01	.7352E-01	.9832E-01
.0120	.2292E+00	.1443E+00	.8939E-01	.7685E-01	.1129E+00
.0130	.2239E+00	.1398E+00	.8881E-01	.7908E-01	.1271E+00
.0140	.2188E+00	.1352E+00	.8723E-01	.8030E-01	.1408E+00
.0150	.2137E+00	.1304E+00	.8479E-01	.8068E-01	.1537E+00
.0160	.2089E+00	.1257E+00	.8165E-01	.8042E-01	.1656E+00
.0170	.2044E+00	.1211E+00	.7794E-01	.7979E-01	.1764E+00
.0180	.2001E+00	.1167E+00	.7379E-01	.7908E-01	.1861E+00
.0190	.1962E+00	.1127E+00	.6931E-01	.7859E-01	.1945E+00
.0200	.1926E+00	.1090E+00	.6461E-01	.7862E-01	.2017E+00

MAGNITUDE OF TRAVELING WAVE

	MODE NUMBER				
TIME	1	2	3	4	5
.0010	.2674E+00	.1436E+00	.1281E-02	-.2197E-02	-.7757E-03
.0020	.2715E+00	.5507E-01	-.2385E-01	-.6377E-02	.2714E-02
.0030	.2126E+00	-.8930E-01	-.1114E-01	.1736E-01	-.2194E-02
.0040	.1041E+00	-.1572E+00	.4286E-01	-.5404E-02	-.5430E-02
.0050	-.2171E-01	-.8381E-01	.2851E-01	-.2495E-01	.1956E-01
.0060	-.1404E+00	.6583E-01	-.5302E-01	.3618E-01	-.3090E-01

TIME	TOTAL ACOUSTIC ENERGY	TIME DERIVATIVE OF TRAVELING WAVE MAGNITUDE				
		MODE NUMBER				
		1	2	3	4	5
.0010	.1468F+00	.3609F+02	-.2521F+02	-.1463F+02	-.1106F+02	-.1397F+01
.0020	.1514F+00	-.2882F+02	-.1379F+03	-.1908F+02	.1349F+02	.7239F+01
.0030	.1558F+00	-.8632F+02	-.1264F+03	.4471F+02	.1495F+02	-.1929F+02
.0040	.1556F+00	-.1221F+03	.2706F+01	.3757F+02	-.5114F+02	.2822F+02
.0050	.1535F+00	-.1283F+03	.1320F+03	-.4740F+02	.3307F+02	-.1408F+02
.0060	.1512F+00	-.1044F+03	.1427F+03	-.4329F+02	.4817F+02	-.2875F+02
.0070	.1464F+00	-.5684F+02	.2432F+02	.7477F+02	-.9669F+02	.9194F+02
.0080	.1504F+00	.2238F+01	-.1136F+03	.9012F+02	.2604F+02	-.1345F+02
.0090	.1540F+00	.5852F+02	-.1477F+03	-.6826F+02	.9984F+02	.1100F+03
.0100	.1555F+00	.9880F+02	-.5025F+02	-.1121F+03	-.1203F+03	-.1552F+01
.0110	.1561F+00	.1144F+03	.8627F+02	.5060F+02	-.1099F+02	-.1530F+03
.0120	.1532F+00	.1030F+03	.1408F+03	.1249F+03	.1436F+03	.2704F+03
.0130	.1460F+00	.6819F+02	.7074F+02	-.2569F+02	-.1103F+03	-.2450F+03
.0140	.1479F+00	.1910F+02	-.5543F+02	-.1268F+03	-.5714F+02	.1107F+03
.0150	.1538F+00	-.3202F+02	-.1256F+03	-.9033F+00	.1616F+03	.1789F+03
.0160	.1556F+00	-.7750F+02	-.8405F+02	.1182F+03	-.8044F+02	-.1567F+03
.0170	.1549F+00	-.9649F+02	.2569F+02	.2510F+02	-.9123F+02	.4160F+03
.0180	.1536F+00	-.9634F+02	.1057F+03	-.1012F+03	.1595F+03	-.2625F+03
.0190	.1483F+00	-.7413F+02	.9095F+02	-.4385F+02	-.5207F+02	.4423F+03
.0200	.1502F+00	-.3574F+02	.6725F+00	.7826F+02	-.1110F+03	.1578F+03

NONLINEAR LOSSLESS ACOUSTICS - SAMPLE CASE 1

INSTANTANEOUS NORMALIZED PRESSURE DISTRIBUTION

	AXIAL LOCATION							
TIME	1	2	3	4	5	6	7	8
.001	.3996E+00	.3706E+00	.3241E+00	.2629E+00	.1910E+00	.1134E+00	.3587E-01	-.3604E-01
.002	.2960E+00	.2868E+00	.2706E+00	.2465E+00	.2133E+00	.1706E+00	.1183E+00	.5038E-01
.003	.1276E+00	.1288E+00	.1314E+00	.1360E+00	.1424E+00	.1491E+00	.1531E+00	.1501E+00
.004	-.1482E-01	-.2736E-02	.1447E-01	.3402E-01	.5419E-01	.7472E-01	.9612E-01	.1181E+00
.005	-.8371E-01	-.8002E-01	-.6965E-01	-.5003E-01	-.2239E-01	.7829E-02	.3341E-01	.4927E-01
.006	-.1159E+00	-.1003E+00	-.8404E-01	-.7524E-01	-.7419E-01	-.8172E-01	-.8710E-01	-.7347E-01
.007	-.9211E-01	-.1121E+00	-.1337E+00	-.1465E+00	-.1462E+00	-.1370E+00	-.1283E+00	-.1285E+00
.008	-.1390E+00	-.1368E+00	-.1375E+00	-.1455E+00	-.1426E+00	-.1863E+00	-.2091E+00	-.2107E+00
.009	-.1900E+00	-.1836E+00	-.1829E+00	-.1931E+00	-.2004E+00	-.2160E+00	-.1937E+00	-.1911E+00
.010	-.2261E+00	-.2622E+00	-.2820E+00	-.2510E+00	-.1574E+00	-.2167E-01	.1129E+00	.1995E+00
.011	-.3329E+00	-.1971E+00	-.3177E-01	.1024E+00	.1463E+00	.1572E+00	.1052E+00	.5324E-01
.012	.1463E+00	.1034E+00	.5177E-01	.1101E-01	-.6386E-02	-.1652E-03	.1892E-01	.3569E-01
.013	.4431E+00	.3237E+00	.1736E+00	.4091E-01	-.6039E-01	-.6515E-01	-.5746E-01	-.3627E-01
.014	.1690E+00	.2761E+00	.3782E+00	.4053E+00	.3238E+00	.1563E+00	-.3917E-01	-.1838E+00
.015	.2596E+00	.1690E+00	.8169E-01	.5179E-01	.9775E-01	.1892E+00	.2627E+00	.2579E+00
.016	.5611E-01	.8834E-01	.1172E+00	.1232E+00	.1027E+00	.7124E-01	.5410E-01	.4918E-01
.017	-.6081E-01	-.1010E-01	.4661E-01	.8306E-01	.8489E-01	.5676E-01	.1941E-01	-.1710E-02
.018	.4322E-01	-.5694E-01	-.1547E+00	-.1896E+00	-.1966E+00	-.2146E-01	.9492E-01	.1517E+00
.019	-.1927E+00	-.7844E-01	.3297E-01	.7410E-01	.2100E-01	-.9113E-01	-.1895E+00	-.2070E+00
.020	-.4993E-01	-.1188E+00	-.1807E+00	-.1919E+00	-.1405E+00	-.5504E-01	.1089E-01	.1168E-01

	AXIAL LOCATION							
TIME	9	10	11	12	13	14	15	16
.001	-.9766E-01	-.1458E+00	-.1791E+00	-.1977E+00	-.2033E+00	-.1986E+00	-.1866E+00	-.1706E+00
.002	-.2319E-02	-.6145E-01	-.1128E+00	-.1524E+00	-.1791E+00	-.1941E+00	-.2005E+00	-.2021E+00
.003	.1357E+00	.1067E+00	.6221E-01	.5089E-02	-.5885E-01	-.1220E+00	-.1771E+00	-.2103E+00
.004	.1382E+00	.1514E+00	.1516E+00	.1327E+00	.9209E-01	.3148E-01	-.4298E-01	-.1221E+00
.005	.5540E-01	.5686E-01	.6041E-01	.6948E-01	.8177E-01	.8757E-01	.7429E-01	.4184E-01
.006	-.5308E-01	-.2965E-01	-.1359E-01	-.1068E-01	-.1445E-01	-.1750E-01	.3770E-02	.5739E-01
.007	-.1389E+00	-.1510E+00	-.1499E+00	-.1214E+00	-.5928E-01	.3118E-01	.1351E+00	.2342E+00
.008	-.2066E+00	-.1621E+00	-.8633E-01	.1188E-01	.1163E+00	.2080E+00	.2716E+00	.3002E+00
.009	-.3372E-01	.7563E-01	.1659E+00	.2125E+00	.2000E+00	.1711E+00	.1274E+00	.1054E+00
.010	.2165E+00	.1725E+00	.1029E+00	.4892E-01	.3548E-01	.5976E-01	.9606E-01	.1137E+00
.011	.3257E-01	.4815E-01	.7988E-01	.9810E-01	.8307E-01	.3477E-01	-.1943E-01	-.5877E-01
.012	.3865E-01	.2514E-01	.1392E-02	-.2250E-01	-.3870E-01	-.4582E-01	-.4865E-01	-.5408E-01
.013	-.3718E-01	-.6121E-01	-.9512E-01	-.1187E+00	-.1187E+00	-.9745E-01	-.7138E-01	-.5897E-01
.014	-.2357E+00	-.1988E+00	-.1230E+00	-.6423E-01	-.6084E-01	-.1097E+00	-.1734E+00	-.2047E+00
.015	.1534E+00	-.1963E-01	-.1924E+00	-.2957E+00	-.2964E+00	-.2147E+00	-.1097E+00	-.4563E-01
.016	.1128E+00	.1581E+00	.1681E+00	.1167E+00	.6304E-02	-.1300E+00	-.2426E+00	-.2909E+00

.017	.9984E-02	.5344E-01	.1103E+00	.1539E+00	.1612E+00	.1231E+00	.4647E-01	-.5041E-01
.018	.1237E+00	.3587E-01	-.5230E-01	-.8241E-01	-.3259E-01	.4876E-01	.1591E+00	.1787E+00
.019	-.1248E+00	.1471E-01	.1317E+00	.1564E+00	.7331E-01	-.4413E-01	-.1688E+00	-.1576E+00
.020	-.6008E-01	-.1656E+00	-.2389E+00	-.2229E+00	-.1037E+00	.7961E-01	.2540E+00	.3511E+00

TIME	AXIAL LOCATION 17	18	19	20
.001	-.1539E+00	-.1396E+00	-.1299E+00	-.1265E+00
.002	-.2019E+00	-.2016E+00	-.2016E+00	-.2017E+00
.003	-.2471E+00	-.2625E+00	-.2694E+00	-.2712E+00
.004	-.1958E+00	-.2550E+00	-.2932E+00	-.3063E+00
.005	-.1222E-01	-.7224E-01	-.1193E+00	-.1371E+00
.006	.1391E+00	.2291E+00	.2996E+00	.3263E+00
.007	.3143E+00	.3689E+00	.3990E+00	.4083E+00
.008	.2977E+00	.2772E+00	.2555E+00	.2465E+00
.009	.1168E+00	.1529E+00	.1905E+00	.2062E+00
.010	.9631E-01	.5163E-01	.5836E-02	-.1333E-01
.011	-.6577E-01	-.4504E-01	-.1715E-01	-.4647E-02
.012	-.6600E-01	-.8259E-01	-.9732E-01	-.1032E+00
.013	-.7027E-01	-.9973E-01	-.1299E+00	-.1426E+00
.014	-.1852E+00	-.1210E+00	-.5364E-01	-.252BE-01
.015	-.5529E-01	-.1239E+00	-.2013E+00	-.2345E+00
.016	-.2641E+00	-.1878E+00	-.1106E+00	-.7867E-01
.017	-.1460E+00	-.2232E+00	-.2720E+00	-.2886E+00
.018	.1063E+00	-.2623E-01	-.1510E+00	-.2017E+00
.019	-.8782E-02	.2210E+00	.4266E+00	.5087E+00
.020	.3437E+00	.2599E+00	.1652E+00	.1246E+00

* CALCULATIONS COMPLETED *

TF-30 Duct Burner at Sea Level

The TF-30 augmentor is represented schematically in Figure 1. A nonlinear instability analysis of its duct burner configuration was conducted using Program NØNLIN, as described in the following section of this report. During that analysis, the sensitivity of the results to a number of physical input items was investigated. The sample case included here is considered to represent the nominal results for the TF-30 duct burner at sea level.

Among the input items not varied as part of the TF-30 sensitivity analysis was the acoustic data. Rather, values of the index of location were calculated using admittances suggested in Reference 6 of $Z_{\ell_1 0} = 0.15$ and $Z_{\ell_1 \ell_2} = 0.25$, and the appropriate values of frequency. The values of frequency were obtained using Program HLMHLT, with the particular computer run appearing as the sample case in Appendix C. As can be seen from the output of that case, Program HLMHLT calculates wave numbers rather than frequencies. The values of frequency must be calculated from

$$\omega_i = \left[R(k_i) \cdot \frac{c}{R_o} \right]_{1 \text{ or } 2}$$

where $R(k_i)$ is the real part of the ith wave number, c is the speed of sound input to HLMHLT, and R_o is the outer radius of the chamber input to HLMHLT. A consistent set of frequencies will be calculated using values appropriate to the chamber either upstream or downstream of the flameholder.

Other physical input items appropriate to the TF-30, which were not varied in the sensitivity analysis, consisted of:

1) Combustion chamber dimensions ~

$\ell_1 = 8.52$ ft, $\ell_2 = 14.1$ ft, and $\ell_3 = 7.0$ ft

2) Fluid properties

$\gamma = 1.3$, $c_1 = 1000$ fps, and $c_2 = 2700$ fps

3) Estimated combustion parameters

$\bar{U}_c = 1000$ fps and $\bar{E} = 2.25 \times 10^7$ (fps)^2

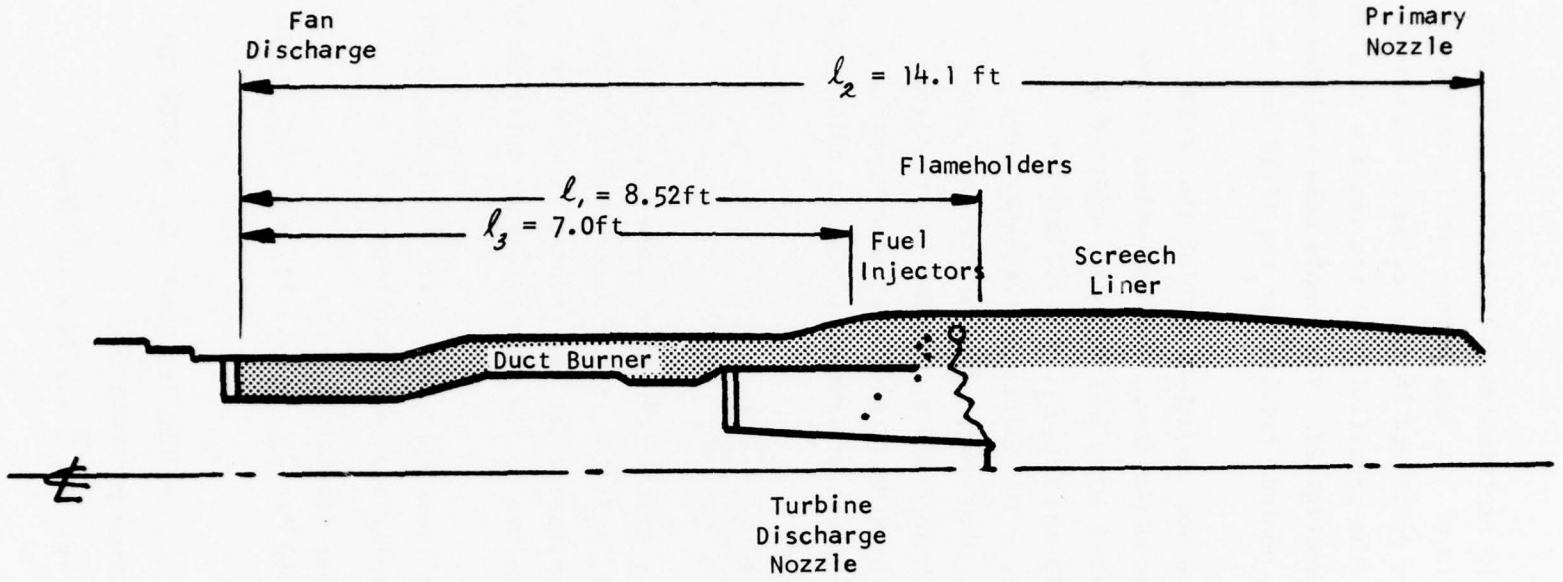

Figure 1. Schematic of the TF-30 Augmentor

Examination of the time-dependent output of Program NØNLIN reveals that this sample case is stable. In particular, the column headed TOTAL ACOUSTIC ENERGY is observed to decrease in essentially a monotonic manner, and at the limiting time of 0.2 sec an overall decrease of one order of magnitude is found. Further, the set of columns headed AMPLITUDE OF TRAVELING WAVE indicates a decrease for each modal component over the time period, although the fourth mode does not decrease as rapidly as the other modes. In the following section it will be seen that the fourth mode tends to be the least stable mode for the TF-30 as it is modeled in Program NØNLIN.

NORTHERN RESEARCH AND ENGINEERING CORPORATION

DATA INPUT SHEET

ENGINEER: M. Platt PROJECT: Nonlinear Combustion Instability PROJECT NO: 1294

TITLE: TF-30 Duct Burner at Sea Level SHEET: 1 OF 1

LOCATION

1 6	7 12	13 18	19 24	25 30	31 36	37 42	43 48	49 54	55 60	61 66	67 72
TF-30 DUCT BURNER - SEA LEVEL						SAMPLE CASE 2					
	16	0	2								
0.		0.200		0.0025							
.08		.08		.08		.08		.08			
.08		.08		.08		.08		.08			
1.3		1000.		2700.		8.52		14.1			
56.717		-.1489		-.05119							
294.847		-.1489		-1.295							
598.341		-.1489		-2.88							
934.141		-.1489		-4.633							
1265.012		-.1489		-6.361							
7.		-2.94		239.3		325.		-1173.9			
1000.		.001		2.25E7		-2.4					

NREC PROGRAM NONLIN

TF-30 DUCT BURNER - SEA LEVEL SAMPLE CASE 2

INPUT DATA

INITIAL TIME, SEC	0.0000
LIMITING TIME, SEC	.2000
COMPUTATIONAL TIME INCREMENT, SEC	.0025
AVERAGING TIME	MODE INDEPENDENT
TOTAL CHAMBER LENGTH, FT	14.100
LENGTH TO FLAMEHOLDER, FT	9.521
LENGTH TO FUEL INJECTOR, FT	7.000
RATIO OF SPECIFIC HEATS	1.300
SOUND VELOCITY UPSTREAM (OF FLAMEHOLDER), FPS	1000.
SOUND VELOCITY DOWNSTREAM (OF FLAMEHOLDER), FPS	2700.
VELOCITY PROFILE UPSTREAM - AXIAL COEF, PER SEC	-2.940
CONSTANT, FPS	325.00
VELOCITY PROFILE DOWNSTREAM - AXIAL COEF, PER SEC	239.300
CONSTANT, FPS	-1173.90
CHARACTERISTIC COMBUSTION VELOCITY, FPS	1000.
CHARACTERISTIC COMBUSTION TIME, SEC	.00100
ENERGY CONTENT, FPS**2	225000000.
UNSTEADY COMBUSTION COEFFICIENT	-2.400000

	ACOUSTIC WAVES			TRAVELING WAVES	
MODE NUMBER	NATURAL FREQUENCY, RAD/SEC	INDEX OF LOCATION, RAD		INITIAL AMPLITUDE OF	
		UPSTREAM	DOWNSTREAM	SIN TERM	COS TERM
1	56.717	-.14890	-.05119	.0800000	.0800000
2	294.847	-.14890	-1.29500	.0800000	.0800000
3	598.341	-.14890	-2.88000	.0800000	.0800000
4	934.141	-.14890	-4.63300	.0800000	.0800000
5	1265.012	-.14890	-6.36100	.0800000	.0800000

TF-30 DUCT BURNER - SEA LEVEL SAMPLE CASE 2

TIME-INDEPENDENT OUTPUT DATA

	MODE NUMBER				
	1	2	3	4	5
RELATIVE AMPLITUDE OF ACOUSTIC WAVE	.1050E+01	-.1342E+01	.2325E+01	-.2685E+01	.2016E+01

INNER-PRODUCT MATRIX(I,J)

I / J	1	2	3	4	5
1	.1451E+02	.1285E+01	.1515E+01	.2254E+00	.7181E+00
2	.1285E+01	.1198E+02	.7763E-01	.8810E+00	.1241E+00
3	.1515E+01	.7763E-01	.2702E+02	-.1805E+00	.7093E+00
4	.2254E+00	.8810E+00	-.1805E+00	.3441E+02	-.8154E-01
5	.7181E+00	.1241E+00	.7093E+00	-.8154E-01	.2059E+02

INVERSE OF IN-PR MATRIX(I,J)

I / J	1	2	3	4	5
1	.7007E-01	-.7447E-02	-.3850E-02	-.2939E-03	-.2268E-02
2	-.7447E-02	.8443E-01	.1678E-03	-.2113E-02	-.2634E-03
3	-.3850E-02	.1678E-03	.3725E-01	.2136E-03	-.1149E-02
4	-.2939E-03	-.2113E-02	.2136E-03	.2912E-01	.1309E-03
5	-.2268E-02	-.2634E-03	-.1149E-02	.1309E-03	.4869E-01

LINEAR COEF MATRIX D(I,J)

I / J	1	2	3	4	5
1	-.1721E+03	-.2816E+03	-.5432E+02	-.3400E+03	-.2121E+03
2	-.2510E+03	-.1898E+03	-.5730E+03	-.1163E+03	-.5728E+03
3	-.1143E+03	-.3870E+02	-.3190E+02	-.5194E+03	-.8576E+02
4	-.8913E+02	-.7348E+02	.1355E+03	-.7432E+01	-.4678E+03
5	-.1293E+03	-.9829E+02	-.6729E+02	.3804E+03	-.4119E+02

LINEAR COEF MATRIX E(I,J)

I / J	1	2	3	4	5
1	.7005E+03	-.2207E+05	-.7474E+05	-.8428E+05	-.2754E+05
2	.8815E+03	-.2834E+05	-.9501E+05	-.1054E+06	-.3332E+05
3	.3006E+03	-.1035E+05	-.3355E+05	-.3515E+05	-.9864E+04
4	.1017E+03	-.4851E+04	-.1355E+05	-.1036E+05	-.7588E+03
5	-.9444E+02	-.1125E+04	.3529E+04	.1606E+05	.1076E+05

NON-LIN COEF MATRIX A(K,I,J)

I / J	1	2	3	4	5
K=1					
1	-.7557E+03	.2472E+03	.4629E+03	.3304E+01	.5204E+03
2	.2472E+03	-.1633E+05	.3566E+04	.5822E+04	-.8391E+03

	3	.4629E+03	.3566F+04	-.1649F+06	.2095F+04	.8956F+04
	4	.3304E+01	.5822F+04	.8095F+04	-.5284F+06	.2200F+05
	5	.5204E+03	-.8391F+03	.8956F+04	.2200F+05	-.5689F+06
K=2	1	.2242E+02	-.1058F+05	.8968F+03	.1386F+04	.4624F+03
	2	-.1058E+05	.3004F+04	-.4473F+05	-.7043F+04	-.3178F+04
	3	.8968E+03	-.4473F+05	.7387F+05	-.2163F+06	-.2970F+05
	4	.1386E+04	-.7043F+04	-.2163F+06	.2485F+06	-.3822F+06
	5	.4624E+03	-.3178F+04	-.2970F+05	-.3822F+06	.2169F+06
K=3	1	.4897E+01	.9458F+02	-.4291F+05	.1402F+04	.1249F+04
	2	.9458E+02	-.7096F+04	.1606F+05	-.7067F+05	-.1040F+05
	3	-.4291E+05	.1606F+05	.3264F+05	.9743F+05	-.1780F+06
	4	.1402E+04	-.7067F+05	.9743F+05	.9400F+05	.1511F+06
	5	.1249E+04	-.1040F+05	-.1780F+06	.1511F+06	.8071F+05
K=4	1	.5066E+00	.4593F+02	.4450F+03	-.1042F+06	.1931F+04
	2	.4593E+02	-.3192F+03	-.2530F+05	.3769F+05	-.8866F+05
	3	.4450E+03	-.2530F+05	.4468F+05	.4296F+05	.9500F+05
	4	-.1042E+06	.3769F+05	.4296F+05	.8113F+05	.5716F+05
	5	.1931E+04	-.8866F+05	.9500F+05	.5716F+05	.6274F+05
K=5	1	.1528E+01	.9516E+01	.3577F+03	.1712F+04	-.1901F+06
	2	.9516E+01	.2343F+03	-.3472F+04	-.8198F+05	.4957F+05
	3	.3577E+03	-.3472F+04	-.8055F+05	.9769F+05	.4667F+05
	4	.1712E+04	-.8198F+05	.9769F+05	.6889F+05	.7923F+05
	5	-.1901E+06	.4957F+05	.4667F+05	.7923F+05	.4433F+05

NON-LIN COEF MATRIX B(K,I,J)

I / J	1	2	3	4	5
K=1					
1	-.2081E+01	-.1976F+01	-.9378F+01	-.1867F+01	-.1799F+02
2	-.1976E+01	-.2396F+00	-.5320F-02	-.6736F+00	-.3030F-01
3	-.9378E+01	-.5320F-02	.1096F+00	.1723F+00	-.1941F+00
4	-.1867E+01	-.6736F+00	.1723F+00	.4672F+00	.4326F-01
5	-.1799E+02	-.3030F-01	-.1941F+00	.4326F-01	.2704F+00
K=2					
1	.2862E+01	-.6022F+00	.1709F+01	-.1577F+02	-.1017F+01
2	-.6022E+00	-.1168F+00	-.7903E+00	.2900F-01	-.8410F+00
3	.1709E+01	-.7903F+00	-.1920F+00	-.2789F+00	.1215F-01
4	-.1577E+02	.2900F-01	-.2789F+00	-.2290F+00	-.1587F-01
5	-.1017E+01	-.8410F+00	.1215F-01	-.1587F-01	-.1236F+00
K=3					
1	.8031E+01	.2146F+01	.2109F+00	.5340F+01	-.7109F+01
2	.2146E+01	.1354F+01	-.1892F+00	-.1094F+01	.5501F-02
3	.2109E+00	-.1892F+00	-.4854F+00	-.8236F-01	-.3730F+00
4	.5340E+01	-.1094F+01	-.8236F-01	-.3206F+00	-.6335F-01
5	-.7109E+01	.5501F-02	-.3730F+00	-.6335F-01	-.1349F+00
K=4					
1	.2212E+01	.1340F+01	.3601F+00	-.3431F+01	.2780F+01
2	.1340E+01	.1300F+00	.1875F+01	-.3314F+00	-.1268F+01
3	.3601E+00	.1875F+01	-.1125F+01	-.5819F+00	-.1126F+00
4	-.3431E+01	-.3314F+00	-.5819F+00	-.3617F+00	-.2705F+00
5	.2780E+01	-.1268F+01	-.1126F+00	-.2705F+00	-.9084F-01
K=5					
1	.2502E+02	.7500F+01	.6163F+01	.6168F+01	-.2795F+00
2	.7500E+01	.6968F+00	.9447F+00	.3641F+01	.4326F-01
3	.6163E+01	.9447F+00	.3796F+01	-.1301F+01	-.2713F+00
4	.6168E+01	.3641F+01	-.1301F+01	-.5230F+00	-.1565F+00
5	-.2795E+00	.4326F-01	-.2713F+00	-.1565F+00	-.1344F+00

TF-30 DUCT BURNER - SEA LEVEL SAMPLE CASE 2

TIME-DEPENDENT OUTPUT DATA

TRAVELING WAVE, AMPLITUDE OF SIN TERM

TIME	MODE NUMBER 1	2	3	4	5
.0050	.7374E-01	.6234E-01	.6620E-01	.8392E-01	.8018E-01
.0100	.6048E-01	.5344E-01	.4961E-01	.8078E-01	.7570E-01
.0150	.5147E-01	.3834E-01	.3488E-01	.7883E-01	.7238E-01
.0200	.2046E-01	.3274E-01	.2684E-01	.7935E-01	.6640E-01
.0250	.1702E-01	.5106E-01	.1501E-01	.7831E-01	.5695E-01
.0300	.8110E-02	.5228E-01	.2993E-02	.7378E-01	.4856E-01
.0350	.3205E-03	.3929E-01	-.4009E-02	.7105E-01	.4352E-01
.0400	.1763E-01	.3280E-01	-.9243E-02	.6958E-01	.3758E-01
.0450	.1062E-01	.4108E-01	-.1770E-01	.6704E-01	.3050E-01
.0500	-.4182E-02	.3442E-01	-.2466E-01	.6279E-01	.2522E-01
.0550	-.8934E-02	.2220E-01	-.2680E-01	.5984E-01	.2236E-01
.0600	.1468E-01	.1784E-01	-.2882E-01	.5749E-01	.1844E-01
.0650	.3468E-02	.2300E-01	-.3376E-01	.5459E-01	.1423E-01
.0700	-.3761E-02	.1545E-01	-.3569E-01	.5093E-01	.1177E-01
.0750	-.1490E-02	.7790E-02	-.3396E-01	.4806E-01	.1055E-01
.0800	.1480E-02	.7219E-02	-.3356E-01	.4551E-01	.7945E-02
.0850	-.1151E-02	.1105E-01	-.3498E-01	.4273E-01	.5601E-02
.0900	.3548E-02	.4499E-02	-.3275E-01	.3959E-01	.4886E-02
.0950	.3517E-02	.7188E-03	-.2988E-01	.3690E-01	.4491E-02
.1000	-.9738E-02	.2383E-02	-.2734E-01	.3442E-01	.2555E-02
.1050	-.6684E-03	.4663E-02	-.2619E-01	.3186E-01	.1329E-02
.1100	.7800E-02	-.5637E-03	-.2169E-01	.2913E-01	.1595E-02
.1150	.1958E-02	-.1872E-02	-.1770E-01	.2666E-01	.1531E-02
.1200	-.8655E-02	.5947E-03	-.1422E-01	.2434E-01	-.6045E-04
.1250	.9708E-03	.1339E-02	-.1376E-01	.2204E-01	-.5882E-03
.1300	.3308E-02	-.2427E-02	-.8958E-02	.1964E-01	.1979E-03
.1350	-.8113E-03	-.2386E-02	-.6284E-02	.1740E-01	.1918E-03
.1400	.1134E-02	.9476E-04	-.5489E-02	.1530E-01	-.1190E-02
.1450	.4439E-03	-.3684E-03	-.2739E-02	.1325E-01	-.1259E-02
.1500	-.4552E-02	-.2678E-02	.9551E-03	.1114E-01	-.2398E-03
.1550	-.6337E-03	-.2080E-02	.1903E-02	.9142E-02	-.3202E-03
.1600	.7859E-02	.7727E-04	.1917E-02	.7278E-02	-.1547E-02
.1650	-.1332E-02	-.1176E-02	.4330E-02	.5468E-02	-.1301E-02
.1700	-.6642E-02	-.2201E-02	.6282E-02	.3636E-02	-.2327E-03
.1750	.9513E-03	-.1554E-02	.5578E-02	.1881E-02	-.4683E-03
.1800	.5078E-02	.1924E-03	.5383E-02	.2544E-03	-.1528E-02

.1450	-.1466E-02	-.1468E-02	.7159E-02	-.1318E-02	-.1065E-02
.1900	-.1216E-02	-.1494E-02	.7393E-02	-.2894E-02	-.6148E-04
.1950	.7107E-03	-.1072E-02	.5847E-02	-.4406E-02	-.4572E-03
.2000	-.2543E-02	.2963E-03	.5760E-02	-.5799E-02	-.1351E-02

TRAVELING WAVE, AMPLITUDE OF COS TERM

TIME	MODE NUMBER 1	2	3	4	5
.0050	.4947E-01	.2682E-01	.8318E-01	.7711E-01	.6701E-01
.0100	.2360E-01	.1038E-01	.8192E-01	.7622E-01	.5658E-01
.0150	.3311E-02	.6554E-03	.7807E-01	.7223E-01	.4600E-01
.0200	.3060E-01	-.1385E-01	.7489E-01	.7066E-01	.3533E-01
.0250	.1790E-01	-.1555E-01	.7501E-01	.7411E-01	.2885E-01
.0300	-.1204E-03	-.2065E-02	.7028E-01	.7576E-01	.2375E-01
.0350	-.1099E-01	.2339E-02	.6384E-01	.7451E-01	.1722E-01
.0400	.1211E-01	-.2750E-02	.5970E-01	.7397E-01	.1061E-01
.0450	.3752E-02	.2495E-02	.5647E-01	.7577E-01	.8254E-02
.0500	.2838E-03	.1344E-01	.4884E-01	.7635E-01	.7020E-02
.0550	.1317E-02	.1304E-01	.4168E-01	.7566E-01	.3587E-02
.0600	-.5308E-02	.6077E-02	.3724E-01	.7515E-01	-.8755E-04
.0650	-.3166E-02	.1054E-01	.3177E-01	.7582E-01	-.3822E-04
.0700	.6046E-02	.1624E-01	.2732E-01	.7583E-01	.6211E-03
.0750	.6470E-02	.1266E-01	.1746E-01	.7535E-01	-.1266E-02
.0800	-.1297E-01	.6040E-02	.1389E-01	.7476E-01	-.3340E-02
.0850	-.1640E-02	.1048E-01	.8110E-02	.7481E-01	-.2268E-02
.0900	.6927E-02	.1275E-01	.1251E-02	.7452E-01	-.1048E-02
.0950	.2376E-02	.8686E-02	-.1851E-02	.7401E-01	-.2334E-02
.1000	-.6113E-02	.3859E-02	-.3781E-02	.7331E-01	-.3551E-02
.1050	.7992E-03	.8394E-02	-.8375E-02	.7296E-01	-.2147E-02
.1100	.8209E-05	.8396E-02	-.1224E-01	.7243E-01	-.9797E-03
.1150	-.1637E-02	.5035E-02	-.1243E-01	.7181E-01	-.2076E-02
.1200	.5487E-02	.2040E-02	-.1290E-01	.7096E-01	-.2770E-02
.1250	.3166E-03	.6238E-02	-.1573E-01	.7033E-01	-.1334E-02
.1300	-.6828E-02	.4812E-02	-.1650E-01	.6961E-01	-.4602E-03
.1350	-.1208E-02	.2505E-02	-.1469E-01	.6883E-01	-.1508E-02
.1400	.9113E-02	.9115E-03	-.1441E-01	.6785E-01	-.1832E-02
.1450	-.1237E-02	.4407E-02	-.1557E-01	.6701E-01	-.4968E-03
.1500	-.5644E-02	.2266E-02	-.1405E-01	.6613E-01	.2073E-04
.1550	.7076E-03	.9790E-03	-.1156E-01	.6520E-01	-.9999E-03
.1600	.2552E-02	.3207E-03	-.1124E-01	.6410E-01	-.1036E-02
.1650	-.8933E-03	.2943E-02	-.1114E-01	.6312E-01	.1412E-03
.1700	.1642E-02	.6634E-03	-.8469E-02	.6210E-01	.3182E-03
.1750	.4634E-03	.1707E-03	-.6391E-02	.6104E-01	-.6481E-03
.1800	-.5456E-02	.8009E-04	-.6423E-02	.5986E-01	-.4504E-03
.1850	.1119E-02	.1818E-02	-.5509E-02	.5876E-01	.5425E-03
.1900	.6275E-02	-.1993E-03	-.2760E-02	.5764E-01	.4302E-03
.1950	-.1194E-02	-.1912E-03	-.1720E-02	.5649E-01	-.4396E-03
.2000	-.6231E-02	.4049E-04	-.2111E-02	.5525E-01	-.5601E-04

AMPLITUDE OF TRAVELING WAVE

TIME	MODE NUMBER 1	2	3	4	5
.0050	.8880E-01	.6786E-01	.1063E+00	.1140E+00	.1045E+00
.0100	.6492E-01	.5443E-01	.9577E-01	.1111E+00	.9451E-01
.0150	.5158E-01	.3834E-01	.8634E-01	.1069E+00	.8576E-01
.0200	.3681E-01	.3555E-01	.7955E-01	.1063E+00	.7521E-01
.0250	.2470E-01	.5338E-01	.7649E-01	.1079E+00	.6384E-01
.0300	.8111E-02	.5232E-01	.7034E-01	.1058E+00	.5406E-01
.0350	.1099E-01	.3936E-01	.6397E-01	.1030E+00	.4680E-01
.0400	.2139E-01	.3291E-01	.6042E-01	.1016E+00	.3905E-01
.0450	.1126E-01	.4115E-01	.5918E-01	.1012E+00	.3160E-01
.0500	.4192E-02	.3695E-01	.5471E-01	.9885E-01	.2618E-01
.0550	.9031E-02	.2575E-01	.4956E-01	.9646E-01	.2264E-01
.0600	.1561E-01	.1885E-01	.4709E-01	.9462E-01	.1844E-01
.0650	.4696E-02	.2530E-01	.4636E-01	.9342E-01	.1423E-01
.0700	.7120E-02	.2241E-01	.4264E-01	.9135E-01	.1179E-01
.0750	.6640E-02	.1487E-01	.3818E-01	.8937E-01	.1063E-01
.0800	.1306E-01	.9412E-02	.3633E-01	.8753E-01	.8619E-02
.0850	.2004E-02	.1523E-01	.3591E-01	.8615E-01	.6043E-02
.0900	.7783E-02	.1352E-01	.3278E-01	.8438E-01	.4995E-02
.0950	.4245E-02	.8716E-02	.2894E-01	.8270E-01	.5062E-02
.1000	.1150E-01	.4536E-02	.2760E-01	.8098E-01	.4375E-02
.1050	.1042E-02	.9602E-02	.2750E-01	.7961E-01	.2525E-02
.1100	.7800E-02	.8415E-02	.2490E-01	.7807E-01	.1872E-02
.1150	.2552E-02	.5372E-02	.2163E-01	.7660E-01	.2580E-02
.1200	.1025E-01	.2125E-02	.2072E-01	.7502E-01	.2771E-02
.1250	.1021E-02	.6380E-02	.2089E-01	.7370E-01	.1458E-02
.1300	.7587E-02	.5389E-02	.1877E-01	.7233E-01	.5010E-03
.1350	.1455E-02	.3460E-02	.1598E-01	.7099E-01	.1520E-02
.1400	.9183E-02	.9164E-03	.1542E-01	.6955E-01	.2185E-02
.1450	.1314E-02	.4422E-02	.1581E-01	.6831E-01	.1353E-02
.1500	.7251E-02	.3508E-02	.1409E-01	.6706E-01	.2407E-03
.1550	.9499E-03	.2299E-02	.1170E-01	.6583E-01	.1053E-02
.1600	.8263E-02	.3299E-03	.1140E-01	.6452E-01	.1861E-02
.1650	.1604E-02	.3169E-02	.1195E-01	.6335E-01	.1309E-02
.1700	.6842E-02	.2299E-02	.1054E-01	.6220E-01	.3942E-03
.1750	.1058E-02	.1564E-02	.8483E-02	.6107E-01	.7396E-03
.1800	.7453E-02	.2084E-03	.8381E-02	.5986E-01	.1593E-02
.1850	.1844E-02	.2337E-02	.9033E-02	.5878E-01	.1195E-02
.1900	.6392E-02	.1507E-02	.7892E-02	.5771E-01	.4346E-03
.1950	.1390E-02	.1089E-02	.6094E-02	.5666E-01	.6343E-03
.2000	.6730E-02	.2990E-03	.6134E-02	.5555E-01	.1352E-02

MAGNITUDE OF TRAVELING WAVE

TIME	MODE NUMBER 1	2	3	4	5

.0050	.6813E-01	.6464E-01	-.7237E-01	-.8706E-01	.7030E-01
.0100	.5240E-01	.7310E-04	.6362E-01	-.6923E-01	.6271E-01
.0150	.4088E-01	-.3693E-01	-.5428E-01	.8723E-01	.5471E-01
.0200	.3148E-01	-.2517E-01	.4668E-01	.5651E-01	.4590E-01
.0250	.1955E-01	.3801E-01	-.4468E-01	-.9195E-01	.4006E-01
.0300	.8056E-02	.3035E-01	.4138E-01	-.5514E-01	.3508E-01
.0350	.4716E-02	-.3211E-01	-.3528E-01	.8948E-01	.2906E-01
.0400	.5724E-02	-.2486E-01	.3030E-01	.4712E-01	.2238E-01
.0450	.2782E-02	.2842E-01	-.2969E-01	-.9014E-01	.1890E-01
.0500	-.1530E-02	.2066E-01	.2811E-01	-.4439E-01	.1667E-01
.0550	-.1514E-02	-.2220E-01	-.2347E-01	.8715E-01	.1315E-01
.0600	.1333E-02	-.1392E-01	.1966E-01	.3837E-01	.9805E-02
.0650	.9091E-03	.1716E-01	-.1967E-01	-.8587E-01	.7336E-02
.0700	-.1315E-02	.1156E-01	.1910E-01	-.3522E-01	.7030E-02
.0750	-.1528E-02	-.1352E-01	-.1551E-01	.8307E-01	.5175E-02
.0800	.8016E-03	-.7060E-02	.1249E-01	.3059E-01	.2316E-02
.0850	.9667E-03	.9678E-02	-.1284E-01	-.8113E-01	.1941E-02
.0900	-.6312E-03	.6559E-02	.1293E-01	-.2751E-01	.2579E-02
.0950	-.1258E-02	-.8198E-02	-.1013E-01	.7860E-01	.1575E-02
.1000	.5853E-03	-.3591E-02	.7661E-02	.2379E-01	-.4790E-03
.1050	.9719E-03	.5475E-02	-.8217E-02	-.7643E-01	-.3447E-03
.1100	-.3373E-03	.3935E-02	.8721E-02	-.2093E-01	.6777E-03
.1150	-.1126E-02	-.5142E-02	-.6526E-02	.7409E-01	.7198E-04
.1200	.4322E-03	-.1822E-02	.4444E-02	.1782E-01	-.1536E-02
.1250	.9199E-03	.3148E-02	-.5097E-02	-.7184E-01	-.1177E-02
.1300	-.2249E-03	.2454E-02	.5866E-02	-.1522E-01	-.3800E-04
.1350	-.1032E-02	-.3330E-02	-.4129E-02	.6961E-01	-.4690E-03
.1400	.3435E-03	-.8657E-03	.2329E-02	.1258E-01	-.1907E-02
.1450	.8611E-03	.1822E-02	-.3010E-02	-.6736E-01	-.1353E-02
.1500	-.1827E-03	.1550E-02	.3941E-02	-.1024E-01	-.2216E-03
.1550	-.9454E-03	-.2202E-02	-.2559E-02	.6520E-01	-.5863E-03
.1600	.2977E-03	-.3243E-03	.9676E-03	.7970E-02	-.1742E-02
.1650	.8029E-03	.1043E-02	-.1431E-02	-.6298E-01	-.1252E-02
.1700	-.1725E-03	.9672E-03	.2654E-02	-.5904E-02	-.1936E-03
.1750	-.8632E-03	-.1470E-02	-.1551E-02	.6087E-01	-.5338E-03
.1800	.2756E-03	-.1245E-04	.1169E-03	.3943E-02	-.1553E-02
.1850	.7451E-03	.5741E-03	-.7353E-03	-.5870E-01	-.1053E-02
.1900	-.1780E-03	.5803E-03	.1801E-02	-.2133E-02	-.7026E-04
.1950	-.7859E-03	-.9813E-03	-.9199E-03	.5664E-01	-.4290E-03
.2000	.2663E-03	.1651E-03	-.3901E-03	.4454E-03	-.1337E-02

TIME	TOTAL ACOUSTIC ENERGY	TIME DERIVATIVE OF TRAVELING WAVE MAGNITUDE				
		MODE NUMBER				
		1	2	3	4	5
.0050	.4056E+00	-.3730E+01	-.6792E+01	-.4741E+02	.6899E+02	.9527E+02
.0100	.3450E+00	-.2540E+01	-.1468E+02	.4323E+02	-.8068E+02	.8729E+02
.0150	.2887E+00	-.1043E+01	-.4602E+00	-.4025E+02	-.5788E+02	.8128E+02
.0200	.2720E+00	-.4654E+01	.4803E+01	.3966E+02	.8452E+02	.7352E+02
.0250	.2571E+00	-.3010E+01	.1495E+02	-.3965E+02	.5328E+02	.6129E+02

.0300	.2249E+00	-.6575E+00	-.1538E+02	.3478E+02	-.8449E+02	.5060E+02
.0350	.2005E+00	.8384E+00	-.5255E+01	-.3216E+02	-.4796E+02	.4479E+02
.0400	.1870E+00	-.2322E+01	.5793E+01	.3238E+02	.8444E+02	.3925E+02
.0450	.1845E+00	-.1161E+01	.1140E+02	-.3211E+02	.4363E+02	.3123E+02
.0500	.1635E+00	.5891E+00	-.1167E+02	.2885E+02	-.8278E+02	.2485E+02
.0550	.1530E+00	.1093E+01	-.2577E+01	-.2633E+02	-.3912E+02	.2234E+02
.0600	.1420E+00	-.1632E+01	.3242E+01	.2457E+02	.8114E+02	.1978E+02
.0650	.1409E+00	-.4796E+00	.7435E+01	-.2648E+02	.3501E+02	.1516E+02
.0700	.1261E+00	.8323E+00	-.7556E+01	.2353E+02	-.7905E+02	.1175E+02
.0750	.1215E+00	.7732E+00	-.9383E+00	-.2103E+02	-.3126E+02	.1115E+02
.0800	.1132E+00	-.1394E+01	.1279E+01	.2121E+02	.7694E+02	.1008E+02
.0850	.1124E+00	-.2148E+00	.5038E+01	-.2127E+02	.2762E+02	.7248E+01
.0900	.1012E+00	.8553E+00	-.4821E+01	.1866E+02	-.7485E+02	.5420E+01
.0950	.9905E-01	.4905E+00	-.3288E+00	-.1629E+02	-.2445E+02	.5707E+01
.1000	.9254E-01	-.1233E+01	.3233E+00	.1650E+02	.7264E+02	.5225E+01
.1050	.9203E-01	-.7484E-01	.3602E+01	-.1474E+02	.2127E+02	.3300E+01
.1100	.8327E-01	.8421E+00	-.3164E+01	.1450E+02	-.7060E+02	.2317E+01
.1150	.8224E-01	.2956E+00	-.1623E+00	-.1233E+02	-.1853E+02	.2990E+01
.1200	.7686E-01	-.1098E+01	-.5979E-01	.1259E+02	.6840E+02	.2716E+01
.1250	.7664E-01	.1281E-01	.2671E+01	-.1301E+02	.1576E+02	.1278E+01
.1300	.6961E-01	.8148E+00	-.2143E+01	.1113E+02	-.6639E+02	.7788E+00
.1350	.6913E-01	.1568E+00	-.1495E+00	-.9165E+01	-.1336E+02	.1613E+01
.1400	.6457E-01	-.9842E+00	-.1806E+00	.9473E+01	.6422E+02	.1392E+01
.1450	.6455E-01	.7250E-01	.2029E+01	-.1004E+02	.1093E+02	.2407E+00
.1500	.5882E-01	.7778E+00	-.1489E+01	.8478E+01	-.6224E+02	.3454E-01
.1550	.5861E-01	.5335E-01	-.1807E+00	-.6708E+01	-.8822E+01	.9216E+00
.1600	.5468E-01	-.8868E+00	-.1896E+00	.7041E+01	.6012E+02	.6924E+00
.1650	.5478E-01	.1161E+00	.1569E+01	-.7725E+01	.6718E+01	-.2752E+00
.1700	.5006E-01	.7343E+00	-.1059E+01	.6435E+01	-.5817E+02	-.2963E+00
.1750	.4998E-01	-.2536E-01	-.2167E+00	-.4836E+01	-.4864E+01	.5968E+00
.1800	.4658E-01	-.8014E+00	-.1546E+00	.5174E+01	.5611E+02	.3290E+00
.1850	.4672E-01	.1496E+00	.1233E+01	-.5936E+01	.3045E+01	-.5113E+00
.1900	.4281E-01	.6871E+00	-.7709E+00	.4882E+01	-.5419E+02	-.4125E+00
.1950	.4278E-01	-.8576E-01	-.2446E+00	-.3430E+01	-.1425E+01	.4362E+00
.2000	.3983E-01	-.7252E+00	-.1057E+00	.3754E+01	.5219E+02	.1457E+00

NREC PROGRAM NONLIN

TF-30 DUCT BURNER - SEA LEVEL SAMPLE CASE 2

INSTANTANEOUS NORMALIZED PRESSURE DISTRIBUTION

TIME	AXIAL LOCATION 1	2	3	4	5	6	7	8
.005	.9179E-01	-.1653E+00	-.3225E+00	-.2084E+00	.1035E+00	.3790E+00	.4450E+00	.3193E+00
.010	.4092E+00	.9806E-01	-.1777E+00	-.2366E+00	-.1061E+00	.4437E-01	.8845E-01	.4807E-01
.015	-.1456E+00	-.5983E-01	.1151E+00	.3130E+00	.3940E+00	.2640E+00	-.8396E-02	-.2190E+00
.020	.1014E+00	.7520E-01	.8624E-01	.1285E+00	.1239E+00	.8069E-02	-.1716E+00	-.2682E+00
.025	.1119E+00	-.1125E+00	-.2838E+00	-.2506E+00	-.3255E-01	.2125E+00	.3304E+00	.2800E+00
.030	.2132E+00	.6205E-02	-.1827E+00	-.2294E+00	-.1387E+00	-.1368E-01	.5378E-01	.5503E-01
.035	-.1828E+00	-.5172E-01	.1337E+00	.2805E+00	.2888E+00	.1311E+00	-.1004E+00	-.2450E+00
.040	.3142E-01	.4928E-01	.8381E-01	.1091E+00	.7898E-01	-.2482E-01	-.1525E+00	-.2089E+00
.045	.1115E+00	-.7611E-01	-.2404E+00	-.2518E+00	-.9706E-01	.1210E+00	.2675E+00	.2666E+00
.050	.1438E+00	.5222E-02	-.1298E+00	-.1762E+00	-.1236E+00	-.2908E-01	.4108E-01	.6012E-01
.055	-.1904E+00	-.3758E-01	.1480E+00	.2615E+00	.2299E+00	.6476E-01	-.1324E+00	-.2315E+00
.060	-.7937E-02	.3082E-01	.7525E-01	.9185E-01	.5419E-01	-.3184E-01	-.1198E+00	-.1485E+00
.065	.1241E+00	-.3906E-01	-.1958E+00	-.2325E+00	-.1188E+00	.7489E-01	.2290E+00	.2525E+00
.070	.1064E+00	.1158E-01	-.8640E-01	-.1281E+00	-.9781E-01	-.2683E-01	.3623E-01	.5969E-01
.075	-.1854E+00	-.2838E-01	.1497E+00	.2424E+00	.1925E+00	.2981E-01	-.1430E+00	-.2150E+00
.080	-.2426E-01	.1930E-01	.6380E-01	.7608E-01	.4041E-01	-.2834E-01	-.9032E-01	-.1048E+00
.085	.1327E+00	-.1548E-01	-.1659E+00	-.2152E+00	-.1257E+00	.4930E-01	.2013E+00	.2356E+00
.090	.7919E-01	.1256E-01	-.5918E-01	-.9351E-01	-.7481E-01	-.2110E-01	.3148E-01	.5330E-01
.095	-.1753E+00	-.2261E-01	.1450E+00	.2243E+00	.1671E+00	.1046E-01	-.1455E+00	-.2021E+00
.100	-.2849E-01	.1189E-01	.5145E-01	.6113E-01	.3112E-01	-.2220E-01	-.6655E-01	-.7413E-01
.105	.1359E+00	-.2257E-02	-.1467E+00	-.2013E+00	-.1264E+00	.3410E-01	.1801E+00	.2184E+00
.110	.5791E-01	.1069E-01	-.4149E-01	-.6810E-01	-.5581E-01	-.1561E-01	.2583E-01	.4379E-01
.115	-.1637E+00	-.1875E-01	.1377E+00	.2078E+00	.1487E+00	-.3669E-03	-.1438E+00	-.1913E+00
.120	-.2666E-01	.7118E-02	.3956E-01	.4713E-01	.2368E-01	-.1613E-01	-.4745E-01	-.5145E-01
.125	.1351E+00	.4992E-02	-.1332E+00	-.1891E+00	-.1237E+00	.2477E-01	.1630E+00	.2020E+00
.130	.4105E-01	.8144E-02	-.2880E-01	-.4832E-01	-.4017E-01	-.1118E-01	.1956E-01	.3310E-01
.135	-.1521E+00	-.1606E-01	.1295E+00	.1926E+00	.1345E+00	-.6305E-02	-.1394E+00	-.1808E+00
.140	-.2190E-01	.4092E-02	.2870E-01	.3423E-01	.1705E-01	-.1099E-01	-.3195E-01	-.3379E-01
.145	.1317E+00	.8875E-02	-.1226E+00	-.1778E+00	-.1190E+00	.1890E-01	.1488E+00	.1868E+00
.150	.2749E-01	.5759E-02	-.1891E-01	-.3231E-01	-.2726E-01	-.7904E-02	.1305E-01	.2258E-01
.155	-.1410E+00	-.1415E-01	.1211E+00	.1786E+00	.1229E+00	-.9384E-02	-.1333E+00	-.1705E+00
.160	-.1588E-01	.2254E-02	.1907E-01	.2250E-01	.1092E-01	-.6918E-02	-.1928E-01	-.1956E-01
.165	.1266E+00	.1081E-01	-.1135E+00	-.1667E+00	-.1130E+00	.1510E-01	.1365E+00	.1727E+00
.170	.1644E-01	.3759E-02	-.1082E-01	-.1905E-01	-.1660E-01	-.5632E-02	.6623E-02	.1254E-01
.175	-.1306E+00	-.1273E-01	.1126E+00	.1655E+00	.1129E+00	-.1077E-01	-.1261E+00	-.1600E+00
.180	-.9494E-02	.1226E-02	.1068E-01	.1201E-01	.5211E-02	-.3834E-02	-.8890E-02	-.7869E-02
.185	.1203E+00	.1158E-01	-.1054E+00	-.1558E+00	-.1064E+00	.1257E-01	.1254E+00	.1595E+00
.190	.7325E-02	.2160E-02	-.4003E-02	-.7938E-02	-.7804E-02	-.4154E-02	.5007E-03	.3754E-02
.195	-.1208E+00	-.1163E-01	.1045E+00	.1532E+00	.1040E+00	-.1117E-01	-.1184E+00	-.1496E+00
.200	-.3252E-02	.7412E-03	.3483E-02	.2735E-02	-.4417E-04	-.1560E-02	-.3402E-03	.1848E-02

TIME	AXIAL LOCATION 9	10	11	12	13	14	15	16
.005	.1414E+00	.4315E-01	.3402E-01	.3154E-01	.3338E-01	.3705E-01	.4045E-01	.4234E-01
.010	.2623E-01	.5258E-01	.6387E-01	.7776E-01	.9142E-01	.1020E+00	.1074E+00	.1063E+00
.015	-.2031E+00	-.6173E-01	-.2425E-01	.1502E-01	.5037E-01	.7666E-01	.9011E-01	.9885E-01
.020	-.1684E+00	.6486E-02	.4634E-01	.8548E-01	.1191E+00	.1430E+00	.1541E+00	.1508E+00
.025	.1270E+00	.5093E-02	-.1326E-01	-.2661E-01	-.3518E-01	-.3954E-01	-.4028E-01	-.3785E-01
.030	.4006E-01	.4070E-01	.4378E-01	.4833E-01	.5314E-01	.5695E-01	.5875E-01	.5796E-01
.035	-.1977E+00	-.6589E-01	-.3423E-01	-.2456E-02	.2533E-01	.4553E-01	.5557E-01	.5418E-01
.040	-.1330E+00	-.1401E-01	.1207E-01	.3720E-01	.5850E-01	.7349E-01	.8036E-01	.7825E-01
.045	.1342E+00	.1389E-02	-.2227E-01	-.4218E-01	-.5722E-01	-.6668E-01	-.7018E-01	-.6764E-01
.050	.4358E-01	.2524E-01	.2263E-01	.2091E-01	.1992E-01	.1941E-01	.1915E-01	.1895E-01
.055	-.1672E+00	-.4581E-01	-.1872E-01	.7459E-02	.2973E-01	.4554E-01	.5308E-01	.5152E-01
.060	-.8833E-01	-.5948E-02	.1128E-01	.2743E-01	.4083E-01	.5007E-01	.5416E-01	.5243E-01
.065	.1353E+00	.1948E-02	-.2355E-01	-.4606E-01	-.6384E-01	-.7553E-01	-.8027E-01	-.7774E-01
.070	.4277E-01	.1723E-01	.1229E-01	.7927E-02	.4468E-02	.2120E-02	.9957E-03	.1119E-02
.075	-.1421E+00	-.2788E-01	-.3583E-02	.1929E-01	.3834E-01	.5160E-01	.5767E-01	.5596E-01
.080	-.5819E-01	-.2122E-03	.1144E-01	.2210E-01	.3076E-01	.3661E-01	.3909E-01	.3797E-01
.085	.1303E+00	.2282E-02	-.2299E-01	-.4576E-01	-.6404E-01	-.7627E-01	-.8139E-01	-.7895E-01
.090	.3768E-01	.1211E-01	.6827E-02	.1951E-02	-.2053E-02	-.4827E-02	-.6138E-02	-.5896E-02
.095	-.1259E+00	-.1709E-01	.5458E-02	.2635E-01	.4352E-01	.5531E-01	.6056E-01	.5877E-01
.100	-.3915E-01	.1762E-02	.9745E-02	.1689E-01	.2260E-01	.2639E-01	.2795E-01	.2713E-01
.105	.1229E+00	.2432E-02	-.2172E-01	-.4368E-01	-.6144E-01	-.7341E-01	-.7848E-01	-.7619E-01
.110	.3060E-01	.8480E-02	.3797E-02	-.5860E-03	-.4224E-02	-.6759E-02	-.7949E-02	-.7692E-02
.115	-.1148E+00	-.1092E-01	.1032E-01	.2982E-01	.4575E-01	.5659E-01	.6133E-01	.5953E-01
.120	-.2618E-01	.2080E-02	.7464E-02	.1220E-01	.1593E-01	.1837E-01	.1934E-01	.1876E-01
.125	.1148E+00	.2505E-02	-.2019E-01	-.4091E-01	-.5774E-01	-.6911E-01	-.7396E-01	-.7183E-01
.130	.2305E-01	.5843E-02	.2161E-02	-.1306E-02	-.4198E-02	-.6217E-02	-.7164E-02	-.6947E-02
.135	-.1063E+00	-.7284E-02	.1280E-01	.3116E-01	.4610E-01	.5622E-01	.6060E-01	.5883E-01
.140	-.1659E-01	.1863E-02	.5291E-02	.8253E-02	.1054E-01	.1202E-01	.1258E-01	.1220E-01
.145	.1067E+00	.2494E-02	-.1865E-01	-.3800E-01	-.5373E-01	-.6438E-01	-.6894E-01	-.6697E-01
.150	.1576E-01	.3921E-02	.1368E-02	-.1049E-02	-.3071E-02	-.4487E-02	-.5153E-02	-.5001E-02
.155	-.9888E-01	-.5059E-02	.1391E-01	.3122E-01	.4527E-01	.5477E-01	.5885E-01	.5714E-01
.160	-.9041E-02	.1534E-02	.3419E-02	.4996E-02	.6180E-02	.6915E-02	.7174E-02	.6956E-02
.165	.9894E-01	.2407E-02	-.1721E-01	-.3516E-01	-.4978E-01	-.5967E-01	-.6392E-01	-.6210E-01
.170	.9070E-02	.2527E-02	.1092E-02	-.2780E-03	-.1432E-02	-.2247E-02	-.2636E-02	-.2560E-02
.175	-.9209E-01	-.3656E-02	.1420E-01	.3047E-01	.4366E-01	.5258E-01	.5639E-01	.5476E-01
.180	-.2883E-02	.1233E-02	.1863E-02	.2321E-02	.2613E-02	.2758E-02	.2778E-02	.2687E-02
.185	.9150E-01	.2265E-02	-.1587E-01	-.3248E-01	-.4600E-01	-.5515E-01	-.5908E-01	-.5740E-01
.190	.3122E-02	.1524E-02	.1132E-02	.7370E-03	.3905E-03	.1350E-03	.1422E-06	-.2448E-06
.195	-.8564E-01	-.2747E-02	.1398E-01	.2921E-01	.4157E-01	.4990E-01	.5347E-01	.5193E-01
.200	.2247E-02	.1001E-02	.5905E-03	.1220E-03	-.3217E-03	-.6625E-03	-.8408E-03	-.9252E-03

* CALCULATIONS COMPLETED *

ANALYSIS OF RESULTS

PRELIMINARY CONSIDERATIONS

General

With the introduction of the present nonlinear theory for unsteady in augmentors, completely computer programmed results for many problem cases can be readily generated. However, the understanding and interpretation of these results require some guidance from previous experiences. These may spring from previous work in nonlinear theories, from experimental results or from previous work in linear theory. In addition to relating these experiences to the results, it is also helpful to establish some simple physical models that will help in understanding the complex results.

It is the purpose of these initial discussions to provide this guidance, the following examples are then easily understood and a discussion of the results can be more fruitful.

Comparison with Linear Theory

In the linear theory the problem is attacked with the objective of finding those conditions where small disturbances will grow. No statement is made regarding the development of these disturbances when they grow, since the theory does not include the terms that describe the finite disturbances. As mentioned previously, such a program was developed by NREC and is called Program REFINE (see Refs 1 and 2).

The linear theory does not allow for interactions between modes and does not calculate the final state of the unstable flow (or limit cycle in mathematical terms). Thus Program REFINE only calculates which mode is unstable. The frequency and mode shape are those calculated with simple acoustic theory.

The present nonlinear program, NØNLIN, considers all modes together and calculates the influence of the amplitude of one mode on the entire system. Thus, given an initial state, NØNLIN will calculate what the final states of the various modes are. When one mode is unstable, the amplitude of that mode will grow to a certain limit and the entire system operates under this oscillatory

behavior. In a linear theory the amplitude would grow to infinity, but now the limit is attained through the stabilizing influence of the stable modes and the effects of the large disturbances. The system then reaches a limit cycle. The frequency of that unstable mode will change (drop) considerably. However, one does not speak of one mode anymore, but rather of the system itself. In fact the system operates in an oscillatory motion at a frequency and amplitude derived from NØNLIN. The frequency has no relationship with the acoustic frequency, but is dependent on all the system variables.

Similarities with Spring-Mass Combinations

From the point of view of elementary vibration theory, NØNLIN can be thought of as modelling the augmentor as a system of a number of spring-mass combinations-- one for each of the principal longitudinal modes of the augmentor duct. Associated with each of these spring-mass combinations is a negative or positive damper corresponding to combustion and throughflow effects. When the damper is negative, the mode is linearly unstable and, alone, its amplitude will become infinite in response to an initial disturbance. On the other hand, when the damper is positive, the mode is linearly stable and its amplitude will decay to zero. However, the spring-mass combinations are coupled to one another via combustion, throughflow and second order effects. (The second order effects are more pronounced at higher amplitudes and the NØNLIN program includes these effects.) As a result, a more complex behavior of the entire system is observed.

The concept of the spring-mass system is illustrated in the sketch below. Combinations 1 and 2 have their own frequency, but when coupled, the entire system will vibrate at a frequency somewhere between the two. Say the amplitudes of 1 and 2 when operating separately are zero and infinity, respectively. When coupled, the energy of the unstable combination 2 can be transferred to the stable combination 1 and the final motion will be of finite amplitude.

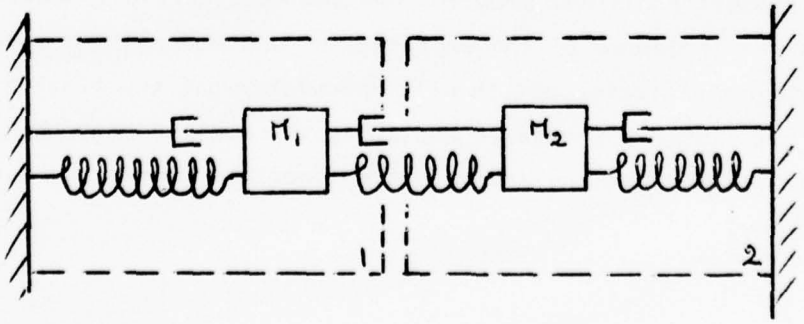

Simple Mode Averaging

In analytical terms, each mode can be represented by the perturbation $\eta = e^{(a+bi)t}$ where $a > 0$ indicates instability and $a < 0$ stability. The frequency is given by b. In most cases where rumble is involved, there are stable and unstable modes. In a crude sense one may assume that the system reaches the limit cycle such that the average value of a is zero, i.e., the system response does not change in time, but oscillates in an unvarying pattern. Thus for a five mode example, $a_1 < 0, a_2 < 0, a_3 < 0, a_5 < 0$ and $a_4 > 0$, then the negative values of a_1, a_2, a_3 and a_5 equal the positive value of such that the average value of $\bar{a}$ is zero. Similarly the frequency values of b_1 through b_5 are averaged such that $\bar{b}$ is somewhere between b_1 and b_5.

Stable and Unstable Modes

A good example of this system behavior is the case of the duct burner running at altitude. As shown later in the examples, the total energy of the unsteady motion has reached a constant value. The amplitude of the individual modes is shown in Figure 2 where those for modes 1, 2, 3 and 5 decrease to a small but constant value and the linearly unstable mode 4 reaches a high, but eventually a constant amplitude. The fact that the unstable mode amplitudes reach finite values and the stable mode amplitudes reach non-zero values is commonly referred to as the principle of the exchange of stabilities (Ref 6). The frequency of the final pressure wave is somewhere between that of the second and third mode and the pressure wave pattern is fairly complicated.

Other Nonlinear Effects

The behavior of the fourth mode amplitudes as presented in Figure 1 shows that it only gradually reaches a limiting value. However, it appears that if nonlinear combustion terms were used, the limiting amplitude would have been reached much sooner since nonlinear combustion terms exercise a stabilizing influence on a system when the amplitudes grow. Nonlinear combustion has been discussed in Reference 2, and it is shown that the value of τ' (see Equation A31) decreases by as much as a factor of five when the amplitude of the perturbations increase. In other words, when more turbulence is produced,

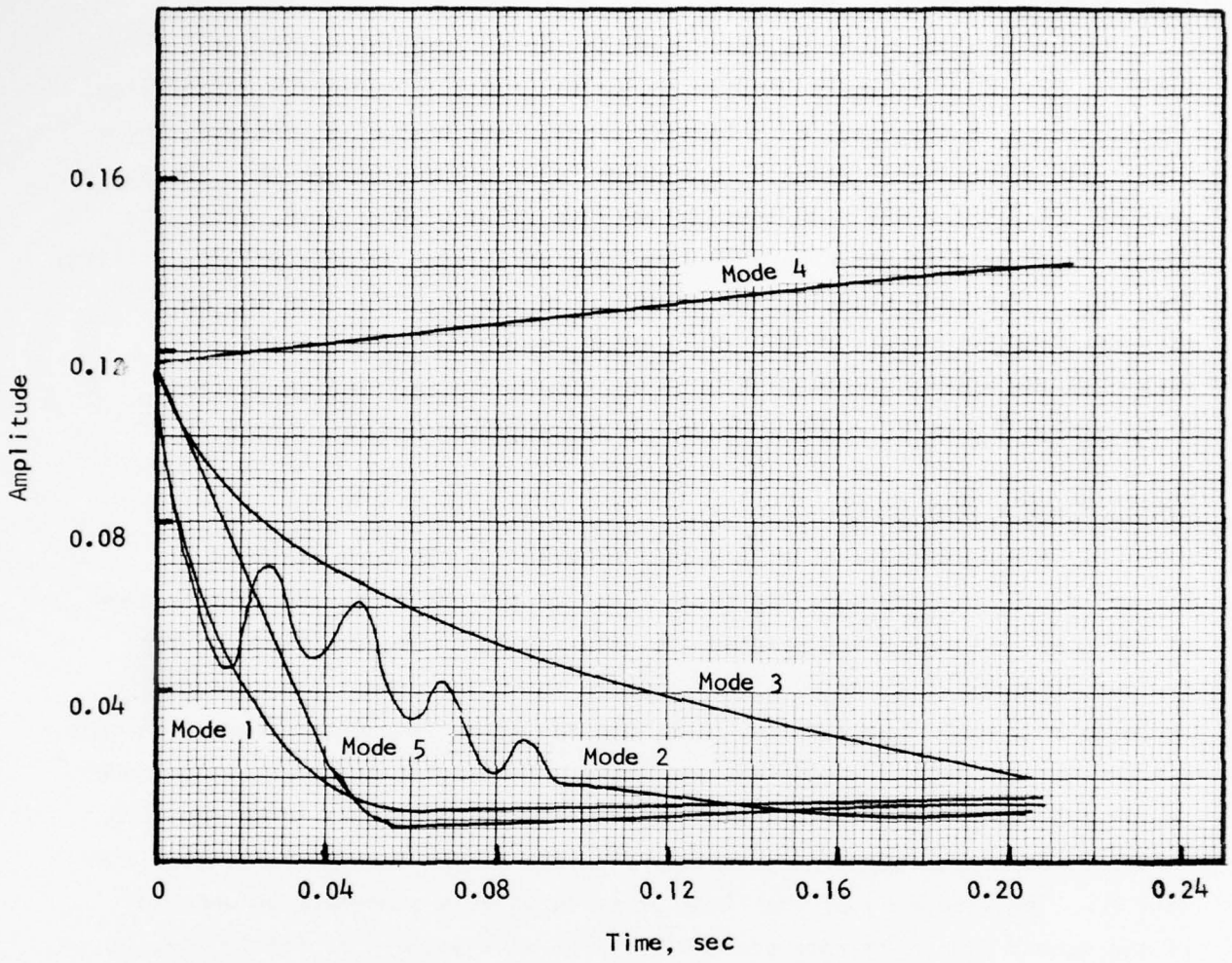

Figure 2. Amplitude Behavior Versus Time for First Five Modes of Duct Burner Case at Altitude

combustion takes place faster and the parametric studies on altitude versus sea level operations show that faster combustion enhances stability. It is clear then that if nonlinear combustion behavior (i.e., $\tilde{\tau}$ dependent on amplitude) were introduced, other limiting amplitudes would have been obtained. Nevertheless, the nature of the solutions would not be different.

Another effect that is not included in the present study concerns nozzle damping. This effect, which exercises a stabilizing influence, can be simulated through a change in the velocity distribution and is discussed in a later section.

Comparison with Other Nonlinear Theories

The results shown above are similar to those obtained by Culick (Ref 3) and the discussion given in Chapter 12 of Reference 3 is very much applicable to the present cases. As shown in Reference 3, the final level of the amplitudes is very much dependent on the initial amplitude of all the modes under consideration, since there is so much interaction of the energies contained in each mode. For example, high initial energy (i.e., amplitude) of the stable modes and low initial energy of the unstable modes will lead to a relatively low amplitude system oscillation. The reverse is also true. In fact, when all initial amplitudes are low, the systems under investigation showed a higher degree of unstableness than the case where all initial amplitudes were high. The reason can be found in the fact that the unstable mode amplitude grows fairly rapidly, but there is not enough energy absorption capability in the stable modes to pull the unstable mode amplitude down.

SENSITIVITY ANALYSIS OF THE TF-30 AT SEA LEVEL

As part of this project, the NØNLIN program was run for a limited number of cases. The results are given in this section for the TF-30 at sea level, and in the following section for the TF-30 at altitude.

The sensitivity analysis of the TF-30 duct burner at sea level was accomplished in two stages. During the first stage, the physical input data followed known values more closely. However, when it was determined

that nozzle damping had an important effect on this case, a second stage of the sensitivity analysis was conducted. In that second stage, certain physical input items were modified from their known values to compensate for the missing damping term as explained below.

First Stage of the Sensitivity Analysis

The baseline case for the first stage of the sensitivity analysis is similar to the sample case included in the previous section, but with the following exceptions:

1) Initial disturbance

$$\left.\begin{matrix}\alpha_k \\ \beta_k\end{matrix}\right\} = 0.2,\ 0.1,\ 10^{-6},\ 10^{-6},\ 10^{-6} \text{ for } = 1,5$$

2) Upstream velocity profile

$$a_1 = -29.4 \text{ sec}^{-1},\ b_1 = 550 \text{ fps}$$

3) Combustion coefficient $\hat{C}_1 = -2.87$

The decelerating flow profile in the upstream chamber is known to be a destabilizing influence, and the time-dependent output for this case was found to be unstable. Examination of the total acoustic energy reveals that a minimum value is calculated at $t = 0.045$ sec, after which the energy increases until the run is aborted at $t = 0.1675$ sec. At that time, the total acoustic energy is two orders of magnitude higher than the initial value. An explanation of this variation is found in the amplitudes of the individual modes. Modes 1 and 2 tend towards stability and initially decrease in amplitude, while the higher three modes tend to be unstable and increase in amplitude. At $t = 0.045$ sec, the amplitude of mode 3 exceeds mode 1 for the first time, becoming the dominant mode. By the time the run is aborted, all of the modes are increasing in amplitude.

The sensitivity of the results to the number of acoustic modes considered in the baseline case was investigated by successively reducing the baseline value of NM = 5. Values of NM = 4 and NM = 3 yielded almost identical behavior of the total acoustic energy with time; in each case a minimum was again reached at $t = 0.045$ sec, while the run was aborted at $t = 0.1675$ sec for NM = 4 but at $t = 0.1875$ sec for NM = 3. A drastic change in behavior, as expected, was encountered for NM = 2. The system became stable and at

t = 0.200 sec the total acoustic energy is ten orders of magnitude lower than the initial value.

The sensitivity of the results to the time-averaging interval was also investigated by varying the baseline value of ITAU = 0. Very similar results were obtained using ITAU = 2, but the instability increased considerably when the time-averaging interval was made mode dependent (ITAU = 1).

The sensitivity of the results to the initial disturbance was investigated by varying the baseline values of α_k and β_k at t_o . Halving the values resulted in a considerable reduction in the total acoustic energy at any point in time. However, a minimum was still reached at t = 0.045 sec, with a steady increase thereafter to values several orders of magnitude higher than the initial value. A more drastic reduction of the values of α_k and β_k at t_o also failed to change the behavior of the total acoustic energy with time.

Finally, the sensitivity of the results to the time step was investigated by varying the baseline value of TSTEP = 0.0025 sec. Both, a larger value of 0.005 sec and a smaller value of 0.001 sec were used, with the results indicating that 0.0025 sec was the largest time step which could be used without compromising the accuracy of the solution.

Effects of Nozzle Damping

The over-all tendency of the sea level case to be unstable because of modes 3, 4, and 5, indicated that a damping term was missing which was relatively more important for the higher modes. Such a term which was not included in Program NONLIN but was available in the earlier linear model of Program REFINE (Refs 1 and 2), is nozzle damping. To determine the importance of this term in the present context, the TF30 duct burner at sea level was analyzed using Program REFINE. The results, which should be sufficiently accurate to determine qualitative effect, are tabulated on the following page in terms of log decrement.

Component Effect	Log Decrement*				
	Mode 1	Mode 2	Mode 3	Mode 4	Mode 5
Throughflow	9.4840	3.1396	-.0578	-.4653	-.2296
Combustion Time	.1652	.0166	-.1396	-.0757	-.1029
Combustion Velocity	.3732	-.1132	.5556	.1978	.1188
Density	.0038	-.4773	-.2997	-.0906	-.0976
Nozzle Damping	-4.3081	**	.2812	.2349	.1240

It can be seen that the effect of nozzle damping is considerable in all modes where it was calculated. However, it is of particular importance in the higher modes where the throughflow effect is not quite so dominant. In fact, it is considered to have sufficient potential for stabilizing the higher modes, that the overall system at sea level will become stable.

Second Stage of the Sensitivity Analysis

In the second stage of the analysis, the upstream thoughflow velocity distribution was modified in the input data to simulate the effect of the missing damping term.

The sensitivity of results to the upstream velocity distribution was investigated initially. The remainder of the input data coincides with that of the TF-30 sample case from the previous section. Figure 3 illustrates the effect on total acoustic energy as the upstream inlet velocity is varied from 550 fps (the value used in the first stage of the sensitivity analysis) to 300 fps (the upstream velocity at the flameholder). It can be seen that, for an upstream deceleration from 550 to 300 fps, curve 1, the system is very unstable with the calculation aborted at t = 0.040 sec. On the other hand, for a constant upstream velocity of 300 fps, curve 5, the system is stable with an overall decrease in total acoustic energy of nearly two orders of magnitude. In between these extremes, other interesting variations are seen to occur. In curve 2, where the upstream deceleration is from 400 to 300 fps, the total acoustic energy is seen to beat at a frequency in the neighborhood

*Please note, a positive decrement indicates a stabilizing effect of the component.

**Not Available.

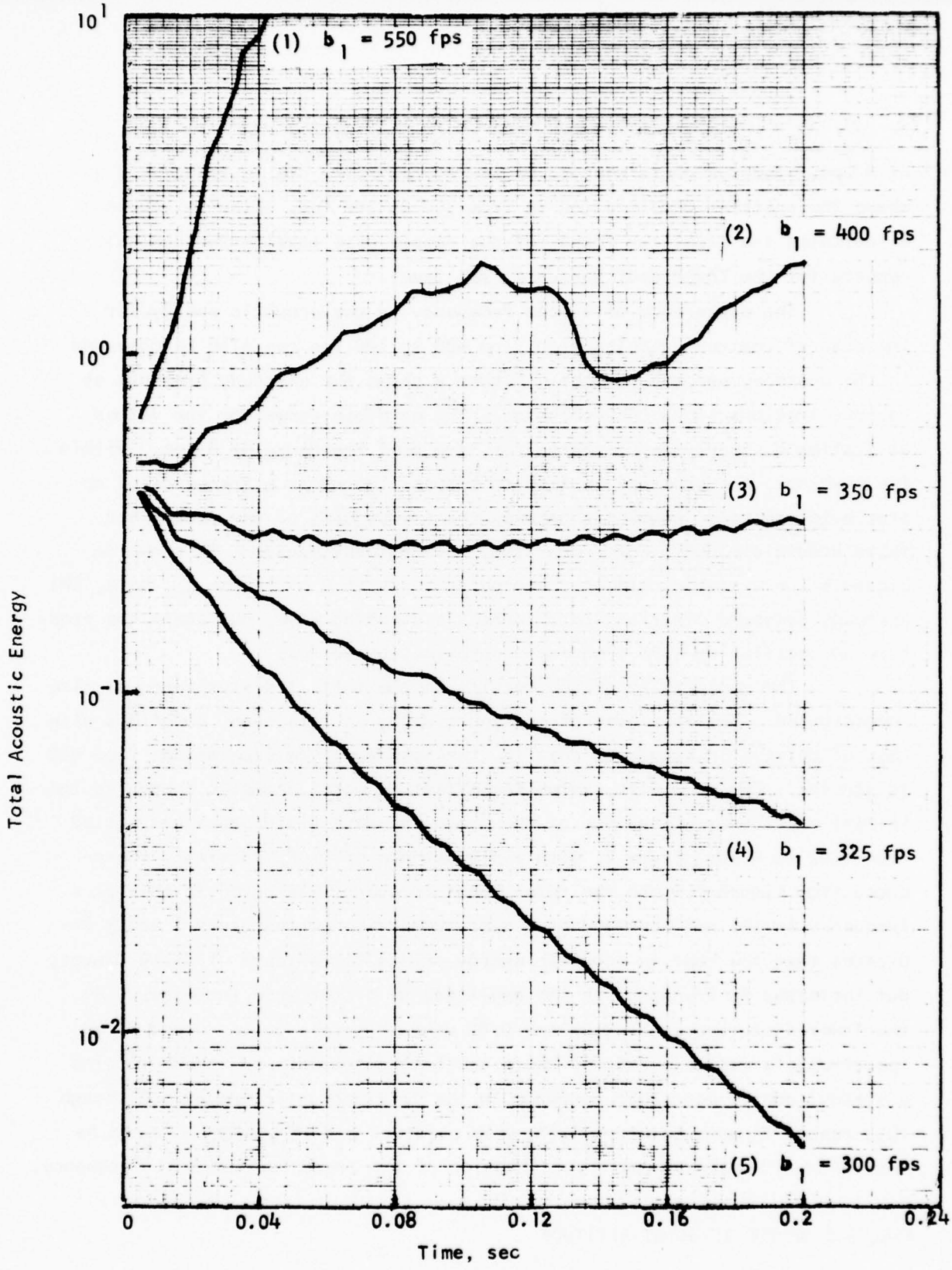

Figure 3. Effect of Upstream Inlet Velocity on the Variation of Total Acoustic Energy with Time

of 8 cps. The system is seen to be nearly neutrally stable in curve 3 where the upstream deceleration is from 350 to 300 fps. Finally, curve 4 indicates the stability found for the sample case itself--the nominal results for the TF-30 duct burner at sea level.

The appearance of a beat frequency in the acoustic energy for the case of upstream deceleration from 400 to 300 fps can also be observed in the unsteady pressure output. Figure 4 shows the unsteady pressure at various stations along the combustor. The envelope drawn for the values at Station 8 clearly demonstrates the same beat frequency of 8 cps. Within the envelope, the pressure is seen to be oscillating at a frequency of approximately 52 cps, somewhere between the frequencies of the second and third acoustic modes. For comparison, the unsteady pressure is shown in Figure 5 for a stable case, corresponding to curve 4 of Figure 3. Here, the unsteady pressure distribution resembles a standing wave, but again the pressure is oscillating at a frequency approximating 52 cps.

The sensitivity of the results to the initial disturbance was also investigated. The remainder of the input data, in this case, coincides with that of curve 2 in Figure 3; that is, the upstream flow decelerates from 400 to 300 fps. Figure 6 illustrates the effect on total acoustic energy as the initial amplitudes α_k and β_k of the traveling wave disturbance are varied from 0.02 to 0.10. Curve 2, with a disturbance of 0.08, is simply reproduced from Figure 3 where the total acoustic energy was noted to beat at a frequency in the neighborhood of 8 cps. Comparison with curves 1 and 3 indicates that the beat in acoustic energy exists for a range of disturbances, but increases in frequency as the amplitude of disturbance increases. At the lower disturbances of 0.04 and 0.02 used to obtain curves 4 and 5, respectively, a limit is reached where the beat disappears and there remains a steady, nearly monotonic increase in the total acoustic energy. Although this result is somewhat surprising when observed out of context, it can be seen to be a straightforward continuation of the trend for the beat frequency.

ANALYSIS OF THE TF-30 AT ALTITUDE

The departure of altitude results from the second-stage TF-30 sea level results was also investigated as part of the program. Three changes in input data were made to represent altitude conditions, as listed on the the following page.

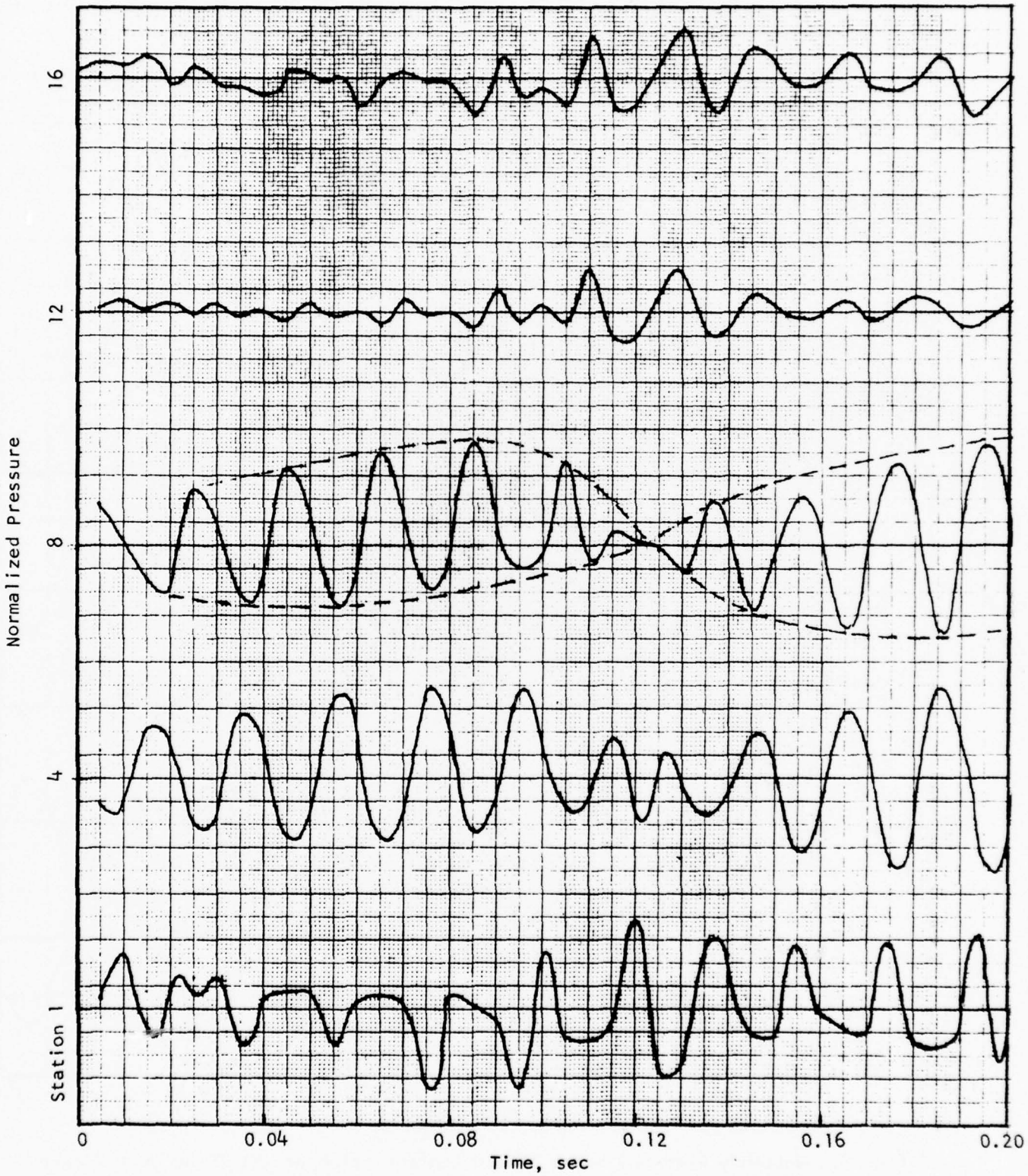

Figure 4. Unsteady Pressure for a Beating Configuration of the TF-30 Duct Burner

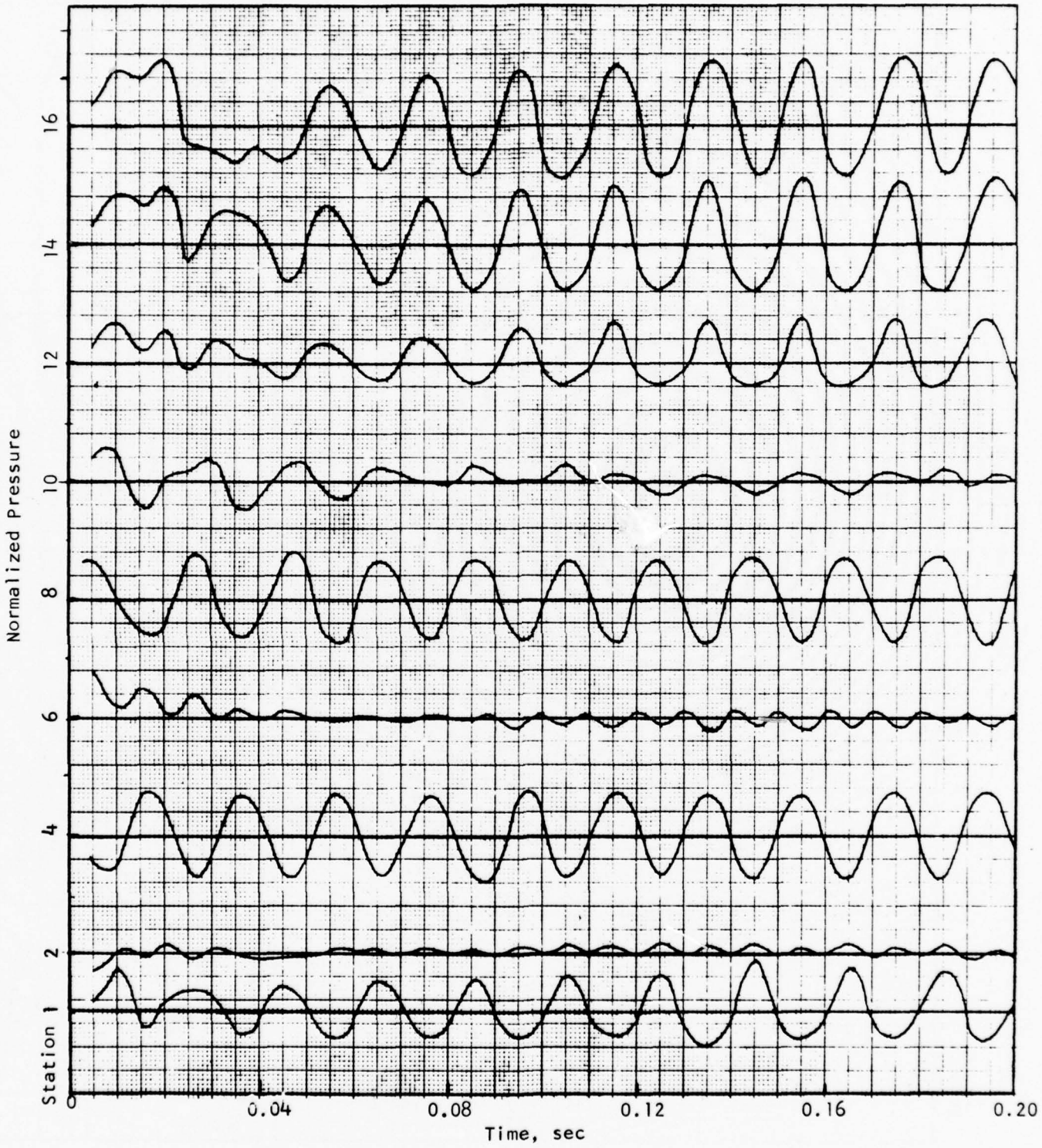

Figure 5. Unsteady Pressure for a Stable Configuration of the TF-30 Duct Burner

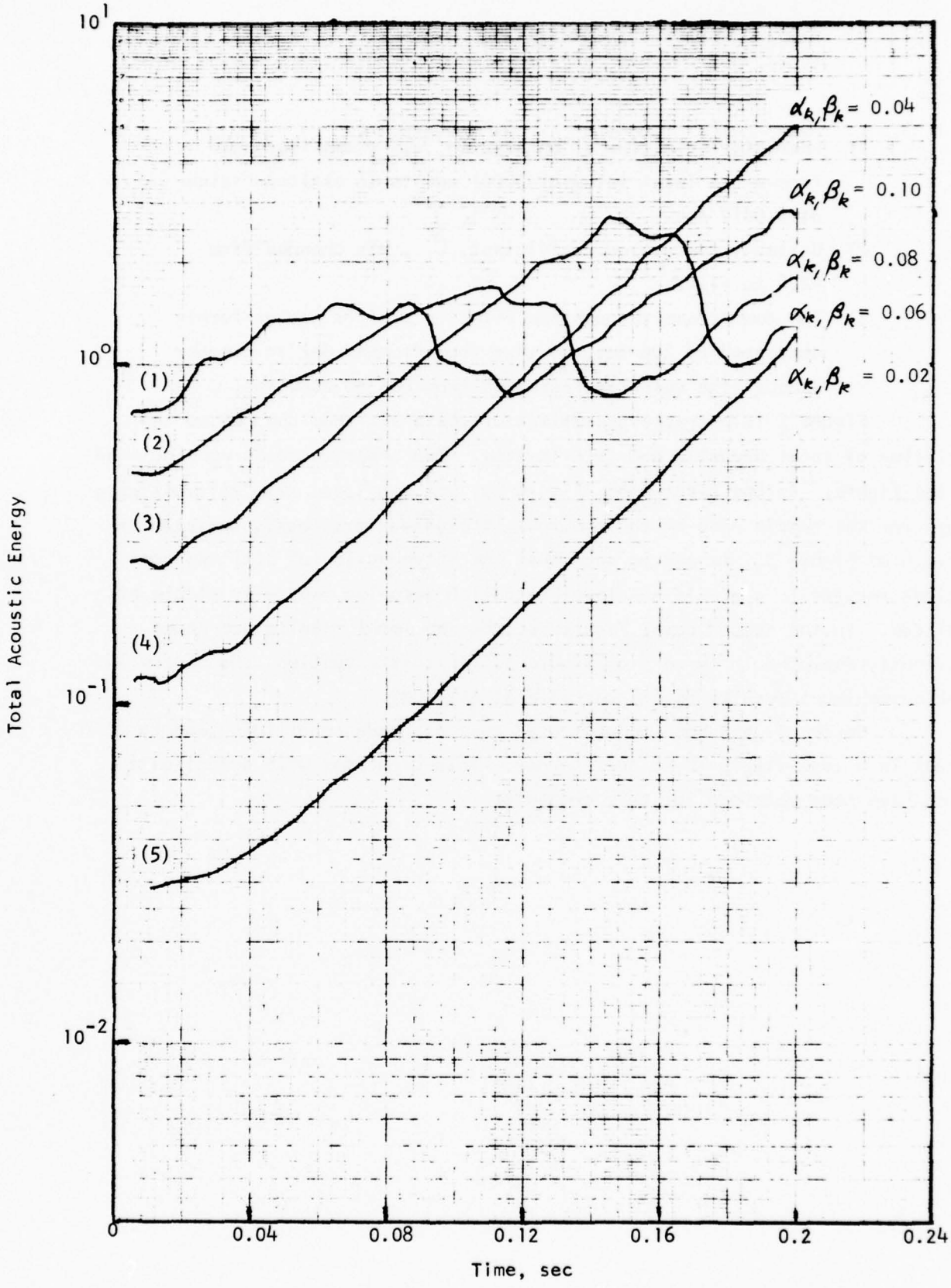

Figure 6. Effect of Initial Disturbance on the Variation of Total Acoustic Energy with Time

1) Characteristic time of combustion, $\bar{\tau}_c$, was increased from a sea level value of 0.001 sec to an altitude value of 0.0017 sec.
2) Unsteady combustion coefficient, $\hat{C}_1$, was changed from -2.4 to -1.42.
3) The downstream throughflow velocity profile was uniformly decreased by 200 fps, so that from flameholder to chamber exhaust the velocity increased from 665 to 2000 fps.

Figure 7 illustrates the effect of these altitude changes on the variation of total acoustic energy with time. Two separate cases are included in the figure. In the first case, Figure 7a, the sea level results are simply those for the sample case of the previous section--as previously depicted in curve 4 of Figure 3. It can be seen that the introduction of altitude conditions results in a stable sea level situation becoming neutrally stable at altitude. In the second case, Figure 7b, the sea level results are those previously depicted in curve 3 of Figure 3. In this situation, the neutrally stable sea level results become unstable at altitude.

Hence, it has been demonstrated that altitude conditions tend to result in a less-stable TF-30 duct burner. This coincides with actual data which have been obtained for this combustor.

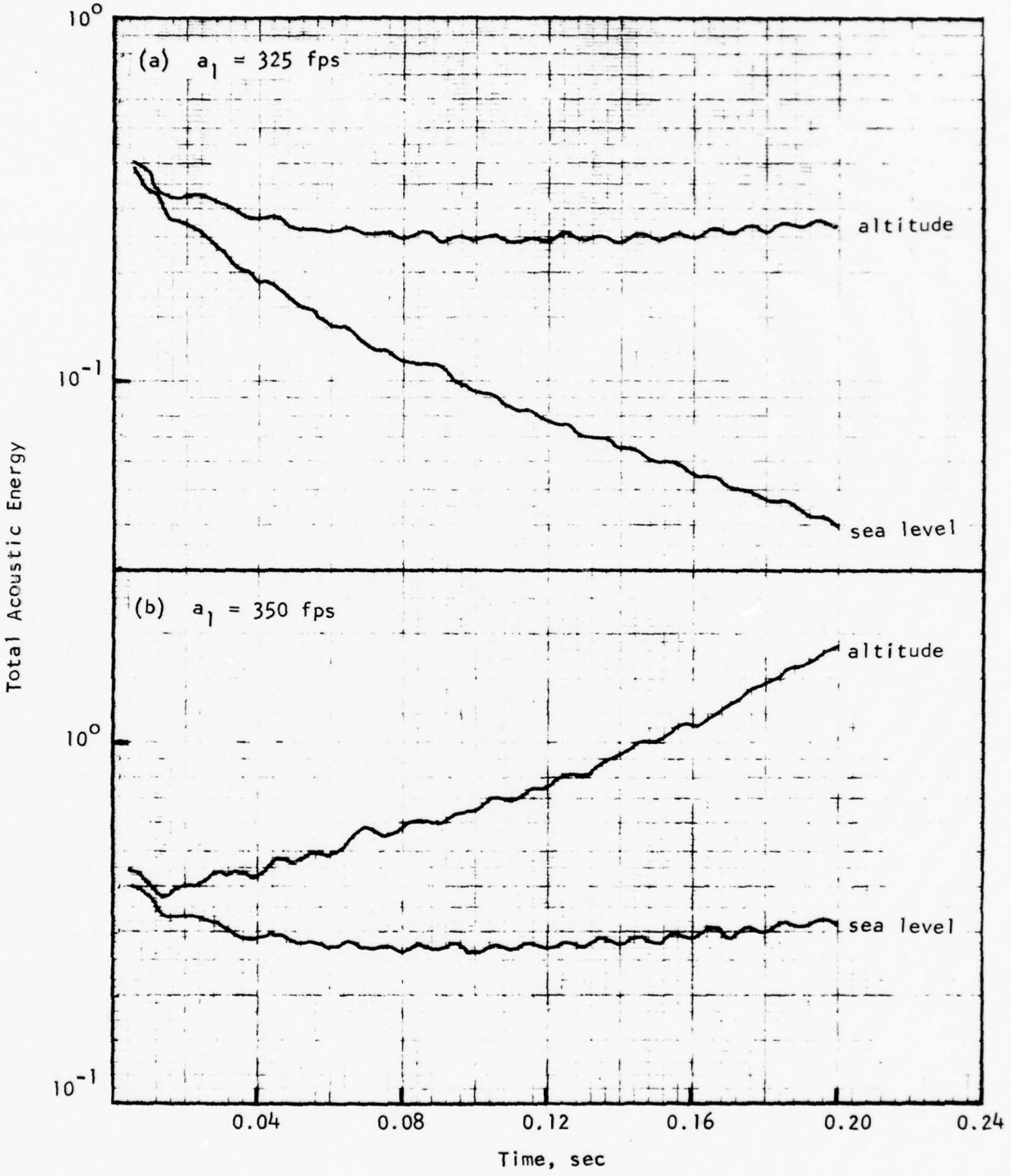

Figure 7. Effect of Altitude on the Variation of Total Acoustic Energy with Time

SUMMARY OF RESULTS

The analytical part of this augmentor instability study concerns the application of a nonlinear analysis to describe the phenomenon of rumble.

Previously, NREC had developed a linear theory which predicted classical combustion instabilities. The present nonlinear theory allows for the inclusion of rumble-related phenomena that the linear theory could not handle. The nonlinear theory follows the approach taken by Culick in an earlier nonlinear acoustic stability analysis. However, the theory stands by itself and uses a combustion model derived in the previous linear stability work. A computer program, NØNLIN, has been developed for the solution of the final equations on a high-speed digital computer.

Analysis of the TF-30 augmentor using Program NØNLIN was brought to a point where the following results are evident:

1) Under certain conditions a system instability is predicted which, after an initial period of adjustment, reaches a state where pressure and flow oscillations are present at a unique frequency and amplitude. Both amplitude and frequency are similar to those observed during rumble in augmentors.
2) The system instability takes place when there is one or more unstable modes that transfer their energies down to the stable modes. The amplitudes of all (both stable and unstable) modes reach limiting values with those of the unstable modes reaching higher values than those of the stable modes. The present nonlinear program allows for this exchange of stabilities.
3) The frequency of the system instability bears no relationship to that of the individual mode, but is in general lower than that of the unstable mode.

4) Current results for the amplitude of the flow oscillations may be slightly off since the effect of amplitude on combustion characteristics has not been incorporated in the current program.

5) Current results for establishing the conditions for stable or rumble operation may be slightly in error since nozzle damping effects were not included. However, the effect of nozzle damping is shown from analyses with the REFINE program to be somewhat equivalent to a reduced velocity drop, upstream of the flameholders. Thus nozzle damping can be simulated by reducing the flow deceleration at the inlet section from that established by geometric considerations.

6) The flow decelerations upstream of the flameholders have a significant effect on augmentor stability. Large velocity decreases make the augmentor unstable.

7) The initial conditions of the perturbations affect the final state of stability in the augmentor. If the initial "kick-off" perturbation is from vortices shed by a flameholder or fuel injectors, then the frequency of this perturbation is potentially significant in starting rumble. Alternatively, if the initial perturbation is a square wave pulse, then the characteristics of the pulse in terms of duration and amplitude may be significant in setting off rumble.

8) The burning rate has an influence on the development of unstable conditions. Long burning times cause more instability than short burning rates. As a consequence, it can be surmised that evaporation rates, fuel-to-air ratios, local temperatures, flameholder shape and level of throughflow velocity have a potential influence on the occurrence of rumble.

9) The pressure waves during rumble show a different pattern when the cause of instability is different. When the main cause of instability is the velocity drop upstream of the

flameholders (see Point 6), then the pressure waves exhibit a definite beat pattern of about 8 cps superposed on the rumble oscillations. However, when the instability is caused by the increased time for combustion (see Point 8), the pressure wave does not show the beat phenomenon.

10) The theory was applied to a duct burner case for which rumble was observed experimentally at altitude operation. The results show that the duct burner is stable at sea level operation. For altitude operation the combustion characteristics change and when these changes were incorporated in the analysis, the results showed rumble to occur and pressure and flow oscillations to exist with a certain amplitude and frequency.

From the results of this study it is recommended that the following tasks be conducted in the future:

1) The theory should be further refined to include other effects, such as nozzle damping and amplitude-dependent combustion terms. From previous experience these terms will have a secondary effect on the results, and mainly affect the final rumble amplitude.
2) The theory should be applied to additional augmentor cases for which experimental data on rumble is available. Two cases covering an afterburner (Ref 7), and a research combustor (Ref 8), are suggested for this purpose. The calculated results should be correlated with the experimental data.
3) The theory should be used to establish the effects of other variables not included in the current parametric study. These comprise, among others, flight Mach number, fuel, flameholder geometry, flow velocity, temperature level, fuel-to-air ratios, and augmentor geometry.
4) After more confidence is gained with the theory through Tasks 1, 2, and 3, flight regimes and augmentor geometries that exhibit rumble should be identified, and courses of action should be examined that show promise of expanding the stable operating regime of augmentors.

APPENDIX A

DERIVATION OF EQUATIONS

1. EQUATIONS OF MOTION

The conservation laws for momentum and energy in a one-dimensional inviscid fluid flow can be written as:

$$\frac{\partial u}{\partial t} + u \frac{\partial u}{\partial z} + \frac{1}{\rho} \frac{\partial p}{\partial z} = 0 \tag{A1}$$

and

$$\frac{\partial p}{\partial t} + u \frac{\partial p}{\partial z} + \gamma p \frac{\partial u}{\partial z} = (\gamma - 1) \omega_c \tag{A2}$$

where ω_c is the rate of heat addition per second per unit mass of fluid.

To explore the nonlinear stability of fluctuations around an equilibrium state of flow, write the physical variables

$$\begin{aligned} p &= \bar{p} + \varepsilon p' \\ u &= \bar{v} + \varepsilon u' \\ \rho &= \bar{\rho} + \varepsilon \rho' \\ \omega_c &= \bar{\omega}_c + \varepsilon \omega_c' \end{aligned} \tag{A3}$$

where the barred quantities are time independent and satisfy the over-all conservation equations

$$\bar{v} \frac{\partial \bar{v}}{\partial z} + \frac{1}{\rho} \frac{\partial \bar{p}}{\partial z} = 0 \tag{A4}$$

$$\bar{v}\frac{\partial \bar{\rho}}{\partial z} + \bar{\rho}\frac{\partial \bar{v}}{\partial z} = (\gamma-1)\bar{\omega}_c \qquad \text{(A5)}$$

Substituting A3 into A1, A2, expanding and eliminating the time independent terms using A4 and A5, yield Equations A7 and A8. Terms of order ε^3 may be dropped when compared with those of ε^2, assuming $\varepsilon \ll 1$. In Equations A7 and A8 the reciprocal of the density is developed as follows:

$$\frac{1}{\rho} = \frac{1}{\bar{\rho}}\left(1 - \frac{\rho'}{\bar{\rho}}\varepsilon + \varepsilon^2\left(\frac{\rho'}{\bar{\rho}}\right)^2 - \cdots\right) \qquad \text{(A6)}$$

In addition the term $\bar{p}$ when appearing at the right-hand side is assumed to be constant across the combustion length, thus $\frac{\partial \bar{p}}{\partial z} = 0$

$$\left[\frac{\partial w'}{\partial t} + \frac{1}{\bar{\rho}}\frac{\partial p'}{\partial z}\right] + \left[\bar{v}\frac{\partial w'}{\partial z} + w'\frac{\partial \bar{v}}{\partial z}\right] + \qquad \text{(A7)}$$

$$+ \left[\frac{1}{\bar{\rho}}\left(\frac{\rho'}{\bar{\rho}}\right)\frac{\partial p'}{\partial z} + w'\frac{\partial w'}{\partial z}\right] = 0$$

and

$$\frac{\partial p'}{\partial t} + \bar{\rho}\bar{c}^2 \frac{\partial m'}{\partial z} = (\gamma-1)\,\omega_c' - \left[\bar{\rho}\frac{\partial \bar{c}}{\partial z}\,\rho' + \frac{\partial \bar{c}}{\partial z}\,\bar{\rho}\,m'\right] - \left[\bar{m}\frac{\partial \bar{c}}{\partial z}\,\rho' + \frac{\partial \bar{c}}{\partial z}\,\bar{\rho}\,\bar{m}\right] \qquad \text{(A8)}$$

The terms on the left can be recognized as the acoustic parts, the terms on the right are the "perturbation terms due to through flow, $\bar{m}$, nonlinear terms m' and combustion, ω_c'.

To eliminate m' as a separate variable on the left-hand side the analysis takes the time derivative of A8 and the spatial derivative of A7 and subtracts the two equations. Using the assumption that flow disturbances are adiabatic implies to lowest order that

$$\frac{1}{\gamma}\frac{\partial p'}{\partial t} = \frac{\partial m'}{\partial z} \qquad \text{(A9)}$$

The resulting equation is:

$$\frac{\partial^2 p'/\bar{p}}{\partial t^2} - \frac{\partial}{\partial z}\left(c^2 \frac{\partial}{\partial z} p'/\bar{p}\right) = (\gamma-1)\frac{\partial}{\partial z}\left[\bar{v}\frac{\partial w'}{\partial z} + w'\frac{\partial \bar{v}}{\partial z}\right]$$

$$- \frac{\partial}{\partial t}\left[\bar{v}\frac{\partial p'/\bar{p}}{\partial z} + (\gamma-1)\frac{\bar{p}}{\bar{T}}\frac{\partial \bar{T}}{\partial z}\right] + \frac{(\gamma-1)}{\bar{p}}\frac{\partial \omega_c'}{\partial t} \qquad \text{(A10)}$$

$$+ (\gamma-1)\frac{\partial}{\partial z}\left[w'\frac{\partial w'}{\partial z} + \frac{1}{\gamma}\frac{\bar{p}}{\bar{T}}\cdot\frac{\partial w'}{\partial t}\right]$$

$$- \frac{\partial}{\partial t}\left[w'\frac{\partial p'/\bar{p}}{\partial z} + (\gamma-1)\frac{\bar{p}}{\bar{T}}\frac{\partial w'}{\partial z}\right]$$

This has the form of a wave equation for $p'/\bar{p}$ (the unsteady pressure component) with amplitude dependent driving terms resulting from interaction of steady through flow, combustion, and nonlinear effects. We treat each of these terms separately, with particular attention focussed on the combustion effects expressed by ω_c'.

For convenience, Equation A10 may be written as

$$\frac{\partial^2 p'/\bar{p}}{\partial t^2} - c^2\frac{\partial^2 p'/\bar{p}}{\partial z^2} = f_v + f_N + f_c \qquad \text{(A11)}$$

One recognizes that the left-hand side of Equation A11 is the general form of the acoustic wave equation when made equal to zero, for which

solutions are known in the form of

$$\frac{p'}{\bar{p}} = \sum_{i=0}^{n} \psi_i(z) \cdot \eta_i(t) \tag{A12}$$

For the pure acoustic case it can also be shown through substitution in Equation A7 and A8 that

$$w' = \sum_{i=1}^{n} \frac{c^2}{\gamma \omega_i^2} \cdot \frac{\partial \psi_i}{\partial z} \cdot \frac{\partial \eta_i}{\partial t} \tag{A13}$$

$$\frac{\partial w'}{\partial t} = - \frac{c^2}{\gamma} \frac{\partial p'|_{\bar{p}}}{\partial z} \tag{A14}$$

$$\frac{\partial w'}{\partial z} = - \frac{1}{\gamma} \frac{\partial p'|_{\bar{p}}}{\partial t} \tag{A15}$$

Assuming that $\eta_i(t) = \alpha \sin \omega t + \beta \cos \omega t$

thus $\partial^2 \eta / \partial t^2 = - \omega^2 \eta$

The terms of the acoustic solution will now be inserted in the disturbance terms, f_v, f_N, and f_c. In the end an equation follows for which the constants of integration α and β are not entirely constant, but have a time dependency. The terms f_v, f_N, and f_c will determine that time dependency.

2. ELIMINATION OF SPATIAL DEPENDENCE

The left-hand side of Equation A11 may be written as:

$$\psi_i \frac{\partial^2 \eta_i}{\partial t} + \omega^2 \psi_i \eta_i \tag{A16}$$

Multiplying Equation A11 by the mode shape ψ_k, and integrating over the entire volume results in

$$\int \psi_k \psi_i (\ddot{\eta}_i + \omega^2 \eta_i) dV = \int \psi_k (f_{\bar{v}} + f_N + f_c) dV \tag{A17}$$

Due to the orthogonality theorems the integral $\int \psi_k \cdot \psi_i \, dV$ is unity when $k = i$, otherwise it vanishes. Thus

$$\ddot{\eta}_i + \omega^2 \eta_i = \int \psi_k f_{\bar{v}} dV + \int \psi_k f_N dV + \int \psi_k f_c dV \tag{A18}$$

The right-hand side should now be evaluated by inserting the appropriate values of $f_{\bar{v}}$, etc. in the equations. This is being accomplished in the next sections.

3. THROUGH FLOW EFFECTS

The terms linear in $\bar{v}$ in Equation A10

$$f_{\bar{v}} = \oint \frac{\partial}{\partial z}\left[\bar{v}\frac{\partial w'}{\partial z} + w'\frac{\partial \bar{v}}{\partial z}\right] - \tag{A19}$$

$$- \frac{\partial}{\partial t}\left[\bar{v}\frac{\partial h'|_{\bar{p}}}{\partial z} + \oint\left(\frac{h'}{\bar{p}}\right)\frac{\partial \bar{v}}{\partial z}\right]$$

become

$$f_v = -2\bar{v}\,\frac{\partial^2 p'|_{\bar{p}}}{\partial z\,\partial t} - (2+f)\frac{\partial \bar{v}}{\partial z}\cdot\frac{\partial p'|_{\bar{p}}}{\partial t} + \qquad \text{(A20)}$$

$$+ f w' \frac{\partial^2 \bar{v}}{\partial z^2}$$

Expanding Equation A20 as $F_v = \int \psi_k f_v \, dV$ and using Equations A12, A13 to convert p' and w' to values of ψ and η it follows that

$$F_v = -2\sum_i \left[\int_0^l \psi_k \bar{v}\,\frac{\partial \psi_i}{\partial z}\,dz\right]\dot{\eta}_i - \qquad \text{(A21)}$$

$$- (2+f)\sum_i \left[\int_0^l \psi_k \frac{\partial \bar{v}}{\partial z}\,\psi_i\,dz\right]\dot{\eta}_i$$

$$+ \sum_i \frac{c^2}{\omega_i^2}\left[\int_0^l \psi_k \frac{\partial^2 \bar{v}}{\partial z^2}\,\frac{\partial \psi_i}{\partial z}\,dz\right]\dot{\eta}_i$$

We assume $\bar{v}$ is a linear function of axial distance downstream, with coefficients constant except at the flameholder. Thus the third term vanishes. The doubly subscripted integrals in the first and second terms will be evaluated below.

For piece-wise linear mean velocity distribution

$$\bar{v} = a_1 z + b_1 \qquad 0 \le z < l_1$$

$$\bar{v} = a_2 z + b_2 \qquad l_1 \le z \le l_2$$

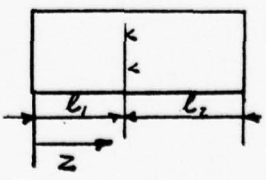

Define

$$F^1_{ki} \equiv \int_0^{\ell_2} \psi_k \, \bar{U} \, \frac{\partial \psi_i}{\partial z} \, dz$$

$$F^2_{ki} \equiv \int_0^{\ell_2} \psi_k \, \frac{\partial \bar{U}}{\partial z} \, \psi_i \, dz$$

Then with $F_v = \hat{D}_{ki} \cdot \dot{\eta}_i$

$$\hat{D}_{ki} = -2 F^1_{ki} - (2 + \gamma) \cdot F^2_{ki}$$

Calculate the contribution to integrals F from chamber 1.

$$F^1_{ki} = \frac{1}{k_i^2 - k_k^2} \left\{ \int_0^{\ell_1} \left(\bar{U} \frac{d\psi_i}{dz} \cdot \frac{d\psi_k}{dz} + \bar{U} k_i^2 \psi_i \psi_k \right. \right.$$

$$\left. \left. - \psi_k \frac{d\psi_i}{dz} a_1 \right) - 2 k_i^2 F^2_{ki} \right\}$$

$$F^2_{ki} = a_1 \frac{1}{k_i^2 - k_k^2} \int_0^{\ell_1} \left(\psi_i \frac{d\psi_k}{dz} - \psi_k \frac{d\psi_i}{dz} \right)$$

These expressions are valid for $i \neq k$

For $i = k$

$$F_{1_{kR}} = \int_0^{\ell_1} \left(\tfrac{1}{2} \bar{v} \psi_R^2 \right) - \frac{a_1}{2} \int_0^{\ell_1} \psi_R^2 \, dz$$

$$F_{2_{kR}} = \frac{1}{2 k_R^2} \int_0^{\ell_1} \left(\bar{v} \left(\frac{d\psi_R}{dz} \right)^2 + \bar{v} k_R^2 \psi_R^2 - \psi_R \frac{d\psi_R}{dz} a_1 \right)$$

Combine these with similar expressions for chamber 2 contribution.

$$F_{1_{ki}} = \frac{1}{\omega_i^2 - \omega_R^2} \left\{ \int_0^{\ell_2} \left(\bar{v} c^2 \frac{d\psi_i}{dz} \frac{d\psi_R}{dz} + \bar{v} \omega_i^2 \psi_i \psi_R - \right.\right.$$

$$\left.\left. - \frac{d\bar{v}}{dz} \psi_R c^2 \frac{d\psi_i}{dz} \right) - 2 \omega_i^2 F_{2_{ki}} \right\} +$$

$$+ \frac{1}{\omega_i^2 - \omega_R^2} \left\{ \left(\bar{v}(\ell_1^-) - \bar{v}(\ell_1^+) \right) \omega_i^2 \psi_i \psi_R \Big|_{z=\ell_1} + \right.$$

$$\left. + (a_2 - a_1) \psi_R c^2 \frac{d\psi_i}{dz} \Big|_{z=\ell_1} + \right.$$

$$\left. + \left(\frac{\bar{v}(\ell_1^-)}{c_1^2} - \frac{\bar{v}(\ell_1^+)}{c_2^2} \right) \cdot c^2 \frac{d\psi_i}{dz} \, c^2 \frac{d\psi_R}{dz} \Big|_{z=\ell_1} \right.$$

$$F_{2_{ki}} = \frac{1}{\omega_i^2 - \omega_R^2} \int_0^{\ell_2} \left\{ \frac{d\bar{v}}{dz} \left(\psi_i c^2 \frac{d\psi_R}{dz} - \psi_R c^2 \frac{d\psi_i}{dz} \right) \right\} +$$

$$+ \frac{(a_1 - a_2)}{\omega_i^2 - \omega_R^2} \left\{ \psi_i c^2 \frac{d\psi_R}{dz} - \psi_R c^2 \frac{d\psi_i}{dz} \right) \Big\} \Big|_{z=\ell_1}$$

For $i = k$

$$F_{1_{kk}} = \int_0^{l_2} \frac{\bar{U}}{2} \psi_k^2 - \frac{1}{2} F_{2_{kk}} \left(\bar{U}(l_1^-) - \bar{U}(l_1^+) \right) \frac{\psi_k^2}{2} \Bigg|_{z=l_1}$$

$$F_{2_{kk}} = \frac{1}{2\omega_k^2} \int_0^{l_2} \left\{ \bar{U} \left(c^2 \frac{d\psi_k^2}{dz} + \omega_k^2 \psi_k^2 \right) - \psi_k c^2 \frac{d\psi_k}{dz} \frac{d\bar{U}}{dz} \right\} +$$

(A22)

$$+ \frac{1}{2\omega_k^2} \left\{ \left(\bar{U}(l_1^-) - \bar{U}(l_1^+) \right) \cdot \omega_k^2 \psi_k^2 \Big|_{z=l_1} + \right.$$

$$+ (a_2 - a_1) \psi_k c^2 \frac{d\psi_k}{dz} \Big|_{z=l_1} +$$

$$\left. + \left(\frac{\bar{U}(l_1^-)}{c_1^2} - \frac{\bar{U}(l_1^+)}{c_2^2} \right) \cdot \left(c^2 \frac{d\psi_k}{dz} \right)^2 \Big|_{z=l_1} \right\}$$

In summary $F_U = \hat{D}_{ki} \cdot \dot{\eta}_i$

NB: In the organ pipe case ($\omega_n = n\omega_1$), an increase in the steady velocity change across the flameholder

$$\bar{U}(l_1^+) - \bar{U}(l_1^-)$$

will increase the decay rate of the acoustic modes.

4. NONLINEAR TERMS

The terms in A10 which are quadratic in fluctuating variables are

$$f_N = \gamma \frac{\partial}{\partial z}\left[u' \frac{\partial u'}{\partial z} + \frac{1}{\gamma} \frac{p'}{\bar{p}} \frac{\partial u'}{\partial t} \right] - \frac{\partial}{\partial t}\left[u' \frac{\partial p'/\bar{p}}{\partial z} + \gamma \frac{p'}{\bar{p}} \frac{\partial u'}{\partial z} \right] \tag{A23}$$

They can be reduced to with A14 and A15

$$f_N = \left(1 + \frac{1}{\gamma}\right)\left\{ \frac{\partial}{\partial t}\left(\frac{p'}{\bar{p}}\right)^2 - 2u' \frac{\partial^2 p'/\bar{p}}{\partial z \partial t} + \frac{p'}{\bar{p}} \frac{\partial^2 p'/\bar{p}}{\partial t^2} - \frac{1}{\gamma} \frac{p'}{\bar{p}} \frac{\partial}{\partial z}\left[c^2 \frac{\partial p'/\bar{p}}{\partial z} \right] \right. \tag{A24}$$

Expanding Equation A20 as $F_N \equiv \int \psi_k f_N \, dV$ and using Equations A12 and A13 to convert p' and u' to values in ψ and η yields

$$F_N = \sum_i \sum_j \left(A_{ijk} \eta_i \eta_j + B_{ijk} \dot{\eta}_i \dot{\eta}_k \right) \tag{A25}$$

In this derivation use is made of an expression used to integrate in parts.

$$\int_0^{\ell_2} c^2 \psi_R \frac{d\psi_i}{dz} \frac{d\psi_j}{dz} dz = \frac{1}{2}\left(\omega_i^2 + \omega_j^2 - \omega_R^2\right) \int_0^{\ell_2} \psi_R \psi_i \psi_j dz$$

$$+ \frac{1}{2} \int_0^{\ell_2} c^2 \left[\frac{d\psi_R}{dz} \psi_i \psi_j - \psi_R \left(\frac{d\psi_i}{dz} \cdot \psi_j + \frac{d\psi_j}{dz} \cdot \psi_i \right) \right] \qquad \text{(A26)}$$

The terms A_{Rij} and B_{Rij} are then

$$A_{Rij} = \left(\frac{1}{\gamma} - 1\right) \frac{\omega_i^2 + \omega_j^2}{2} \int_0^{\ell_2} \psi_R \psi_i \psi_j dz$$

$$B_{Rij} = \left\{ 1 - \frac{1}{2\gamma} \left(\frac{\omega_j^2 - \omega_R^2}{\omega_i^2} + \frac{\omega_i^2 - \omega_R^2}{\omega_j^2} \right) \right\} \int_0^{\ell_2} \psi_R \psi_i \psi_j dz \qquad \text{(A27)}$$

$$+ \frac{1}{2\gamma} \left(\frac{1}{\omega_i^2} + \frac{1}{\omega_j^2} \right) \cdot \int_0^{\ell_2} c^2 \left\{ \psi_R \left(\frac{d\psi_i}{dz} \psi_j + \frac{d\psi_j}{dz} \psi_i \right) - \right.$$

$$\left. - \frac{d\psi_R}{dz} \psi_i \psi_j \right\}$$

Inspection of the above expression for F_N shows that only the symmetric parts of A_{Rij}, B_{Rij} are required for further calculation.

Thus we have replaced

$$A_{Rij} = \tfrac{1}{2}\left(A_{Rij} + A_{Rji}\right) \qquad \text{(A28)}$$

$$B_{Rij} = \tfrac{1}{2}\left(B_{Rij} + B_{Rji}\right)$$

In this manner only one integral requires being integrated. This is

$$\int_0^{l_2} \psi_R \psi_i \psi_j \, dz \qquad \text{(A29)}$$

where $\psi_R = R_R \cos\left(K_R z + \theta_R\right) \qquad 0 \leq z < l_1$

and $\psi_R = \cos\left(\hat{K}_R z + \hat{\theta}_R\right) \qquad l_1 \leq z \leq l_2$

The values of ψ_R are given mode shapes and are previously calculated or given quantities.

Since

$$\cos k_R z \cdot \cos k_i z \cdot \cos k_j z =$$

$$\frac{1}{4}\left[\cos\left(k_R + k_i + k_j\right)z + \cos\left(k_R + k_i - k_j\right)z + \right.$$

$$\left. + \cos\left(k_R - k_i + k_j\right)z + \cos\left(k_R - k_i - k_j\right)z\right.$$

we have (see Section B)

$$\int_0^{\ell_2} \psi_k \psi_i \psi_j \, dz =$$

$$\frac{1}{4} \sum_{m=1}^{4} \int_0^{\ell_1} \frac{\sin(p_m z + \theta_m)}{p_m} \cdot R_k R_i R_j \quad \text{(A30)}$$

$$+ \frac{1}{4} \sum_{m=1}^{4} \int_{\ell_1}^{\ell_2} \frac{\sin(\hat{p}_m z + \hat{\theta}_m)}{\hat{p}_m}$$

where

$$p_1 \equiv K_k + K_i + K_j$$

$$p_2 \equiv K_k + K_i - K_j$$

$$p_3 \equiv K_k - K_i + K_j$$

$$p_4 \equiv K_k - K_i - K_j$$

and

$$\theta_1 \equiv \theta_k + \theta_i + \theta_j$$

$$\theta_2 \equiv \theta_k + \theta_i - \theta_j$$

$$\theta_3 \equiv \theta_k - \theta_i + \theta_j$$

$$\theta_4 \equiv \theta_k - \theta_i - \theta_j$$

θ becomes $\hat{\theta}$ when θ_R, θ_i, θ_j are replaced by $\hat{\theta}_R$, $\hat{\theta}_i$, $\hat{\theta}_j$.

5. UNSTEADY COMBUSTION

The unsteady heat release term f_c from Equation A11 may be written as

$$f_c = \frac{\gamma - 1}{\bar{p}} \frac{\partial \omega_c'}{\partial t} \tag{A31}$$

The unsteady heat release was formulated in previous work at NREC (Ref 1) and may be written as

$$\omega_c'(z',t) = \frac{\bar{\rho}\bar{E}}{\bar{\tau}} \cdot e^{-\frac{z'}{\bar{U}\bar{\tau}}} \left\{ \frac{\rho'}{\bar{\rho}}(z',t) - \frac{\tau'}{\bar{\tau}}(z',t) + \right.$$
$$+ \int_0^{z'} \frac{\tau'}{\bar{\tau}}(y,t) \cdot \exp\left(i\omega_0 \frac{(z'-y)}{\bar{U}}\right) \frac{dy}{\bar{U}\bar{\tau}} +$$
$$\left. + \int_0^{z'} \frac{U'}{\bar{U}}(y,t) \cdot \exp\left(i\omega_0 \cdot \frac{z'-y}{\bar{U}}\right) \frac{dy}{\bar{U}\bar{\tau}} \right. \tag{A31}$$

where z' is the axial coordinate downstream from the flameholder; y is the same as z' but has been inserted in the integral terms for distinction (see sketch on the following page).

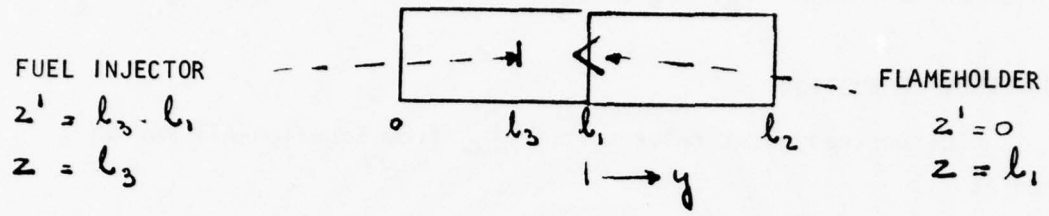

Equation A31 contains terms in ρ and τ which have to be expressed in p'. Using previous formulations:

$$\frac{\rho'}{\bar{\rho}} = \frac{1}{\gamma}\frac{p'}{\bar{p}} \qquad \frac{\tau'}{\bar{\tau}} = -\hat{C}_1 \frac{p'}{\bar{p}}$$

Equation A31 can then be rewritten as

$$\omega_c'(z',t) = \frac{\bar{\rho}\bar{E}}{\bar{\tau}}\, e^{-\frac{z'}{\bar{v}\bar{\tau}}} \left[\left(\frac{1}{\gamma} - \hat{C}_1\right)\frac{p'}{\bar{p}}(z',t) + \right.$$
$$+ \int_0^{z'} \left(\hat{C}_1 \frac{p'}{\bar{p}}\left(y, t + \frac{y-z'}{\bar{v}}\right) + \right. \qquad \text{(A32)}$$
$$\left. \left. + \frac{u'}{\bar{v}}\left(y, t + \frac{y-z'}{\bar{v}}\right)\right) \frac{dy}{\bar{v}\bar{\tau}} \right]$$

Note that the cumulative integral terms in A31 and A32 result from transforming the moving coordinate system/Lagrangean to a fixed coordinate system/Eulerian, they may be considered hueristically as the weighted sum of time delay terms.

In order to emphasize this interpretation, and generalize the combustion model to an arbitrary acoustic disturbance written as a sum of harmonic components, the complex phase factors in A31 can be rewritten in terms of time delays. Thus for a disturbance harmonic in time, the following replacements were made.

$$\frac{u'}{\bar{U}}(y,t)\cdot \exp\left[i\,\frac{\omega_0}{\bar{U}}(z'-y)\right] \qquad \text{(A33)}$$

with

$$\frac{u'}{\bar{U}}\left(y, t+\frac{z'-y}{\bar{U}}\right)$$

In order to eliminate the spatial distribution it was explained before that the form of A18 must be evaluated.

$$F_c \equiv \int \psi_k f_c \, dz = \left(\frac{-1}{\bar{P}}\right)\int_0^{\ell_2} \psi_k \frac{\partial \omega_c'}{\partial t}\, dz \qquad \text{(A33)}$$

The terms in ω_c' may now be individually evaluated.

The resulting expression is written in terms of the following integrals, which are evaluated in Section 9 of this appendix.

$$I_{1_{ki}} \equiv \int_0^{\ell_{21}} \hat{\psi}_k(z') \sin\left(\omega_i \frac{z'}{\bar{U}}\right) e^{-\frac{z'}{\bar{U}\tau}}\, dz'$$

$$I_{2_{ki}} \equiv \int_0^{\ell_{21}} \hat{\psi}_k(z') \cos\left(\omega_i \frac{z'}{\bar{U}}\right) \cdot e^{-\frac{z'}{\bar{U}\tau}}\, dz'$$

$$I_{3_{Ri}} \equiv \int_0^{l_{21}} \hat{\psi}_R(z') \; e^{-\frac{z'}{\bar{v}\tau}} \; dz'$$

$$I_{4_{Ri}} \equiv \int_0^{l_{21}} \hat{\psi}_R(z') \cdot \hat{\psi}_i(z') \; e^{-\frac{z'}{\bar{v}\tau}} \; dz' \qquad \text{(A34)}$$

$$I_{5_{Ri}} \equiv \int_0^{l_{21}} \hat{\psi}_R(z') \; \frac{d\hat{\psi}_i}{dz}(z') \; e^{-\frac{z'}{\bar{v}\tau}} \; dz'$$

In the above use of the second chamber variable z' is emphasized by writing

$$\hat{\psi}_R(z') \equiv \psi_R(z' + l_1) = \psi_R(z) \qquad \text{(A35)}$$

With EquationsA12 the pressure term can be written as

$$\int_0^{l_{21}} \frac{p'}{\bar{p}}(z',t) \; e^{-\frac{z'}{\bar{v}\tau}} \; \psi_R(z') \, dz' =$$

$$= \sum_{i=1} \eta_i(t) \cdot I_{4_{Ri}} \qquad \text{(A34)}$$

where $I_{4_{Ri}}$ is defined above.

The contribution of noncumulative terms in $\partial w_c' / \partial t$ to F_c is then written

$$C_w \cdot \left(\frac{1}{\gamma} - \hat{C}_1 \right) \sum_{i=1}^{n} \dot{\eta}_i(t) \cdot \bar{I}_{4i} \tag{A35}$$

where the constant C_w is

$$C_w = \frac{\bar{\bar{E}}\,\gamma(\gamma-1)}{\bar{\bar{c}}\;c_2^2} \tag{A36}$$

For convenience in evaluating the contribution of the cumulative terms in w_c' define also the following double integrals which are reduced to a linear combination of the $\bar{I}_1$ ---- $\bar{I}_5$ in Section 10 of this appendix.

$$\hat{\hat{C}}_{ki} \equiv \int_0^{\ell_{21}} \bar{F}_{ki}(y) \cos\left(\omega_i \frac{y}{\bar{\bar{c}}}\right) dy$$

$$\hat{\hat{S}}_{ki} \equiv \int_0^{\ell_{21}} \bar{F}_{ki}(y) \sin\left(\omega_i \frac{y}{\bar{\bar{c}}}\right) dy \tag{A37}$$

where

$$\bar{F}_{ki}(y) \equiv \int_y^{\ell_{21}} \hat{\psi}_i(z'-y) \cdot \psi_k(z') \cdot e^{-\frac{z'}{\bar{\bar{c}}\tau}} dz' \tag{A38}$$

The effect of the cumulative pressure term then can be found as:

$$\int_0^{z'} e^{-\frac{z'}{\bar{v}\bar{\tau}}} \cdot \frac{p'}{\bar{p}}\left(y, t + \frac{y-z'}{\bar{v}}\right) dy = \sum_i \sum_k F_{ki}\,\eta_i \qquad \text{(A39)}$$

Using the expressions of A12 and A13 together with an integration by parts produces the identity for the cumulative term containing the unsteady velocity.

$$\int_0^{z'} \frac{w'\left(y, t + \frac{y-z'}{\bar{v}}\right)}{\bar{v}}\, dy =$$

$$= \sum_i \frac{c_2^2}{\gamma\,\omega_i^2}\left\{ \frac{d\psi_i}{dz'}(z') \cdot \eta_i(t) - \right.$$

$$\left. - \frac{d\psi_i}{dz'}(l_1^+) \cdot \eta_i\left(t - \frac{z'}{\bar{v}}\right)\right\} \qquad \text{(A40)}$$

$$+ \frac{1}{\gamma}\int_0^{z'} \frac{p'}{\bar{p}}\left(y, t + \frac{y-z'}{\bar{v}}\right) dy$$

Using this expression combine the cumulative terms in ω_o' and carry out the spatial integration over them implied in A33. It is convenient to reverse of orders of integration, performing the Galerkin method integral over z' before the moving average integral over the space lag variable y.

$$\frac{\bar{\rho}\bar{E}}{\bar{T}} \int_0^{z} \int_0^{z'} \left\{ \left(\hat{C}_1 \cdot \frac{p'}{\bar{p}} + \frac{w'}{\bar{v}} \right) e^{-\frac{z'}{\bar{v}\bar{\tau}}} \cdot \frac{dy}{\bar{v}\bar{\tau}} \right\} dz =$$

$$C_w \cdot \left(\hat{C}_1 + \frac{1}{\gamma} \right) \cdot \frac{1}{\bar{v}\bar{\tau}} \cdot \sum_i \int_0^{\ell_{2i}} \eta_i \left(t - \frac{y}{\bar{v}} \right) \cdot F_{R_i}(y)\, dy \qquad \text{(A41)}$$

$$+ C_w \frac{1}{\bar{v}\bar{\tau}} \cdot \sum_i \left\{ \eta_i(t) \left(I_{R_i}^{5} - \frac{d\psi_i}{dz}(\ell_i^+)\, I_{R_i}^{2} \right) + \right.$$

$$\left. + \dot{\eta}_i(t) \cdot \frac{1}{\omega_i} \left(\frac{d\psi_i}{dz}(\ell_i^+)\, I_{R_i}^{1} \right) \right\}$$

As shown in the discussion of the time-averaging method, if the perturbing effects of flow and combustion are not too large, the coefficient $\eta_i(t)$ will behave over short periods like a sinusoid of frequency ω_i, with coefficients that show only slight variation over the hot chamber transit time. Thus the time-delay effects in the combustion model will be simplified using

$$\eta_i\left(t - \frac{z}{\bar{v}}\right) \simeq \eta_i(t) \cos\left(\omega_i \frac{z}{\bar{v}}\right) - \frac{1}{\omega_i} \dot{\eta}_i(t) \cdot \sin\left(\omega_i \frac{z}{\bar{v}}\right) \qquad \text{(A42)}$$

$$\dot{\eta}_i\left(t - \frac{z}{\bar{v}}\right) \simeq \dot{\eta}_i(t) \cos\left(\omega_i \frac{z}{\bar{v}}\right) + \omega_i\, \eta_i(t) \sin\left(\omega_i \frac{z}{\bar{v}}\right)$$

Take the time derivative of A41 above using Equation A42 to expand the function of retarded argument in the first term. The cumulative contribution to $\bar{F}_z$ is written

$$\frac{C_w}{\bar{v}\bar{t}} \left\{ \sum_i \eta_i(b) \left[\left(\hat{C}_1 + \frac{1}{\gamma} \right) \omega_i \cdot \hat{\hat{S}}_{ki} - \frac{c_2^2}{\gamma \omega_i^2} \cdot \frac{d\psi_i}{d2}\left(l_1^+\right) \bar{I}_{1_{ki}} \right] \right.$$

$$\left. + \sum_i \dot{\eta}_i(b) \left[\left(\hat{C}_1 + \frac{1}{\gamma} \right) \cdot \hat{\hat{C}}_{ki} + \frac{c_2^2}{\gamma \omega_i^2} \left(\bar{I}_{5_{ki}} - \frac{d\psi_i}{d2}\left(l_1^+\right) \bar{I}_{2_{ki}} \right) \right] \right\}$$

(A43)

6. SUMMARY OF EQUATIONS

The previous derivations have resulted in an equation for A18 as follows

$$\ddot{\eta}_i + \omega^2 \eta_i = F_K$$

where

$$F_k = \sum_i \left(D_{ki} \dot{\eta}_i + E_{ki} \eta_i \right) + \sum_i \sum_j \left(A_{kij} \eta_i \eta_i + B_{kij} \dot{\eta}_i \dot{\eta}_k \right)$$

(A44)

and from A22, A35 and A43

$$D_{ki} = -2\,\bar{F}^{1}_{ki} - (2+\gamma)\,\bar{F}^{2}_{ki} +$$

$$+ \frac{C_w}{\bar{v}\,\bar{t}}\left[\left(\hat{\bar{C}}_1 + \frac{1}{\gamma}\right)\cdot\hat{\hat{C}}_{ki} + C_w\left(\frac{1}{\gamma} - \hat{\bar{C}}_1\right)\cdot\bar{I}^{4}_{ki} + \right. \tag{A45}$$

$$\left. + \left(\frac{C_2^2}{\gamma\,\omega_i^2}\right)\left(\bar{I}^{5}_{ki} - \frac{d\psi_i}{dz}\left(l_1^{+}\right)\,\bar{I}^{2}_{ki}\right)\right]$$

The doubly subscripted integrals $\bar{F}^{1}_{ki}$ and $\bar{F}^{2}_{ki}$ (see A22) which contain respectively, the function, $\bar{v}$ and its first derivative are evaluated before.

From A43:

$$\bar{E}_{ki} = \frac{C_w}{\bar{v}\,\bar{t}}\left\{\left(\hat{\bar{C}}_1 + \frac{1}{\gamma}\right)\cdot\omega_i\,\hat{\hat{S}}_{ki} - \right.$$

$$\left. - \left(\frac{C_2^2}{\gamma\,\omega_i}\right)\cdot\frac{d\psi_i}{dz}\left(l_1^{+}\right)\,\bar{I}^{1}_{ki}\right\} \tag{A46}$$

The values for A_{kij} and B_{kij} are given by A27 as follows:

$$A_{kij} = \left(\frac{1}{\gamma} - 1\right)\left(\frac{\omega_i^2 + \omega_j^2}{2}\right)\cdot\int_0^{l_2}\psi_k\,\psi_i\,\psi_j\,dz.$$

$$B_{kij} = \left\{ 1 + \frac{1}{2j} \cdot \left(\frac{\omega_k^2 - \omega_j^2}{\omega_i^2} + \frac{\omega_k^2 - \omega_i^2}{\omega_j^2} \right) \right\} \int \psi_k \psi_i \psi_j \, dz$$

$$+ \frac{1}{2j} \left(\frac{1}{\omega_i^2} + \frac{1}{\omega_j^2} \right) \Bigg|_0^{l_z} c^2 \left[\psi_k \cdot \left(\frac{d\psi_i}{dz} \psi_j - \frac{d\psi_j}{dz} \psi_i \right) \right. \tag{A27}$$

$$\left. - \frac{d\psi_k}{dz} \psi_i \psi_j \right]$$

7. CORRELATION BETWEEN PREVIOUS ANALYSES

NREC has previously conducted a linearized combustion stability program (Refs 1 and 2). To establish the link between the present theory and that developed before, one should compare only diagonal terms in the matrices $\mathbf{D}$ and $\vec{\mathbf{E}}$; i.e., $i = k$. Contributions to D_{kk} from the various combustion effects may be listed for reference. Corresponding to the four terms in A34, these are:

1) from density fluctuation in a fluid fuel element

$$\frac{1}{\gamma} C_w I_{4kk} \tag{A47}$$

2) from fluctuation in the rate of combustion

$$-\hat{C}_1 C_w I_{4_{kk}} \tag{A48}$$

3) from resultant fluctuation in the remaining fuel content of a fuel element

$$C_w \frac{1}{\bar{U}\bar{\tau}} \hat{C}_1 \hat{\hat{C}}_{kk} \tag{A49}$$

4) from translation of the combustion description to a fixed Eulerian frame

$$\frac{1}{\gamma}\left(\frac{C_w}{\bar{U}\bar{\tau}}\right)\cdot\left\{\hat{\hat{C}}_{kk} + \frac{C_2^2}{\omega_k^2}\left(I_{\bar{5}_{kk}} - \frac{d\psi}{dz}\left(l_1^+\right)\cdot I_{2_{kk}}\right)\right\} \tag{A50}$$

This last term can be rewritten using integration by parts to yield

$$\frac{1}{\gamma}\frac{C_w}{\omega_k\bar{\tau}}\cdot\left(\frac{C_2}{\bar{U}}\right)^2\left\{\frac{\omega_k}{\bar{U}}\hat{\hat{C}}_{kk} - \psi_k\left(l_1^+\right) I_{1_{kk}}\right\} \tag{51}$$

This yields the basic link to previous NREC work in linear high frequency stability analysis. In terms of the first order frequency shift calculated by REFINE our linear stability coefficients D_{kk} and E_{kk} become

$$Re\left(\Delta\omega_k^2\right) = -E_{kk}. \tag{A52}$$

$$Im\left(\Delta\omega_k^2\right) = \omega_k D_{kk}.$$

Using formulae A47-A51, a term-by-term identification of the various contributions to these quantities is possible (see Ref 1, pages 193-194).

Note that combustion time fluctuations spatially redistribute the heat release of an element through the two effects accounted for in A49. In slowly varying low frequency modes for which

$$\frac{\omega_i(\ell_2-\ell_1)}{\bar{v}} < 1 \tag{A53}$$

the combination of these terms is

$$\simeq \hat{C}_1 C_w \int \psi_k(z)\, e^{-\frac{z'}{\bar{v}\bar{\tau}}} \left\{ \int_0^z \psi_k(z-y)\,dy - \bar{v}\bar{\tau}\,\psi_k(z) \right\} \tag{A54}$$

If A53 is obeyed it will follow that

$$\frac{\omega_k}{c_2}\left(\bar{v}\bar{\tau}\right) < 1 \tag{A55}$$

i.e., the k^{th} waveform will not oscillate appreciably in the interval $(\ell_1, \ell_1 + \bar{v}\bar{\tau})$. Thus A54 will be quite small.

8. TIME AVERAGING

Equation A44 represents a set of coupled second order differential equations that may be solved numerically at great expense. Following Culick, the equations may be reduced to a set of first order equations, assuming the solution is of the form

$$\eta_k(t) = \alpha_k \sin(\omega_k t) + \beta_k \cos(\omega_k t) \qquad \text{(A56)}$$

where α and β are slowly varying functions in time. The timewise variation of α and β can be obtained through averaging the fast oscillations of terms containing ω_k.

We obtain the coefficients $\eta_k(t)$ by solving the set of coupled, weakly nonlinear differential equations

$$\ddot{\eta}_k + \omega_k \eta_k = F_k \qquad \text{(A57)}$$

where the nonlinear forcing function F_k is

$$F_k = \sum_i \left(D_{ki} \dot{\eta}_i + E_{ki} \eta_i \right) + \sum_i \sum_j \left(A_{kij} \eta_i \eta_j + B_{kij} \dot{\eta}_i \dot{\eta}_j \right) \qquad \text{(A58)}$$

If F_k were absent the general solution of A57 would be

$$\eta_k = \alpha_k \sin(\omega_k t) + \beta_k \cos(\omega_k t) \qquad \text{(A56)}$$

We assume the solution of A57 can be parameterized this way with α, β slowly varying functions of time; i.e., we assume the average fractional change in α, β is small over a time period $2\pi/\omega_k$.

Substitute the above form for η_k into A57 and expand ignoring terms containing $\ddot{\alpha}$, $\ddot{\beta}$.

$$F_k(t) = 2\omega_k \left(\dot{\alpha}_k \cos \omega_k t - \dot{\beta}_k \sin \omega_k t \right) \qquad \text{(A58)}$$

AD-A060 073 NORTHERN RESEARCH AND ENGINEERING CORP CAMBRIDGE MASS F/G 21/2
FLAMEHOLDER COMBUSTION INSTABILITY STUDY. VOLUME I. ANALYTICAL --ETC(U)
MAY 78 W JANSEN, M PLATT, G E SMITH F33615-76-C-2112
UNCLASSIFIED NREC-1294-1 AFAPL-TR-78-27-VOL-1 NL

2 OF 2
AD
A060073

END
DATE
FILMED
12-78
DDC

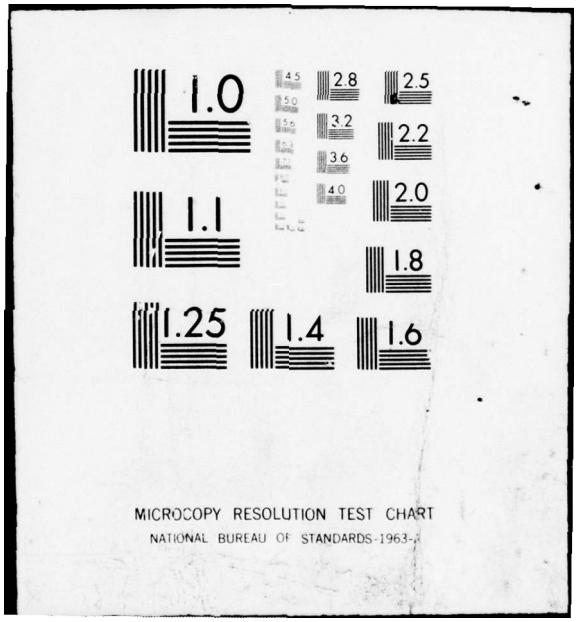
1.0
1.1
1.25
1.4
1.6
1.8
2.0
2.2
2.5
2.8
3.2
3.6
4.0
4.5
5.0
MICROCOPY RESOLUTION TEST CHART
NATIONAL BUREAU OF STANDARDS-1963-A

We now multiply by $\sin(\omega_k t)$ and integrate over the time interval $(t, t+\bar{\tau})$. Since α, β vary slowly we can move them outside the integral:

$$\tfrac{1}{2}\int_t^{t+\bar{\tau}} F_K \cdot \sin\omega_k t' dt' = \omega_k \dot{\alpha}_k \int_t^{t+\bar{\tau}} \sin\omega_k t' \cdot \cos\omega_k t' \, dt' - \omega_k \dot{\beta}_k \int_t^{t+\bar{\tau}} \sin^2\omega_k t' \, dt' \tag{A59}$$

$$\tfrac{1}{2}\int_t^{t+\bar{\tau}} F_K \cos\omega_k t' dt' = \omega_k \dot{\alpha}_k \int_t^{t+\bar{\tau}} \cos^2\omega_k t' \, dt - \omega_k \dot{\beta}_k \int_t^{t+\bar{\tau}} \sin\omega_k t' \cdot \cos\omega_k t' \, dt' \tag{A60}$$

If $\bar{\tau}$ is a multiple of $2\pi/\omega_k$ these become

$$\dot{\alpha}_k = \frac{1}{\omega_k \bar{\tau}} \int_t^{t+\bar{\tau}} F_k(t') \cos\omega t' dt' \tag{A61}$$

$$\dot{\beta}_k = \frac{-1}{\omega_k \bar{\tau}} \int_t^{t+\bar{\tau}} F_k(t') \sin\omega t' dt' \tag{A62}$$

with

$$\int_t^{t+\frac{2\pi}{\omega}} \cos^2\omega t \, dt = \frac{\bar{\tau}}{2} = \frac{\pi}{\omega} \; ; \int_t^{t+\frac{2\pi}{\omega}} \sin\omega t \cos\omega t \, dt = 0$$

Note that using the parameterized form A56 for η_i yields

$$\dot{\eta}_i(t) = \left\{ \omega_i \alpha_i(t) + \dot{\beta}_i(t) \right\} \cdot \cos \omega_i t + \left\{ -\omega_i \beta_i(t) + \dot{\alpha}_i(t) \right\} \cdot \sin \omega_i t \tag{A63}$$

We now expand our form of the forcing function F_R (see A58) assuming from the slow variation of α_i, β_i over a period that on the average

$$\frac{1}{\omega_i} \frac{\dot{\beta}_i}{\alpha_i} << 1 \qquad \frac{1}{\omega_i} \frac{\dot{\alpha}_i}{\beta_i} << 1 \tag{A64}$$

Thus in calculating the time average of F_R we assume

$$\dot{\eta}_i = \omega_i \left(\alpha_i \cos \omega_i t - \beta_i \sin \omega_i t \right) \tag{A65}$$

We do not use this approximation to evaluate the left-hand side of A57; it would amount to ignoring contributions of the magnitude of leading terms (see right-hand side of A58). The result would be equations identical to A61, A62 but with the parameter τ now arbitrary. Although derivations of A61, A62 do proceed this way and specific applications do suggest the use, for example, of a value for τ_R based on the fundamental frequency, no limits of validity for this assumption are available. The generalization of A61, A62 to arbitrary τ is

$$\begin{bmatrix} \dot{\alpha}_k \\ \dot{\beta}_k \end{bmatrix} = \frac{1}{2\omega_k} \cdot \frac{1}{\Delta} \begin{bmatrix} \langle S_k S_k \rangle - \langle S_k C_k \rangle \\ \langle S_k C_k \rangle - \langle C_k C_k \rangle \end{bmatrix} \cdot$$

$$\cdot \begin{bmatrix} \int F_k \cos \omega_k t' dt' \\ \int F_k \sin \omega_k t' dt' \end{bmatrix} \qquad \text{(A66)}$$

where

$$\Delta \equiv \langle C_k C_k \rangle \langle S_k S_k \rangle - \langle S_k C_k \rangle^2$$

In the above, the time averaging integrals have been abbreviated; e.g.,

$$\langle S_k C_k \rangle \equiv \int_t^{t+\tau} \sin(\omega_k t') \cos(\omega_k t') dt' \qquad \text{(A67)}$$

Use of a nonstandard value for τ_k causes changes in the resulting amplitudes α_i, β_i that must be compared with the neglect of terms $\ddot{\alpha}_i$, $\ddot{\beta}_i$ on the left-hand side of A58 and use of the approximate formula for η_i (Equation A65) on the right-hand side.

If the energy stored in the i^{th} harmonic is written

$$E_i = \left(\frac{\eta_i}{\omega_i}\right)^2 + \eta_i^2 \qquad \text{(A68)}$$

We can expand and time average it as above to yield

$$\langle E_i \rangle_{AV} \approx E_0(t)\left[1 + \frac{1}{\omega_i}\frac{\dot{\beta}_i}{\alpha_i}\right] \approx E_0(t)\left[1 - \frac{1}{\omega_i}\frac{\dot{\alpha}_i}{\beta_i}\right] \tag{A69}$$

Thus the above assumption is equivalent to assuming $\underline{E} = \underline{E}_0$ in evaluating $\dot{\alpha}_i, \dot{\beta}_i$. (For an analytic and numerical check of this assumption in the lossless nonlinear acoustics problem, the organ-pipe situation can be considered.)

The expansion of A61, A62 is simplified by setting

$$\langle S_i C_k \rangle \equiv \int_t^{t+\bar{\tau}} \sin(\omega_i t') \cos(\omega_k t')\, dt'$$

$$\langle S_i S_j C_k \rangle \equiv \int_t^{t+\bar{\tau}} \sin(\omega_i t') \sin(\omega_j t') \cos(\omega_k t')\, dt'$$

Then

$$\dot{\alpha}_k = \frac{1}{\omega_k \bar{\tau}} \cdot \left\{ \sum_i^{\bar{}} \left(E_{ki}\alpha_i - D_{ki}\omega_i\beta_i\right)\cdot\langle S_i C_k\rangle + \right.$$

$$\left. + \sum_i^{\bar{}} \left(E_{ki}\beta_i + D_{ki}\omega_i\alpha_i\right)\cdot\langle C_i C_k\rangle + \right.$$

$$+ \sum_i \sum_j \left[A_{Rij}\,\alpha_i\beta_j - \omega_i\omega_j B_{Rij}\,\beta_i\alpha_j \right] \cdot 2\langle S_i C_j C_k \rangle$$

$$+ \sum_i \sum_j \left(A_{Rij}\,\beta_i\beta_j + \omega_i\omega_j B_{Rij}\,\alpha_i\alpha_j \right) \cdot \langle C_i C_j C_k \rangle \qquad \text{(A70)}$$

$$+ \sum_i \sum_j \left(A_{Rij}\,\alpha_i\alpha_j + \omega_i\omega_j B_{Rij}\,\beta_i\beta_j \right) \cdot \langle S_i S_j C_k \rangle \Bigg\}$$

$$\dot{\beta}_R = -\frac{1}{\omega_R \tau} \Bigg\{ \sum_i \left(E_{Ri}\,\alpha_i - D_{Ri}\,\omega_i\beta_i \right) \cdot \langle S_i S_k \rangle +$$

$$+ \sum_i \left(E_{Ri}\,\beta_i + D_{Ri}\,\omega_i\alpha_i \right) \cdot \langle C_i S_k \rangle +$$

$$+ \sum_i \sum_j \left(A_{Rij}\,\alpha_i\beta_j - \omega_i\omega_j B_{Rij}\,\beta_i\alpha_j \right) \cdot 2\langle S_i C_j S_k \rangle \qquad \text{(A71)} +$$

$$+ \sum_i \sum_j \left(A_{Rij}\,\alpha_i\alpha_j + \omega_i\omega_j B_{Rij}\,\beta_i\beta_j \right) \cdot \langle S_i S_j S_k \rangle +$$

$$+ \sum_i \sum_j \left(A_{Rij}\,\beta_i\beta_j + \omega_i\omega_j B_{Rij}\,\alpha_i\alpha_j \right) \cdot \langle C_i C_j S_k \rangle \Bigg\}$$

Equations A70 and A71 are used to determine the stability of the combustion process. All terms are known. The terms D, E, A and B are given in Equations A45, A46, and A27 respectively.

9. EVALUATION OF COMBUSTION INTEGRALS

a. Integrals I_1 and I_2

We evaluate the following integrals

$$I_{1_{ki}} \equiv \int_0^{l_{21}} \hat{\psi}_k(z') \sin\left(\frac{\omega_i z'}{\bar{U}}\right) e^{-\frac{z'}{\bar{U}\tau}} dz' \tag{A72}$$

$$I_{2_{ki}} \equiv \int_0^{l_{21}} \hat{\psi}_k(z') \cos\left(\frac{\omega_i z'}{\bar{U}}\right) \cdot e^{-\frac{z'}{\bar{U}\tau}} dz' \tag{A73}$$

where the caret over ψ signifies that we integrate (over z') over the length of the hot chamber; i.e.,

$$\hat{\psi}_k(z') = \psi_k(l_1 + z') = \psi_k(z) \tag{A74}$$

where $l_2 \equiv l_2 - l_1$ is the hot chamber length. For any two smooth functions $f(z)$, $g(z)$ we have, using integration by parts:

$$\int_a^b f \frac{d^2 g}{dz^2} dz - \int_a^b g \frac{d^2 f}{dz^2} dz = \tag{A75}$$

$$= \Big|_a^b \left(f \frac{dg}{dz} - g \frac{df}{dz} \right)$$

Note that because the hot chamber sound speed is taken to be constant we have as acoustic wave equation in chamber two:

$$\frac{d^2\psi_k}{dz^2} + \left(\frac{\omega_k}{c_2}\right)^2 \psi_k = 0 \tag{A76}$$

Substitute in the identity A75 above

$$g = \psi_k$$

$$f = \sin\frac{\omega_i z'}{\bar{U}}\, e^{-\frac{z'}{\bar{U}\bar{\tau}}} \tag{A77}$$

and eliminate derivatives of ψ_k using the wave equation A76, then

$$\left[\left(\frac{\omega_i}{\bar{U}}\right)^2 - \left(\frac{\omega_k}{c_2}\right)^2 - \left(\frac{1}{\bar{U}\bar{\tau}}\right)^2\right] \underline{I}^1_{ki} + 2\left(\frac{1}{\bar{U}\bar{\tau}}\right)\frac{\omega_i}{\bar{U}} \cdot \underline{I}^2_{ki} =$$

$$= \int_0^{l_{21}} e^{-\frac{z'}{\bar{U}\bar{\tau}}} \cdot \left\{ \frac{d\hat{\psi}_k}{dz'} \sin\left(\frac{\omega_i z'}{\bar{U}}\right) - \right. \tag{A78}$$

$$\left. - \hat{\psi}_k \left(\frac{\omega_i}{\bar{U}} \cos\left(\frac{\omega_i z'}{\bar{U}}\right) - \frac{1}{\bar{U}\bar{\tau}} \sin\left(\frac{\omega_i z'}{\bar{U}}\right)\right)\right\}.$$

Now substitute in A75

$$q = \psi_k$$

$$f = \cos\frac{\omega_i z'}{\bar{v}}\, e^{-z'/\bar{v}\bar{\tau}} \tag{A79}$$

and simplify as above

$$\left\{\left(\frac{\omega_i}{\bar{v}}\right)^2 - \left(\frac{\omega_k}{c_2}\right)^2 - \left(\frac{1}{\bar{v}\bar{\tau}}\right)^2\right\} \cdot \bar{I}^2_{k_i} - 2\left(\frac{1}{\bar{v}\bar{\tau}}\right)\frac{\omega_i}{\bar{v}} \cdot \bar{I}^1_{k_i} =$$

$$= \int_0^{l_{z1}} e^{-\frac{z'}{\bar{v}\bar{\tau}}} \left\{ \frac{d\psi_k}{dz'} \cos\left(\frac{\omega_i z'}{\bar{v}}\right) + \right. \tag{A80}$$

$$\left. + \psi_k \cdot \left(\frac{\omega_i}{\bar{v}} \sin\left(\frac{\omega_i z'}{\bar{v}}\right) + \frac{1}{\bar{v}\bar{\tau}} \cos\left(\frac{\omega_i z'}{\bar{v}}\right)\right)\right\}$$

The pair of linear equations A78, A80 can then be solved algebraically for $\bar{I}_1$, $\bar{I}_2$. Writing R_2, R_3 for the RHS of A78 and A80 respectively and defining

$$L_2 \equiv \left(\frac{\omega_i}{\bar{v}}\right)^2 - \left(\frac{\omega_k}{c_2^2}\right)^2 - \left(\frac{1}{\bar{v}\bar{\tau}}\right)^2 \tag{A81}$$

A78 and A80 become

$$L_2 \bar{I}_1 + \left(\frac{2}{\bar{v}\bar{\tau}}\right)\left(\frac{\omega_i}{\bar{v}}\right) \cdot \bar{I}_2 = R_2 \tag{A82}$$

$$L_2 \bar{I}_2 - \left(\frac{2}{\bar{U}\bar{\tau}}\right)\left(\frac{\omega_i}{\bar{U}}\right)\bar{I}_1 = R_3 \qquad \text{(A83)}$$

Solving A82 and A83

$$\bar{I}^1_{R_i} = \frac{L_2 R_2 - \frac{2}{\bar{U}\bar{\tau}} \cdot \frac{\omega_i}{\bar{U}} \cdot R_3}{L_2^2 + \left(\frac{2}{\bar{U}\bar{\tau}} \cdot \frac{\omega_i}{\bar{U}}\right)^2} \qquad \text{(A84)}$$

$$\bar{I}^2_{R_i} = \frac{L_2 R_3 + \frac{2}{\bar{U}\bar{\tau}} \cdot \frac{\omega_i}{\bar{U}} \cdot R_2}{L_2^2 + \left(\frac{2}{\bar{U}\bar{\tau}} \cdot \frac{\omega_i}{\bar{U}}\right)^2} \qquad \text{(A85)}$$

b. Combustion Integral I_3

The integral $I_{3_{Ri}}$

$$I_{3_{Ri}} \equiv \int_0^{l_{21}} \hat{\psi}_R(z') \cdot e^{-\frac{z'}{\bar{U}\bar{\tau}}}\, dz'$$

can be evaluated using integration by parts to yield

$$-\left[\left(\frac{\omega_R}{c_2}\right)^2 + \left(\frac{1}{\bar{U}\bar{\tau}}\right)^2\right] \cdot \bar{I}^3_{R_i} = \int_0^{l_{21}} \left[e^{-\frac{z_1}{\bar{U}\bar{\tau}}} \cdot \left(\frac{d\hat{\psi}_R}{dz} + \frac{1}{\bar{U}\bar{\tau}}\psi_R\right)\right]$$

$$\equiv R_1 \qquad \text{(A86)}$$

c. Combustion Integrals I_4 and I_5

We evaluate the pair $I_{4_{ki}}$ and $I_{5_{ki}}$:

$$I_{4_{ki}} \equiv \int_0^{l_{21}} \hat{\psi}_k(z') \cdot \hat{\psi}_i(z') \cdot e^{-z'/\bar{v}\bar{\tau}} \, dz'$$

$$I_{5_{ki}} \equiv \int_0^{l_{21}} \hat{\psi}_k(z') \, \frac{d\hat{\psi}_i}{dz'}(z') \, e^{-z'/\bar{v}\bar{\tau}} \, dz'$$

with the same method used above for I_1, I_2.

$$\left[\left(\frac{\omega_i}{c_2}\right)^2 - \left(\frac{\omega_k}{c_2}\right)^2 - \left(\frac{1}{\bar{v}\bar{\tau}}\right)^2\right] \cdot I_{4_{ki}} + 2\left(\frac{1}{\bar{v}\bar{\tau}}\right) \cdot I_{5_{ki}} = \tag{A87}$$

$$= \int_0^{l_{21}} e^{-\frac{z'}{\bar{v}\bar{\tau}}} \left\{ \hat{\psi}_i \frac{d\hat{\psi}_k}{dz} - \hat{\psi}_k \frac{d\hat{\psi}_i}{dz} + \frac{1}{\bar{v}\bar{\tau}} \hat{\psi}_i \hat{\psi}_k \right\}$$

$$\left[\left(\frac{\omega_i}{c_2}\right)^2 - \left(\frac{\omega_k}{c_2}\right)^2 - \left(\frac{1}{\bar{v}\bar{\tau}}\right)^2\right] I_{5_{ki}} - 2\left(\frac{1}{\bar{v}\bar{\tau}}\right)\left(\frac{\omega_i}{c_2}\right)^2 \cdot I_{4_{ki}} = \tag{A88}$$

$$= \int_0^{l_{21}} e^{-\frac{z'}{\bar{v}\bar{\tau}}} \left\{ \frac{d\hat{\psi}_k}{dz} \frac{d\hat{\psi}_i}{dz} + \left(\frac{\omega_i}{c_2}\right)^2 \hat{\psi}_i \hat{\psi}_k + \frac{1}{\bar{v}\bar{\tau}} \hat{\psi}_k \frac{d\hat{\psi}_i}{dz} \right\}$$

Write R_4, R_5 for the right-hand sides of these two equations and define

$$\mathcal{L}_4 \equiv \left(\frac{\omega_i}{c_2}\right)^2 - \left(\frac{\omega_k}{c_2}\right)^2 - \left(\frac{1}{\bar{U}\bar{t}}\right)^2$$

Then

$$\underset{ki}{I_4} = \frac{\mathcal{L}_4 R_4 - \frac{2}{\bar{U}\bar{t}} R_5}{\mathcal{L}_4^2 + \left(\frac{2}{\bar{U}\bar{t}} \cdot \frac{\omega_i}{c_2}\right)^2} \tag{A89}$$

$$\underset{ki}{I_5} = \frac{\left(\frac{2}{\bar{U}\bar{t}} \cdot \frac{\omega_i}{c_2}\right)^2 R_4 + \mathcal{L}_4 R_5}{\mathcal{L}_4^2 + \left(\frac{2}{\bar{U}\bar{t}} \cdot \frac{\omega_i}{c_2}\right)^2} \tag{A90}$$

10. REDUCTION OF THE DOUBLE INTEGRALS IN COMBUSTION

For the cumulative (time-delay) contributions to the heat release rate we require the (doubly-subscripted) integrals:

$$\hat{\hat{S}}_{ki} = \int_0^{l_{21}} F_{ki}(y) \sin\left(\frac{\omega_i y}{\bar{U}}\right) dy$$

$$\hat{\hat{C}}_{ki} = \int_0^{l_{21}} F_{ki}(y) \cos\left(\frac{\omega_i y}{\bar{U}}\right) dy \tag{A37}$$

where

$$\bar{F}_{Ri}(y) = \int_{y}^{l_{21}} \hat{\psi}_i(z'-y)\,\hat{\psi}_R(z')\,e^{-\frac{z'}{\bar{U}\tau}}\,dz \qquad \text{(A38)}$$

where we measure the integration variables over the hot chamber (y, z) as distances downstream from the flameholder, and write:

$$\hat{\psi}_R(z') \equiv \psi_R(l_1+z') = \psi_R(z) \qquad \text{(A35)}$$

Also define here

$$SINL \equiv \sin\left(\frac{\omega_i l_{21}}{\bar{U}}\right)$$

$$COSL \equiv \cos\left(\frac{\omega_i l_{21}}{\bar{U}}\right)$$

$$EXPL \equiv \exp\left(-\,l_{21}/\bar{U}\tau\right)$$

Note: the first two of these depend on the second index (i) of the integrals we are evaluating. Noting that $\bar{F}_{Ri}(y)$ contains the argument y as both a limit of integration and a parameter in the integrand, we use Leibniz' rule:

$$\frac{d}{dy}\left(-\bar{F}_{Ri}(y)\right) = -\int_{l_{21}}^{y} \frac{d\hat{\psi}_i(z'-y)}{dz'}\,\hat{\psi}_k(z')\,e^{-\frac{z'}{\bar{v}\bar{\tau}}}\,dz' + \tag{A91}$$

$$+\ \psi_i(l_1)\,\hat{\psi}_k(y)\,e^{y/\bar{v}\bar{\tau}}$$

$$\frac{d^2}{dy^2}\left(-\bar{F}_{Ri}(y)\right) + \left(\frac{\omega_i}{c_2}\right)^2\left(-\bar{F}_{Ri}(y)\right) =$$

$$= e^{-y/\bar{v}\bar{\tau}}\left\{\psi_i(l_1)\left[\frac{d\hat{\psi}_k(y)}{dy} - \frac{1}{\bar{v}\bar{\tau}}\,\hat{\psi}_k(y)\right]\right. \tag{A92}$$

$$\left. - \frac{d\psi_i}{dy}(l_1^+)\,\psi_k(y)\right\}$$

From the above

$$\bar{F}_{ki}(l_{21}) = 0$$

$$\bar{F}_{ki}(0) = \bar{I}_{4_{ki}}$$

$$-\frac{d\bar{F}_{ki}}{dy}(l_{21}) = \psi_i(l_1)\,\psi_k(l_2)\,e^{-\frac{l_{21}}{\bar{v}\bar{\tau}}}$$

$$-\frac{d\bar{F}_{ki}}{dy}(0) = \bar{I}_{\bar{\sigma}_{ki}} + \psi_i(l_1)\,\psi_k(l_1)$$

Using integration by parts directly, we write

$$\int_0^{l_{21}} \cos\left(\frac{\omega_i y}{\bar{v}}\right) \cdot \frac{d^2\left(-\bar{F}_{ki}(y)\right)}{dy^2}\, dy =$$

$$= \left(\frac{\omega_i}{\bar{v}}\right)^2 \hat{\hat{C}}_{ki} +$$

$$+ \int_0^{l_{21}} \left\{ \cos\left(\frac{\omega_i y}{\bar{v}}\right) \frac{d(-\bar{F}_{ki})}{dy} - \left(\frac{\omega_i}{\bar{v}}\right) \sin\left(\frac{\omega_i y}{\bar{v}}\right) F_{ki} \right\} = \tag{A93}$$

$$= \left(\frac{\omega_i}{\bar{v}}\right)^2 \hat{\hat{C}}_{ki} +$$

$$+ \cos L \cdot \psi_i(l_1)\,\psi_k(l_2)\, e^{-\frac{l_{21}}{\bar{v}\bar{\tau}}} - \bar{I}_{\bar{\sigma}_{ki}} - \psi_i(l_1)\psi_k(l_1)$$

$$\int_0^{l_{21}} \sin\left(\frac{\omega_i y}{\bar{v}}\right) \frac{d^2}{dy^2}\left(-\bar{F}_{ki}(y)\right) dy =$$

$$= \left(\frac{\omega_i}{\bar{v}}\right)^2 \hat{\hat{S}}_{ki} +$$

$$+ \int_0^{l_{21}} \left\{ \sin\left(\frac{\omega_i y}{\bar{v}}\right) \frac{d\left[-\bar{F}_{ki}(y)\right]}{dy} + \bar{F}_{ki}(y) \cdot \left(\frac{\omega_i}{\bar{v}}\right) \cdot \cos\left(\frac{\omega_i y}{\bar{v}}\right) \right. \tag{A94}$$

$$= \left(\frac{\omega_i}{\bar{v}}\right)^2 \hat{\hat{S}}_{ki} + SINL \cdot \psi_i(l_1)\psi_k(l_2) \cdot e^{-l_{21}/\bar{v}\bar{\tau}} - \frac{\omega_i}{\bar{v}} I_{4_{ki}}$$

Multiply Equation A92 by $\sin\left(\frac{\omega_i y}{\bar{v}}\right)$ or $\cos\left(\frac{\omega_i y}{\bar{v}}\right)$ and integrate over the hot chamber.

$$\int_0^{l_{21}} \sin \frac{\omega_i y}{\bar{v}} \frac{d^2}{dy^2}\left(-\bar{F}_{ki}(y)\right) dy =$$

(A95)

$$= \left(\frac{\omega_i}{c_2}\right)^2 \hat{\hat{S}}_{ki} +$$

$$+ \psi_i(l_1)\left\{ SINL\ \psi_k(l_2) e^{-\frac{l_{21}}{\bar{v}\bar{\tau}}} - \left(\frac{\omega_i}{\bar{v}}\right) I_{2_{ki}} \right\} - \frac{d\psi_i}{dy}(l_1^+) I_{1_{ki}}$$

$$\int_0^{l_{21}} \cos\frac{\omega_i y}{\bar{v}} \frac{d^2}{dy^2}\left(-\bar{F}_{ki}(y)\right) dy =$$

$$= \left(\frac{\omega_i}{c_2}\right)^2 \hat{\hat{C}}_{ki} +$$

$$+ \psi_i(l_1)\left[\cos L \cdot \psi_k(l_2)\, e^{-\frac{l_{21}}{\bar{v}}\bar{z}} - \psi_k(l_1) + \left(\frac{\omega_i}{\bar{v}}\right) \bar{I}_{k'i}\right] \quad \text{(A96)}$$

$$- \frac{d\psi}{dy}(l_1^+)\, \bar{I}^2_{ki}$$

Equate the RHS of Equations A94 and A95:

$$\hat{\hat{S}}_{ki} = \frac{1}{\left[\left(\frac{\omega_i}{\bar{v}}\right)^2 - \left(\frac{\omega_i}{c_2}\right)^2\right]} \left[\left(\frac{\omega_i}{\bar{v}}\right)\bar{I}^4_{ki} - \left(\frac{\omega_i}{\bar{v}}\right)\psi_i(l_1)\,\bar{I}^2_{ki} - \frac{d\psi_i}{dy}(l_1^+)\,\bar{I}^1_{k'i}\right] \quad \text{(A97)}$$

Equate the RHS of Equations A93 and A96:

$$\hat{\hat{C}}_{ki} = \frac{1}{\left[\left(\frac{\omega_i}{\bar{v}}\right)^2 - \left(\frac{\omega_i}{c_2}\right)^2\right]} \cdot \left[\bar{I}^5_{ki} + \frac{\omega_i}{\bar{v}} \cdot \psi_i(l_1) \cdot \bar{I}_{ki} - \frac{d\psi_i}{dy}(l_1^+) \cdot \bar{I}^2_{ki}\right] \quad \text{(A98)}$$

11. TRIPLE SINE AND COSINE TIME AVERAGED INTEGRALS

At various times in the derivation of the final equations integrals of triple triginometric functions are encountered. They are derived below.

$$\int_t^{t+\bar{\tau}} \cos\omega_i t' \cdot \cos\omega_j t' \cdot \sin\omega_k t'\, dt' =$$

$$= \frac{1}{4}\left[\frac{2}{p_1} \sin p_1\left(t+\frac{\bar{\tau}}{2}\right) \cdot \sin\frac{p_1\bar{\tau}}{2} + \right.$$

$$+ \frac{2}{p_2} \sin p_2\left(t+\frac{\bar{\tau}}{2}\right) \cdot \sin\frac{p_2\bar{\tau}}{2} +$$

$$+ \frac{2}{p_3} \sin p_3\left(t+\frac{\bar{\tau}}{2}\right) \cdot \sin\frac{p_3}{2}\bar{\tau} +$$

$$\left. + \frac{2}{p_4} \sin p_4\left(t+\frac{\bar{\tau}}{2}\right) \cdot \sin\frac{p_4\bar{\tau}}{2} \right]$$

$$\int_t^{t+\bar{\tau}} \cos\omega_i t' \cdot \cos\omega_j t' \cdot \cos\omega_k t'\, dt' =$$

$$= \frac{1}{4}\left[\frac{2}{p_1} \cos p_1\left(t+\frac{\bar{\tau}}{2}\right) \cdot \sin\frac{p_1\bar{\tau}}{2} + \right.$$

$$+ \frac{2}{p_2} \cos p_2\left(t+\frac{\bar{\tau}}{2}\right) \sin\frac{p_2\bar{\tau}}{2} +$$

$$+ \frac{2}{p_3} \cos p_3\left(t+\frac{\bar{\tau}}{2}\right) \cdot \sin\frac{p_3\bar{\tau}}{2} +$$

$$\left. + \frac{2}{p_4} \cos p_4\left(t+\frac{\bar{\tau}}{2}\right) \cdot \sin\frac{p_4\bar{\tau}}{2} \right]$$

where

$$p_1 \equiv \omega_k + \omega_i - \omega_j$$

$$p_2 \equiv \omega_k - \omega_i + \omega_j$$

$$p_3 \equiv \omega_k + \omega_i + \omega_j$$

$$p_4 \equiv \omega_k - \omega_i - \omega_j$$

$$\int_t^{t+\bar{\tau}} \sin\omega_i t' \cdot \sin\omega_j t' \cdot \sin\omega_k t' \, dt =$$

$$= \frac{1}{4}\left[\frac{2}{p_1} \sin p_1\left(t+\frac{\bar{\tau}}{2}\right) \cdot \sin\frac{p_1\bar{\tau}}{2} + \right.$$

$$+ \frac{2}{p_2} \sin p_2\left(t+\frac{\bar{\tau}}{2}\right) \cdot \sin\frac{p_2\bar{\tau}}{2} -$$

$$- \frac{2}{p_3} \sin p_3\left(t+\frac{\bar{\tau}}{2}\right) \cdot \sin\frac{p_3\bar{\tau}}{2} -$$

$$\left. - \frac{2}{p_4} \sin p_4\left(t+\frac{\bar{\tau}}{2}\right) \cdot \sin\frac{p_4\bar{\tau}}{2} \right]$$

$$\int_{t}^{t+\tau} \sin \omega_j t \cdot \cos \omega_i t \cdot \sin \omega_k t \, dt =$$

$$= \frac{1}{4}\left[\frac{2}{p_1} \cos p_1\left(t + \frac{\tau}{2}\right) \cdot \sin \frac{p_1 \tau}{2} - \right.$$

$$- \frac{2}{p_2} \cos p_2\left(t + \frac{\tau}{2}\right) \cdot \sin \frac{p_2 \tau}{2} -$$

$$- \frac{2}{p_3} \cos p_3\left(t + \frac{\tau}{2}\right) \cdot \sin \frac{p_3 \tau}{2} +$$

$$\left. + \frac{2}{p_4} \cos p_4\left(t + \frac{\tau}{2}\right) \cdot \sin \frac{p_4 \tau}{2} \right]$$

where

$p_{1..}$ is as before

12. EVALUATION OF ORTHOGONALITY MATRIX

In the following the orthogonality matrix

$$\int_{0}^{l_2} \psi_k(z) \cdot \psi_i(z) \, dz$$

in terms of the values of the acoustic nodes k and i at the flameholder and the end boundaries is evaluated.

For $i \neq k$

$$\int_0^{l_2} \psi_k \psi_i \, dz = \frac{1}{(\omega_i^2 - \omega_k^2)} \Big|_0^{l_2} \left(\frac{d\psi_k}{dz} \psi_i - \frac{d\psi_i}{dz} \psi_k \right)$$

For $i = k$

$$\int_0^{l_2} \psi_k \psi_k \, dz = \frac{1}{2\omega_k^2} \cdot \left\{ c_2^2 \frac{d\psi_k}{dz}(l_2) \left[l_2 \cdot \frac{d\psi_k}{dz}(l_2) - \psi_k(l_2) \right] + \right.$$

$$+ l_2 \cdot \omega_k^2 \cdot \psi_k^2(l_2) +$$

$$+ \psi_k(0) \cdot \frac{d\psi_k}{dz}(0) \cdot c_1^2 +$$

$$\left. + l_1 \cdot \left[\frac{1}{c_1^2} - \frac{1}{c_2^2} \right] \cdot \left[c_2^2 \frac{d\psi_k}{dz} l_1^+ \right]^2 \right\}$$

With

$$\psi_i = R_i \cos(k_i z + \theta_i) \qquad 0 \leq z \leq l_1$$
$$\psi_j = R_j \cos(k_j z + \theta_j)$$

$$\psi_i = \cos(\hat{k}_i z + \hat{\theta}_i) \qquad l_1 < z \leq l_2$$
$$\psi_j = \cos(\hat{k}_j z + \hat{\theta}_j)$$

Then

$$\int_0^{l_2} \psi_i \, \psi_j \, dz =$$

$$= R_i R_j \left\{ \cos\left[(k_i + k_j) \cdot \frac{l_1}{2} + (\theta_i + \theta_j) \right] \cdot \frac{\sin\left[(k_i + k_j) \cdot \frac{l_1}{2} \right]}{(k_i + k_j)} + \right.$$

$$\left. + \cos\left[(k_i - k_j) \cdot \frac{l_1}{2} + (\theta_i - \theta_j) \right] \cdot \frac{\sin\left[(k_i - k_j) \cdot \frac{l_1}{2} \right]}{(k_i - k_j)} \right\} +$$

$$+ \left\{ \cos\left[(\hat{k}_i + \hat{k}_j) \cdot \left(\frac{l_1 + l_2}{2} \right) + (\hat{\theta}_i + \hat{\theta}_j) \right] \cdot \frac{\sin\left[(\hat{k}_i + \hat{k}_j) \cdot \left(\frac{l_2 - l_1}{2} \right) \right]}{(\hat{k}_i + \hat{k}_j)} \right.$$

$$\left. + \cos\left[(\hat{k}_i - \hat{k}_j) \cdot \left(\frac{l_1 + l_2}{2} \right) + (\hat{\theta}_i - \hat{\theta}_j) \right] \cdot \frac{\sin\left[(\hat{k}_i - \hat{k}_j) \cdot \left(\frac{l_2 - l_1}{2} \right) \right]}{(\hat{k}_i - \hat{k}_j)} \right\}$$

When $i = j$ the second, fourth terms become respectively,

$$\frac{l_1}{2} \quad ; \left(\frac{l_2 - l_1}{2}\right)$$

APPENDIX B

SOURCE LISTING OF PROGRAM NØNLIN

```
      PROGRAM NONLIN(INPUT,OUTPUT,TAPE5=INPUT,TAPE6=OUTPUT)

C           ANALYSIS OF NONLINEAR COMBUSTION STABILITY

      COMMON/CIN/COMENT(18),NM,TZERO,TFIN,TSTEP,AFIRST(5),BFIRST(5),
     1GAM,C1,C2,FL1,FL2,W(5),THU(5),THD(5),VELC,A1,A2,R1,R2,FL3,FUFL,
     2TAUR,EBAR,C1TL,C2TL,NZSTEP,NPRINT,ITAU
      COMMON /COUT/HOED(5),R(5),ORTH(5,5),OORM(5),ORTI(5,5),DCOEF(5,5),
     1ECOEF(5,5),ACOEF(5,5,5),BCOEF(5,5,5),PS2(5),PSD2(5),PSU(5),
     2PSDU(5),TAU,ISTORE,INST,IFIN,TIME(40),TA(40,5),TB(40,5),TSQ(40,5),
     3TETA(40,5),TETD(40,5),TEN(40),TPR(40,40)

      DIMENSION QA(5),QB(5),ARTH(5,10),A(5),B(5),PA(5),PB(5),
     1ETA(5),ETD(5),PRSS(40)
      DIMENSION DTEMP(5,5),ETEMP(5,5),ATEMP(5,5,5),BTEMP(5,5,5)
      DIMENSION PPA(5),PPB(5)
      EXTERNAL DERIV
      DATA PI/3.1415926536/

C     CALL SUBROUTINE INPUT TO READ AND WRITE THE INPUT DATA

   10 CALL INPUT
      INST=0
      IFIN=0

C     CALL SUBROUTINE ORTHOG TO CALCULATE INNER-PRODUCT MATRIX

      CALL ORTHOG
      NMP=NM+1
      NM2=2*NM
      DO 100 I=1,NM
      DO 50 J=1,NM
   50 ARTH(I,J)=ORTH(I,J)
      DO 75 J=NMP,NM2
   75 ARTH(I,J)=0.0
      INM=I+NM
  100 ARTH(I,INM)=1.0

C     CALL SUBROUTINE SIMEQ TO INVERT INNER-PRODUCT MATRIX

      CALL SIMEQ(ARTH,ORTI,DET,NM,NM,1,LSGN,LEXP,5,10,5)

C      CALL SUBROUTINE LINCOF TO CALCULATE COMBUSTION CONTRIBUTION

      CALL LINCOF

C      CALL SUBROUTINE ARMAT TO CALCULATE ACOEF AND BCOEF

      CALL ARMAT
      DO 110 K=1,NM
      DO 110 I=1,NM
      DTEMP(K,I)=DCOEF(K,I)
      ETEMP(K,I)=ECOEF(K,I)
      DO 110 J=1,NM
      ATEMP(K,I,J)=ACOEF(K,I,J)
  110 BTEMP(K,I,J)=BCOEF(K,I,J)
      DO 140 K=1,NM
```

```
      DO 140 I=1,NM
      DDC=0.0
      EEC=0.0
      DO 130 J=1,NM
      DDC=DDC+ORTI(K,J)*DTEMP(J,I)
      EEC=EEC+ORTI(K,J)*ETEMP(J,I)
      AAC=0.0
      BBC=0.0
      DO 120 L=1,NM
      AAC=AAC+ORTI(K,L)*ATEMP(L,I,J)
  120 BBC=BBC+ORTI(K,L)*BTEMP(L,I,J)
      ACOEF(K,I,J)=AAC
  130 BCOEF(K,I,J)=BBC
      DCOEF(K,I)=DDC
  140 ECOEF(K,I)=EEC

C     CALL SUBROUTINE OUTPT1 TO PRINT TIME-INDEPENDENT OUTPUT

      CALL OUTPT1
      DELZ=EL2/FLOAT(NZSTEP)
      EL21=EL2-EL1
      IF(ITAU.NE.1)  TAU=2.0*PI/W(1)
      ITIME=1
      ISTORE=0
      T=TZERO
      TP=T
      DO 150 I=1,NM
      A(I)=AFIRST(I)
      B(I)=BFIRST(I)
      PA(I)=A(I)
      PB(I)=B(I)
      QA(I)=0.0
  150 QB(I)=0.0

C     CALL SUBROUTINE RUNKUT TO PERFORM TIME INTEGRATION

  200 CALL RUNKUT(TP,TSTEP,PA,QA,PB,QB,DERIV,NM)
      CALL DERIV(TP,PA,PPA,PB,PPB)
      DO 300 I=1,NM
      PAI=PA(I)
      PBI=PB(I)
      WI=W(I)
      SINWT=SIN(WI*TP)
      COSWT=COS(WI*TP)
      ETA(I)=PAI*SINWT+PBI*COSWT
      DETA=WI*(PAI*COSWT-PBI*SINWT)
  300 ETD(I)=DETA+(PPA(I)*SINWT+PPB(I)*COSWT)/TSTEP
      ENERGY=0.0
      DO 400 I=1,NM
      ETAI=ETA(I)
      PS2I=PS2(I)
      PSUI=PSU(I)
      DI=ETD(I)/W(I)**2
      DO 400 J=1,NM
      DVAR=C2**2*PS2I*PSD2(J)-C1**2*PSUI*PSDU(J)
      ORTHJ=ORTH(J,I)
      VAR=DVAR+W(J)**2*ORTHJ
```

```
      TERM1=VAR*DI*ETD(J)/W(J)**2+ETAI*ETA(J)*ORTH.I
  400 ENERGY=ENERGY+0.5*TERM1/GAM
      Z=0.0
      DO 500 IZ=1,NZSTEP
      PRP=0.0
      Z=Z+DELZ
      DO 450 I=1,NM
      IF(Z.GT.EL1) GO TO 410
      SPATI=R(I)*COS(W(I)*Z/C1+THU(I))
      GO TO 450
  410 SPATI=COS(W(I)*Z/C2+THD(I))
  450 PRP=PRP+ETA(I)*SPATI
  500 PRSS(IZ)=PRP
      T=TP
      DO 550 I=1,NM
      A(I)=PA(I)
      B(I)=PB(I)
      IF (A(I).GT.1.0.OR.B(I).GT.1.0) INST=1
  550 CONTINUE
      IF (T.GE.TFIN-1.0E-6) IFIN=1
      IF (ITIME.NE.NPRINT*(ITIME/NPRINT).AND.IFIN+INST.EQ.0) GO TO 750
      ISTORE=ISTORE+1
      TIME(ISTORE)=T
      DO 600 I=1,NM
      TA(ISTORE,I)=A(I)
      TB(ISTORE,I)=B(I)
      TSQ(ISTORE,I)=SQRT(A(I)**2+B(I)**2)
      TETA(ISTORE,I)=ETA(I)
  600 TETD(ISTORE,I)=ETD(I)
      DO 650 IZ=1,NZSTEP
  650 TPR(ISTORE,IZ)=PRSS(IZ)
      TEN(ISTORE)=ENERGY
      IF (IFIN+INST.EQ.0.AND.ISTORE.LT.40) GO TO 750

C     CALL SUBROUTINE OUTPT2 TO PRINT TIME-DEPENDENT OUTPUT

  700 CALL OUTPT2
      IF (IFIN+INST.GT.0) GO TO 10
      ISTORE=0
  750 ITIME=ITIME+1
      GO TO 200
      END
```

```
      SUBROUTINE INPUT
      COMMON/CIN/COMENT(18),NM,TZERO,TFIN,TSTEP,AFIRST(5),BFIRST(5),
     1GAM,C1,C2,EL1,EL2,W(5),THU(5),THD(5),VELC,A1,A2,B1,B2,EL3,FUEL,
     2TAUB,EBAR,C1TL,C2TL,NZSTEP,NPRINT,ITAU
      DATA HDASH/10H----------/,HDOT/10H../
      DATA HSTOP/4HSTOP/
      READ(5,10) COMENT
   10 FORMAT(18A4)
      IF(COMENT(1).EQ.HSTOP) STOP
      READ(5,20) NM,NZSTEP,ITAU,NPRINT
   20 FORMAT (12I6)
      IF(NM.LT.1) NM=5
      IF(NZSTEP.LT.1) NZSTEP=40
      IF (NPRINT.LT.1) NPRINT=1
      READ(5,40) TZERO,TFIN,TSTEP
   40 FORMAT(6E12.5)
      IF(TFIN.LT.TZERO) TFIN=TZERO+1.0
      IF (TSTEP.LE.0.0) TSTEP=0.005
      READ(5,40) (AFIRST(I),I=1,NM)
      READ(5,40) (BFIRST(I),I=1,NM)
      READ(5,40) GAM,C1,C2,EL1,EL2
      IF(GAM.LE.0.0) GAM=1.4
      READ(5,50) (W(I),THU(I),THD(I),I=1,NM)
   50 FORMAT (3E12.5)
      READ(5,40) EL3,A1,A2,B1,B2
      READ(5,40)       VELC,TAUB,EBAR,C1TL
      WRITE(6,100) (HDASH,I=1,5)
  100 FORMAT (1H1/////////////38X,4H----,5A10///38X,2HAN          ///36X,
     1
     256H  NNN       NNN  RRRRRRRRRR   EEEEEEEEEE     CCCCCCCCC    /36X,
     356H  NNNN      NNN  RRRRRRRRRRR  EEEEEEEEEE    CCCCCCCCCCC   /36X,
     456H  NNNNN     NNN  RRR       RRR  EEE          CCC       CCC  /36X,
     556H  NNNNNN    NNN  RRR       RRR  EEE          CCC            /36X,
     656H  NNNNNNN   NNN  RRRRRRRRRRR  EEEEEEEE     CCC            /36X,
     756H  NNN NNNN NNN  RRRRRRRRRR   EEEEEEEE     CCC            /36X,
     856H  NNN  NNNNNNN  RRR RRRR      EEE          CCC            /36X,
     956H  NNN   NNNNNN  RRR  RRRR     EEE          CCC            /36X,
     156H  NNN    NNNNN  RRR   RRRR    EEE          CCC       CCC  /36X,
     256H  NNN     NNNN  RRR    RRRR   EEEEEEEEEEE  CCCCCCCCCCC   /36X,
     356H  NNN      NNN  RRR     RRRR  EEEEEEEEEEE   CCCCCCCCC
     4                                                ///71X,
     516HCOMPUTER PROGRAM)
      WRITE(6,110) (HDASH,I=1,5)
  110 FORMAT(/////38X,17HPROGRAM NONLIN -//
     148X,44HANALYSIS OF NONLINEAR COMBUSTION INSTABILITY///
     238X,4H----,5A10)
      WRITE(6,120) COMENT,(HDASH,I=1,9)
  120 FORMAT(1H1/1X,19HNREC PROGRAM NONLIN///30X,18A4/30X,
     12H--,7A10///          61X,A10/61X,10HINPUT DATA/61X,A10)
      WRITE(6,130) (HDOT,I=1,3),TZERO,(HDOT,J=1,3),TFIN,
     1          (HDOT,K=1,2),TSTEP
  130 FORMAT(///33X,24HINITIAL TIME, SEC........,3A10,F12.4/33X,
     124HLIMITING TIME, SEC.......   3A10,F12.4/33X,
     234HCOMPUTATIONAL TIME INCREMENT, SEC.,2A10,F12.4)
      IF (ITAU-1) 150,135,165
  135 WRITE (6,140) (HDOT,I=1,4)
  140 FORMAT(    33X,14HAVERAGING TIME,          4A10,14HMODE DEPENDENT)
```

```
      GO TO 170
  150 WRITE(6,160) (HDOT,I=1,4)
  160 FORMAT (     33X, 14HAVERAGING TIME,       4A10,16HMODE INDEPENDENT)
      GO TO 170
  165 WRITE (6,166) (HDOT,I=1,4)
  166 FORMAT (33X,14HAVERAGING TIME,4A10,12H  MIXED MODE)
  170 WRITE(6,180) (HDOT,I=1,3),EL2,(HDOT,J=1,2),EL1,(HDOT,K=1,2),EL3
  180 FORMAT(/33X,24HTOTAL CHAMBER LENGTH, FT,3A10,F12.3/
     133X,34HLENGTH TO FLAMEHOLDER, FT.........   2A10,F12.3/
     233X,34HLENGTH TO FUEL INJECTOR, FT.......   2A10,F12.3)
      WRITE(6,190) (HDOT,I=1,3),GAM,C1,C2
  190 FORMAT(/33X,24HRATIO OF SPECIFIC HEATS.,3A10,F12.3/
     133X,54HSOUND VELOCITY UPSTREAM (OF FLAMEHOLDER), FPS.........,
     2F12.0/
     333X,54HSOUND VELOCITY DOWNSTREAM (OF FLAMEHOLDER), FPS........
     4F12.0)
      WRITE(6,200) A1,B1,A2,B2
  200 FORMAT (/33X,54HVELOCITY PROFILE UPSTREAM   - AXIAL COEF, PER SEC.
     1....., F12.3/69X,18HCONSTANT, FPS.....,F12.2/
     233X,54HVELOCITY PROFILE DOWNSTREAM - AXIAL COEF, PER SEC......
     3F12.3/69X,18HCONSTANT, FPS.....,F12.2)
      WRITE(6,210)                    HDOT,VELC,HDOT,TAUB,(HDOT,J=1,3),
     1EBAR,HDOT,C1TL
  210 FORMAT (/
     133X,44HCHARACTERISTIC COMBUSTION VELOCITY, FPS.....,A10,F12.0/
     233X,44HCHARACTERISTIC COMBUSTION TIME, SEC.........,A10,F12.5/
     333X,24HENERGY CONTENT, FPS**2..,3A10,F12.0/
     433X,44HUNSTEADY COMBUSTION COEFFICIENT.............,A10,F12.6)
      WRITE(6,250) (HDASH,I=1,8),(I,W(I),THU(I),THD(I),AFIRST(I),
     1                           BFIRST(I),I=1,NM)
  250 FORMAT(///  51X,14HACOUSTIC WAVES,18X,15HTRAVELING WAVES/
     140X,5H-----,3A10,5X,1H-,2A10/
     241X,7HNATURAL,5X,22HINDEX OF LOCATION, RAD,5X,20HINITIAL AMPLITUDE
     3 OF/   31X,4HMODE,5X,10HFREQUENCY,3X,2H--,2A10/
     430X,6HNUMBER,5X,7HRAD/SEC,6X,8HUPSTREAM,3X,10HDOWNSTREAM,5X,
     58HSIN TERM,5X,8HCOS TERM/
     630X,6H------,4X,9H---------,4X,9H---------,3X,A10,5X,8H--------,
     75X,8H--------//(33X,I1,F13.3,2F13.5,2F13.7))
      RETURN
      END
```

```
      SUBROUTINE ORTHOG

C     CALCULATION OF INNER-PRODUCT MATRIX

      COMMON/CIN/COMENT(18),NM,TZERO,TFIN,TSTEP,AFIRST(5),BFIRST(5),
     1GAM,C1,C2,EL1,EL2,W(5),THU(5),THD(5),VELC,A1,A2,B1,B2,EL3,FUEL,
     2TAUR,EBAR,C1TL,C2TL,NZSTEP,NPRINT,ITAU
      COMMON /COUT/HOED(5),R(5),ORTH(5,5),OORM(5),ORTI(5,5),DCOEF(5,5),
     1ECOEF(5,5),ACOEF(5,5,5),BCOEF(5,5,5),PS2(5),PSD2(5),PSU(5),
     2PSDU(5),TAU,ISTORE,INST,IFIN,TIME(40),TA(40,5),TB(40,5),TSQ(40,5),
     3TETA(40,5),TETD(40,5),TEN(40),TPR(40,40)

      DO 10 I=1,NM
      COS1=COS(W(I)*EL1/C1+THU(I))
      COS2=COS(W(I)*EL1/C2+THD(I))
      PAR=COS1*COS2
      RELSQ=COS2**2+(C2/C1)**2*(1.0-COS2**2)
   10 R(I)=SQRT(RELSQ)*SIGN(1.0,PAR)
      DO 100 J=1,NM
      WJ=W(J)
      THUJ=THU(J)
      THDJ=THD(J)
      DO 70 I=1,NM
      WI=W(I)
      P1=(WI+WJ)*EL1/C1
      SIN1=SIN(P1/2.0)*EL1/P1
      TERM1=COS(P1/2.0+THU(I)+THUJ)*SIN1
      IF(I.NE.J) GO TO 40
      TERM2=EL1/2.0
      GO TO 50
   40 P2=(WI-WJ)*EL1/C1
      SIN2=SIN(P2/2.0)*EL1/P2
      TERM2=COS(P2/2.0+THU(I)-THUJ)*SIN2
   50 P3=(EL1+EL2)/2.0
      P4=(EL2-EL1)/2.0
      SIN3=SIN((WI+WJ)*P4/C2)*C2/(WI+WJ)
      TERM3=COS((WI+WJ)*P3/C2+THD(I)+THDJ)*SIN3
      IF(I.NE.J) GO TO 60
      TERM4=P4
      GO TO 70
   60 SIN4=SIN((WI-WJ)*P4/C2)*C2/(WI-WJ)
      TERM4=COS((WI-WJ)*P3/C2+THD(I)-THDJ)*SIN4
   70 ORTH(I,J)=R(I)*R(J)*(TERM1+TERM2)+TERM3+TERM4
  100 OORM(J)=ORTH(J,J)
      RETURN
      END
```

```
      SUBROUTINE  SIMEQ(A,X,DET,NR,NS,NDEX,LSGN,LEXP,NRD,NCD,NSD)

C               A - MATRIX AUGMENTED BY CONSTANT VECTORS
C               X - SOLUTION MATRIX
C               DET - DETERMINANT, NORMALIZED
C               NR - NO OF ROWS
C               NS - NO OF SOLUTIONS
C               NDEX - -1 -DET ONLY
C                       0  -SOLUTION ONLY
C                      +1 -BOTH DET AND SOLUTION
C               LSGN - AS OUTPUT = 0 UNLESS SINGULAR
C                      OTHERWISE = ROW OF SINGULARITY
C               LEXP - EXPONENT INDICATOR FOR DET
C                      DETERMINANT=DET*10.**LEXP
C          1000 SERIES SETS UP SOLUTION TYPE

      DIMENSION A(NRD,NCD),X(NRD,NSD)
 1000 IF (NDEX) 1800, 1500, 1200
 1200 ASSIGN 4100 TO MRIPAS
      ASSIGN 3100 TO NRIPAS
      GO TO 1900
 1500 ASSIGN 5000 TO MRIPAS
      ASSIGN 3100 TO NRIPAS
      GO TO 2000
 1800 ASSIGN 4100 TO MRIPAS
      ASSIGN 4000 TO NRIPAS
 1900 LSGN=1
      LEXP=0
      DET=1.0
C          2000 SERIES TRIANGULARIZES MATRIX
 2000 NC=NR+NS
      I=1
C          2100 SERIES MAXIMIZES PIVOTAL ELEMENT
 2100 S= ABS(A(I,I))
      J=I
      IF (I-NR) 2110,2150,3000
 2110 K=I+1
 2120 T= ABS(A(K,I))
      IF (T .LE. S) GO TO 2130
      S=T
      J=K
 2130 K=K+1
      IF (K .LE. NR) GO TO 2120
 2150 IF (S .EQ. 0.0) GO TO 9000
C          2200 SERIES INTERCHANGES ROWS IF NECESSARY
 2200 IF (J .LE. I) GO TO 2500
      LSGN=-LSGN
      K=I
 2250 R=A(I,K)
      A(I,K)=A(J,K)
      A(J,K)=R
      K=K+1
      IF (K .LE. NC) GO TO 2250
C          2500 SERIES THEN REDUCES WITH ZERO CHECK
 2500 J=I+1
 2510 IF (J .LE. NC) GO TO 2520
      I=I+1
```

```
      GO TO 2100
 2520 IF (A(I,J).EQ.0.0) GO TO 2590
      A(I,J)=A(I,J)/A(I,I)
      K=I+1
 2530 IF (K .GT. NR) GO TO 2590
      A(K,J)=A(K,J)-A(I,J)*A(K,I)
      K=K+1
      GO TO 2530
 2590 J=J+1
      GO TO 2510
C          3000 SERIES COMPUTES SOLUTION
 3000 GO TO NRIPAS, (3100,4000)
 3100 K=1
 3200 L=NR+K
      X(NR,K)=A(NR,L)
      I=NR-1
 3300 J=I+1
      R=0.0
 3400 R=R+A(I,J)*X(J,K)
      J=J+1
      IF (J .LE. NR) GO TO 3400
      X(I,K)=A(I,L)-R
      I=I-1
      IF (I .GT. 0) GO TO 3300
      K=K+1
      IF (K .LE. NS) GO TO 3200
C          4000 SERIES COMPUTES DETERMINANT
 4000 GO TO MRIPAS, (4100,5000)
 4100 I=1
 4200 R=A(I,I)
      CALL  POUR(R,LEXP)
      DET=DET*R
      CALL  POUR(DET,LEXP)
      I=I+1
      IF (I .LE. NR) GO TO 4200
      S=LSGN
      DET=S*DET
 5000 LSGN=0
      RETURN
 9000 DET=0.0
      LSGN=I
      RETURN
      END
```

```
      SUBROUTINE  POWR(R,L)
C          CONTROLS OVERFLOW FOR R BY EXTRACTING POWERS OF 10
C               R - NUMBER
C               L - RESULTANT POWER OF 10
      ASSIGN 20 TO IB
   10 S= ABS(R)
      GO TO IB, (20,40)
   20 IF (S .LT. 1.0E+9) GO TO 30
      R=R*1.0E-10
      L=L+10
      GO TO 10
   30 ASSIGN 40 TO IB
   40 IF (S .GT. 1.0E-9) GO TO 50
      R=R*1.0E+10
      L=L-10
      GO TO 10
   50 RETURN
      END
```

```
      SUBROUTINE LINCOF

C     CALCULATION OF COEFFICIENTS FOR LINEAR TERMS, DCOEF AND ECOEF,
C     FROM COMBUSTION MODEL

      COMMON/CIN/COMENT(18),NM,TZERO,TFIN,TSTEP,AFIRST(5),BFIRST(5),
     1GAM,C1,C2,FL1,FL2,W(5),THU(5),THD(5),VELC,A1,A2,B1,B2,FL3,FUEL,
     2TAUR,EBAR,C1TL,C2TL,NZSTEP,NPRINT,ITAU
      COMMON /COUT/HOED(5),R(5),ORTH(5,5),OORM(5),ORTI(5,5),DCOEF(5,5),
     1ECOEF(5,5),ACOEF(5,5,5),BCOEF(5,5,5),PS2(5),PSD2(5),PSU(5),
     2PSDU(5),TAU,ISTORE,INST,IFIN,TIME(40),TA(40,5),TB(40,5),TSQ(40,5),
     3TETA(40,5),TETD(40,5),TEN(40),TPR(40,40)

      DIMENSION PS3(5),PSD3(5),AMP1(5),AMPD1(5)
      C2SI=1.0/C2**2
      FL21=FL2-FL1
      VT=1.0/(VELC*TAUR)
      EXPL=EXP(-FL21*VT)
      CW=GAM*(GAM-1.0)*EBAR/(C2**2*TAUR)
      VEL2=A2*FL2+B2
      VELU=B1
      VELD=(A1-A2)*FL1+(B1-B2)
      DMACH=(A1*FL1+B1)/C1**2-(A2*FL1+B2)/C2**2
      DO 10 I=1,NM
      WI=W(I)
      RI=R(I)
      THUI=THU(I)
      THDI=THD(I)
      PSU(I)=RI*COS(THUI)
      PSDU(I)=-WI*RI*SIN(THUI)/C1
      PS2(I)=COS(WI*FL2/C2+THDI)
      PSD2(I)=-WI*SIN(WI*FL2/C2+THDI)/C2
      PS3(I)=RI*COS(WI*FL3/C1+THUI)
      PSD3(I)=-RI*WI*SIN(WI*FL3/C1+THUI)/C1
      AMP1(I)=COS(WI*FL1/C2+THDI)
   10 AMPD1(I)=-C2*WI*SIN(WI*FL1/C2+THDI)
      DO 100 K=1,NM
      WK=W(K)
      PSD2K=PSD2(K)
      PS2K=PS2(K)
      PSDUK=PSDU(K)
      PSUK=PSU(K)
      AMPD1K=AMPD1(K)
      AMP1K=AMP1(K)
      DO 100 I=1,NM
      WI=W(I)
      SINL=SIN(WI*FL21/VELC)
      COSL=COS(WI*FL21/VELC)
      PSD2I=PSD2(I)
      PS2I=PS2(I)
      PSDUI=PSDU(I)
      PSUI=PSU(I)
      AMPD1I=AMPD1(I)
      AMP1I=AMP1(I)
      IF(K.NE.I) GO TO 40
      FF2U=VEL2*((C2*PSD2K)**2+(WK*PS2K)**2)
     C        -PS2K*PSD2K*C2**2*A2
```

```
      FF2D=VELU*((C1*PSDUK)**2+(WK*PSUK)**2)
     C       -PSUK*PSDUK*C1**2*A1
      DSCNT=VELD*(WK*AMP1K)**2+(A2-A1)*AMP1K*AMPD1K
     C        +DMACH*AMPD1K**2
      FF2=0.5*(FF2U-FF2D+DSCNT)/WK**2
      DSCT1=VELD*AMP1K**2
      FF1=0.5*(VEL2*PS2K**2+DSCT1-VELU*PSUK**2-FF2)
      GO TO 50
   40 FF2U = A2*C2**2*(PS2I*PSD2K-PS2K*PSD2I)
      FF2D = A1*C1**2*(PSUI*PSDUK-PSUK*PSDUI)
      DSCNT=(A1-A2)*(AMP1I*AMPD1K-AMP1K*AMPD1I)
      FF2=(FF2U-FF2D+DSCNT)/(WI**2-WK**2)
      FF1U=VEL2*(C2**2*PSD2I*PSD2K+WI**2*PS2I*PS2K)
     C       -A2*C2**2*PS2K*PSD2I
      FF1D=VELU*(C1**2*PSDUI*PSDUK+WI**2*PSUI*PSUK)
     C       -A1*C1**2*PSUK*PSDUI
      DSCNT=VELD*WI**2*AMP1I*AMP1K+(A2-A1)*AMP1K*AMPD1I
     C       +DMACH*AMPD1K*AMPD1I
      FF1=(FF1U-FF1D+DSCNT-2.0*WI**2*FF2)/(WI**2-WK**2)
   50 PL1=(WK/C2)**2+VT**2
      PL2=(WI/VELC)**2-PL1
      PL4=(WI/C2)**2-PL1
      PR2=CW*(WI*AMP1K/VELC+EXPL*(PSD2K*SINL
     C                            -PS2K*(WI*COSL/VELC-VT*SINL)))
      PR3=CW*(EXPL*(PSD2K*COSL+PS2K*(WI*SINL/VELC+VT*COSL))
     C                             -AMPD1K*C2SI-AMP1K*VT)
      PR4=CW*((AMP1K*AMPD1I-AMP1I*AMPD1K)*C2SI-VT*AMP1I*AMP1K
     C          +EXPL*(PS2I*PSD2K-PS2K*PSD2I+VT*PS2I*PS2K))
      PR5=CW*(EXPL*(PSD2K*PSD2I+WI**2*PS2I*PS2K*C2SI+VT*PS2K*PSD2I)
     C    -(AMPD1K*AMPD1I*C2SI+WI**2*AMP1K*AMP1I+VT*AMP1K*AMPD1I)*C2SI)
      PAR=2.0*WI*VT/VELC
      HINT1=(PL2*PR2-PAR*PR3)/(PL2**2+PAR**2)
      HINT2=(PAR*PR2+PL2*PR3)/(PL2**2+PAR**2)
      PAR=2.0*WI*VT/C2
      HINT4=(PL4*PR4-2.0*VT*PR5)/(PL4**2+PAR**2)
      HINT5=(PL4*PR5+2.0*VT*PR4*(WI/C2)**2)/(PL4**2+PAR**2)
      DEN=1.0/((WI/VELC)**2-(WI/C2)**2)
      HINTS=DEN*(WI*(HINT4-AMP1I*HINT2)/VELC
     C        -AMPD1I*HINT1/C2**2)
      HINTC=DEN*(HINT5+WI*HINT1*AMP1I/VELC-AMPD1I*HINT2*C2SI)
      TERM1=-2.0*FF1-(2.0+GAM)*FF2
      TERM2=HINT4/GAM
      TERM3=-C1TL*HINT4
      TERM4=C1TL*HINTC*VT
      TERM5=(HINTC+(C2**2*HINT5-AMPD1I*HINT2)/WI**2)*VT/GAM
      DCOEF(K,I)=TERM1+TERM2+TERM3+TERM4+TERM5
      FCOEF(K,I)=WI*VT*((C1TL+1.0/GAM)*HINTS-AMPD1I*HINT1/
     C              (GAM*WI**2))
  100 CONTINUE
      RETURN
      END
```

```
      SUBROUTINE ARMAT
C     CALCULATION OF COEFFICIENTS FOR NONLINEAR TERMS, ACOEF AND BCOEF
      COMMON/CIN/COMENT(18),NM,TZERO,TFIN,TSTEP,AFIRST(5),BFIRST(5),
     1GAM,C1,C2,EL1,EL2,W(5),THU(5),THD(5),VELC,A1,A2,B1,B2,EL3,FUEL,
     2TAUB,EBAR,C1TL,C2TL,NZSTEP,NPRINT,ITAU
      COMMON /COUT/HOED(5),R(5),ORTH(5,5),OORM(5),ORTI(5,5),OCOEF(5,5),
     1ECOEF(5,5),ACOEF(5,5,5),BCOEF(5,5,5),PS2(5),PSD2(5),PSU(5),
     2PSDU(5),TAU,TSTORE,INST,IFIN,TIME(40),TA(40,5),TB(40,5),TSO(40,5),
     3TETA(40,5),TETD(40,5),TEN(40),TPR(40,40)
      DIMENSION TH(4),P(4)
      DO 250 K=1,NM
      WK=W(K)
      WK2=WK**2
      THUK=THU(K)
      THDK=THD(K)
      DO 250 I=1,NM
      WI=W(I)
      WI2=WI**2
      THUI=THU(I)
      THDI=THD(I)
      DO 250 J=1,I
      WJ=W(J)
      WJ2=WJ**2
      THUJ=THU(J)
      THDJ=THD(J)
      P(1)=(WI+WJ+WK)/C1
      P(2)=(WI+WJ-WK)/C1
      P(3)=(WI-WJ+WK)/C1
      P(4)=(WI-WJ-WK)/C1
      TH(1)=THUI+THUJ+THUK
      TH(2)=THUI+THUJ-THUK
      TH(3)=THUI-THUJ+THUK
      TH(4)=THUI-THUJ-THUK
      TERM1=0.0
      DO 100 ID=1,4
      PAR=ABS(P(ID)*EL1)
      IF(PAR.GT.0.01) GO TO 50
      TERM1=TERM1+EL1*COS(TH(ID))/2.0
      GO TO 100
   50 SINID=SIN(P(ID)*EL1/2.0)/P(ID)
      TERM1=TERM1+COS(P(ID)*EL1/2.0+TH(ID))*SINID
  100 CONTINUE
      TH(1)=THDI+THDJ+THDK
      TH(2)=THDI+THDJ-THDK
      TH(3)=THDI-THDJ+THDK
      TH(4)=THDI-THDJ-THDK
      TERM2=0.0
      DO 200 ID=1,4
      P(ID)=P(ID)*C1/C2
      PAR=ABS(P(ID)*EL2)
      IF(PAR.GT.0.01) GO TO 150
      TERM2=TERM2+(EL2-EL1)*COS(TH(ID))/2.0
      GO TO 200
  150 SINID=SIN(P(ID)*(EL2-EL1)/2.0)/P(ID)
```

```
      TERM2=TERM2+COS(P(ID)*(FL1+FL2)/2.0+TH(ID))*SINID
  200 CONTINUE
      PHI2=R(I)*R(J)*R(K)*TERM1/2.0+TERM2/2.0
      VAR=(WI2-WK2)/WJ2+(WJ2-WK2)/WI2
      TERM=(1.0-0.5*VAR/GAM)*PHI2
      TERM2=C2**2*((PSD2(I)*PS2(J)+PSD2(J)*PS2(I))*PS2(K)
     C        -PSD2(K)*PS2(I)*PS2(J))    -C1**2*((PSDU(I)*PSU(J)+
     2        PSDU(J)*PSU(I))*PSU(K)-PSDU(K)*PSU(J)**2)
      BCOEF(K,I,J)=TERM+0.5*(1.0/WI**2+1.0/WJ**2)*TERM2/GAM
      BCOEF(K,J,I)=BCOEF(K,I,J)
      ACOEF(K,I,J)=0.5*(1.0/GAM-1.0)*(WI2+WJ2)*PHI2
  250 ACOEF(K,J,I)=ACOEF(K,I,J)
      RETURN
      END
```

```
      SUBROUTINE OUTPT1

      COMMON/CIN/COMENT(18),NM,TZERO,TFIN,TSTEP,AFIRST(5),BFIRST(5),
     1GAM,C1,C2,EL1,EL2,W(5),THU(5),THD(5),VELC,A1,A2,B1,B2,EL3,FUEL,
     2TAUR,EBAR,C1TL,C2TL,NZSTEP,NPRINT,ITAU
      COMMON /COUT/HOED(5),R(5),ORTH(5,5),OORM(5),ORTI(5,5),DCOEF(5,5),
     1ECOEF(5,5),ACOEF(5,5,5),BCOEF(5,5,5),PS2(5),PSD2(5),PSU(5),
     2PSDU(5),TAU,TSTORE,INST,IFIN,TIME(40),TA(40,5),TB(40,5),TSO(40,5),
     3TETA(40,5),TETD(40,5),TEN(40),TPR(40,40)

      DIMENSION HED(5)
      DATA HED/1H1,1H2,1H3,1H4,1H5/,HBL/1H /
      DATA HDASH/10H----------/
      WRITE(6,10) COMENT,(HDASH,I=1,13)
   10 FORMAT(1H1/1X,19HNPSC PROGRAM NONLIN///30X,18A4/30X,2H--,7A10///
     151X,3A10     /52X,28HTIME-INDEPENDENT OUTPUT DATA/     51X,3A10)
      DO 20 J=1,5
      HOED(J)=HBL
      IF(J.LE.NM) HOED(J)=HED(J)
   20 CONTINUE
      WRITE(6,30)   (HDASH,I=1,6),(HOED(J),J=1,5),(HDASH,K=1,6)
   30 FORMAT(///83X,11HMODE NUMBER/56X,5H-----,6A10/52X,5A13/56X,
     15H-----,6A10)
      WRITE(6,40) (R(J),J=1,NM)
   40 FORMAT (11X,35HRELATIVE AMPLITUDE OF ACOUSTIC WAVE,10X,5E13.4)
      WRITE(6,50) (HDASH,I=1,7),(HOED(J),J=1,5),(HDASH,K=1,7)
   50 FORMAT(/46X,5H-----,7A10/11X,25HINNER-PRODUCT MATRIX(I,J),13X,
     15HI / J,A11   ,4A13/46X,5H-----,7A10)
      DO 60 I=1,NM
   60 WRITE(6,70) I,(ORTH(I,J),J=1,NM)
   70 FORMAT(51X,I1,4X,5E13.4)
      WRITE(6,80) (HDASH,I=1,7),(HOED(J),J=1,5),(HDASH,K=1,7)
   80 FORMAT (/46X,5H-----,7A10/11X,28HINVERSE OF IN-PR MATRIX(I,J),10X,
     15HI / J,A11   ,4A13/46X,5H-----,7A10)
      DO 90 I=1,NM
   90 WRITE(6,70) I,(ORTI(I,J),J=1,NM)
      WRITE(6,100) (HDASH,I=1,7),(HOED(J),J=1,5),(HDASH,K=1,7)
  100 FORMAT(/46X,5H-----,7A10/11X,25HLINEAR COEF MATRIX D(I,J),13X,
     15HI / J,A11   ,4A13/46X,5H-----,7A10)
      DO 110 I=1,NM
  110 WRITE(6,70) I,(DCOEF(I,J),J=1,NM)
      WRITE(6,120) (HDASH,I=1,7),(HOED(J),J=1,5),(HDASH,K=1,7)
  120 FORMAT(/46X,5H-----,7A10/11X,25HLINEAR COEF MATRIX E(I,J),13X,
     15HI / J,A11   ,4A13/46X,5H-----,7A10)
      DO 130 I=1,NM
  130 WRITE(6,70) I,(ECOEF(I,J),J=1,NM)
      WRITE(6,140)   (HDASH,I=1,7),(HOED(J),J=1,5),(HDASH,K=1,7)
  140 FORMAT(//46X,5H-----,7A10/11X,28HNON-LIN COEF MATRIX A(K,I,J),
     110X,5HI / J,A11,  4A13/46X,5H-----,7A10)
      DO 160 K=1,NM
      WRITE(6,150) K,(ACOEF(K,1,J),J=1,NM)
  150 FORMAT(/22X,2HK=,I1,26X,1H1,4X,5E13.4)
      IF(NM.EQ.1) GO TO 160
      DO 155 I=2,NM
  155 WRITE(6,70) I,(ACOEF(K,I,J),J=1,NM)
  160 CONTINUE
      WRITE(6,170) (HDASH,I=1,7),(HOED(J),J=1,5),(HDASH,K=1,7)
```

```
170 FORMAT(//46X,5H-----,7A10/11X,28HNON-LIN COEF MATRIX B(K,I,J),
   110X,5HI / J,A11,  4A13/46X,5H-----,7A10)
    DO 180 K=1,NM
    WRITE(6,150) K,(BCOEF(K,1,J),J=1,NM)
    IF(NM.EQ.1) GO TO 180
    DO 175 I=2,NM
175 WRITE(6,70) I,(BCOEF(K,I,J),J=1,NM)
180 CONTINUE
    RETURN
    END
```

```
      SUBROUTINE RUNKUT(X,DELX,Y,QY,Z,QZ,FUNCTN,NM)

C     SOLUTION OF SIMULTANEOUS SETS OF FIRST-ORDER ORDINARY
C     DIFFERENTIAL EQUATIONS BY THE GILL VARIATION OF THE
C     RUNGE-KUTTA METHOD

      DIMENSION Y(5),Z(5),QY(1),QZ(1),YPRIME(5),ZPRIME(5)
      DIMENSION A(4),B(4),C(4),D(4)
      DATA (A(I),I=1,4)/0.5,0.2928932,1.7071068,0.1666667/,(B(I),I=1,4)
     1/2.0,1.0,1.0,2.0/,(C(I),I=1,4)/0.5,0.2928932,1.7071068,0.5/,
     2(D(I),I=1,4)/0.0,0.5,0.0,0.5/
      DO 100 K=1,4
      X=X+D(K)*DELX
      CALL FUNCTN(X,Y,YPRIME,Z,ZPRIME)
      AK=A(K)
      BK=B(K)
      CK=C(K)
      DO 100 I=1,NM
      DELY=YPRIME(I)
      DIFF=AK*(DELY-BK*QY(I))
      Y(I)=Y(I)+DIFF
      QY(I)=QY(I)+3.0*DIFF-CK*DELY
      DELZ=ZPRIME(I)
      DIFF=AK*(DELZ-BK*QZ(I))
      Z(I)=Z(I)+DIFF
  100 QZ(I)=QZ(I)+3.0*DIFF-CK*DELZ
      RETURN
      END
```

```
      SUBROUTINE DERIV(TP,PA,PPA,PB,PPB)

C     CALCULATION OF DERIVATIVES FOR SIN AND COS TERM AMPLITUDES
C     OF TRAVELING WAVE

      COMMON/CIN/COMENT(18),NM,TZERO,TFIN,TSTEP,AFIRST(5),BFIRST(5),
     1GAM,C1,C2,FL1,FL2,W(5),THU(5),THD(5),VELC,A1,A2,B1,B2,FL3,FUEL,
     2TAUB,EBAR,C1TL,C2TL,NZSTEP,NPRINT,ITAU
      COMMON /COUT/HOED(5),R(5),ORTH(5,5),OORM(5),ORTI(5,5),DCOEF(5,5),
     1ECOEF(5,5),ACOEF(5,5,5),BCOEF(5,5,5),PS2(5),PSD2(5),PSU(5),
     2PSDU(5),TAU,ISTORE,INST,IFIN,TIME(40),TA(40,5),TB(40,5),TSO(40,5),
     3TETA(40,5),TETD(40,5),TEN(40),TPR(40,40)

      DIMENSION PA(5),PPA(5),PB(5),PPB(5)
      DATA PI/3.1415926536/
      DO 100 K=1,NM
      WK=W(K)
      IF(ITAU.EQ.1)  TAU=2.0*PI/WK
      IF (ITAU.NE.2) GO TO 20
      IK=2
      IF (K.EQ.1) IK=1
      TAU=2.0*PI/W(IK)
   20 TWT=TSTEP/(WK*TAU)
      PPA(K)=0.0
      PPB(K)=0.0
      DO 100 I=1,NM
      WI=W(I)
      PAI=PA(I)
      PBI=PB(I)
      DO 100 J=1,NM
      WJ=W(J)
      PAJ=PA(J)
      PBJ=PB(J)
      VAR=ACOEF(K,I,J)*PAI*PBJ-WI*WJ*BCOEF(K,I,J)*PBI*PAJ
      CALL TRISIN(3,TP,TAU,WI,WJ,WK,TINT)
      APX=2.0*VAR*TINT
      CALL TRISIN(2,TP,TAU,WI,WJ,WK,TINT)
      APY=2.0*VAR*TINT
      IF (J.GT.I) GO TO 50
      V1=ACOEF(K,I,J)*PBI*PBJ+WI*WJ*BCOEF(K,I,J)*PAI*PAJ
      CALL TRISIN(4,TP,TAU,WI,WJ,WK,T1)
      PARA=V1*T1
      CALL TRISIN(3,TP,TAU,WK,WI,WJ,TINT)
      PARB=V1*TINT
      V2=ACOEF(K,I,J)*PAI*PAJ+WI*WJ*BCOEF(K,I,J)*PBI*PBJ
      CALL TRISIN(2,TP,TAU,WI,WK,WJ,T2)
      PARA=PARA+V2*T2
      CALL TRISIN(1,TP,TAU,WK,WI,WJ,TINT)
      PARB=PARB+V2*TINT
      APX=APX+PARA
      APY=APY+PARB
      IF(I.EQ.J) GO TO 50
      APX=APX+PARA
      APY=APY+PARB
   50 PPA(K)=PPA(K)+TWT*APX
  100 PPB(K)=PPB(K)-TWT*APY
      DO 200 K=1,NM
```

```
      APX=0.0
      APY=0.0
      WK=W(K)
      IF(ITAU.EQ.1)    TAU=2.0*PI/WK
      IF (ITAU.NE.2) GO TO 120
      IK=2
      IF (K.EQ.1) IK=1
      TAU=2.0*PI/W(IK)
  120 TWT=TSTEP/(WK*TAU)
      DO 150 I=1,NM
      WI=W(I)
      PAR=DCOEF(K,I)*WI*PA(I)+ECOEF(K,I)*PB(I)
      CALL BISIN(1,TP,TAU,WI,WK,TINT)
      APX=APX+PAR*TINT
      CALL BISIN(2,TP,TAU,WK,WI,TINT)
      APY=APY+PAR*TINT
      PAR=ECOEF(K,I)*PA(I)-DCOEF(K,I)*WI*PB(I)
      CALL BISIN(2,TP,TAU,WI,WK,TINT)
      APX=APX+PAR*TINT
      CALL BISIN(3,TP,TAU,WK,WI,TINT)
  150 APY=APY+PAR*TINT
      PPA(K)=PPA(K)+TWT*APX
  200 PPB(K)=PPB(K)-TWT*APY
      RETURN
      END
```

```
      SUBROUTINE TRISIN(INDX,TP,TAU,WX,WY,WZ,TINT)

      TINT=0.
      TAUT=0.5*TAU
      TT=TP+TAUT
      ERR=0.001/TAU
      P1=WX+WY-WZ
      P2=WX-WY+WZ
      P3=WX+WY+WZ
      P4=WX-WY-WZ
      AP1=ABS(P1)
      AP2=ABS(P2)
      AP3=ABS(P3)
      AP4=ABS(P4)
      SIN1=SIN(P1*TAUT)
      SIN2=SIN(P2*TAUT)
      SIN3=SIN(P3*TAUT)
      SIN4=SIN(P4*TAUT)
      GO TO (10,20,30,40), INDX

C     INTEGRATE SIN(I)*SIN(J)*SIN(K)

   10 IF(AP1.LT.ERR) GO TO 12
      TINT=2.0*SIN1*SIN(P1*TT)/P1
   12 IF(AP2.LT.ERR) GO TO 14
      TINT=TINT+2.0*SIN2*SIN(P2*TT)/P2
   14 IF(AP3.LT.ERR) GO TO 16
      TINT=TINT-2.0*SIN3*SIN(P3*TT)/P3
   16 IF(AP4.LT.ERR) GO TO 18
      TINT=TINT-2.0*SIN4*SIN(P4*TT)/P4
   18 TINT=TINT/4.0
      RETURN

C     INTEGRATE COS(I)*SIN(J)*SIN(K)

   20 TINT=TAU
      IF (AP1.GT.ERR) TINT=2.0*SIN1*COS(P1*TT)/P1
      TINT=TINT-TAU
      IF (AP2.GT.ERR) TINT=TINT+TAU-2.0*SIN2*COS(P2*TT)/P2
      TINT=TINT-TAU
      IF (AP3.GT.ERR) TINT=TINT+TAU-2.0*SIN3*COS(P3*TT)/P3
      TINT=TINT+TAU
      IF (AP4.GT.ERR) TINT=TINT-TAU+2.0*SIN4*COS(P4*TT)/P4
      TINT=TINT/4.0
      RETURN

C     INTEGRATE COS(I)*COS(J)*SIN(K)

   30 IF(AP1.LT.ERR) GO TO 32
      TINT=2.0*SIN1*SIN(P1*TT)/P1
   32 IF(AP2.LT.ERR) GO TO 34
      TINT=TINT+2.0*SIN2*SIN(P2*TT)/P2
   34 IF(AP3.LT.ERR) GO TO 36
      TINT=TINT+2.0*SIN3*SIN(P3*TT)/P3
   36 IF(AP4.LT.ERR) GO TO 38
      TINT=TINT+2.0*SIN4*SIN(P4*TT)/P4
   38 TINT=TINT/4.0
```

```
      RETURN

C       INTEGRATE COS(I)*COS(J)*COS(K)

   40 TINT=TAU
      IF (AP1.GT.ERR) TINT=2.0*SIN1*COS(P1*TT)/P1
      TINT=TINT+TAU
      IF (AP2.GT.ERR) TINT=TINT-TAU+2.0*SIN2*COS(P2*TT)/P2
      TINT=TINT+TAU
      IF (AP3.GT.ERR) TINT=TINT-TAU+2.0*SIN3*COS(P3*TT)/P3
      TINT=TINT+TAU
      IF (AP4.GT.ERR) TINT=TINT-TAU+2.0*SIN4*COS(P4*TT)/P4
      TINT=TINT/4.0
      RETURN
      END
```

```
      SUBROUTINE BISIN(INDX,TP,TAU,WY,WX,TINT)

      P1=WY+WX
      P2=WY-WX
      TAUT=0.5*TAU
      ERR=ABS(P2*TAU)
      TT=TP+TAUT
      IF (INDX-2) 10,20,30

C        COS(WY*T)*COS(WX*T)

   10 TINT= COS(P1*TT)*SIN(P1*TAUT)/P1+TAUT
      IF(ERR.GT.0.001) TINT=TINT-TAUT+COS(P2*TT)*SIN(P2*TAUT)/P2
      RETURN

C       SIN(WY*T)*COS(WX*T)

   20 TINT= SIN(P1*TT)*SIN(P1*TAUT)/P1
      IF(ERR.GT.0.001) TINT=TINT+SIN(P2*TT)*SIN(P2*TAUT)/P2
      RETURN

C        SIN(WY*T)*SIN(WX*T)

   30 TINT= -COS(P1*TT)*SIN(P1*TAUT)/P1+TAUT
      IF(ERR.GT.0.001) TINT=TINT-TAUT+COS(P2*TT)*SIN(P2*TAUT)/P2
      RETURN
      END
```

```
      SUBROUTINE OUTPT2

      COMMON/CIN/COMENT(18),NM,T7ERO,TFIN,TSTEP,AFIRST(5),BFIRST(5),
     1GAM,C1,C2,FL1,FL2,W(5),THU(5),THD(5),VELC,A1,A2,B1,B2,FL3,FUEL,
     2TAUB,EBAR,C1TL,C2TL,N7STEP,NPRINT,ITAU
      COMMON /COUT/HOED(5),R(5),ORTH(5,5),OORM(5),ORTI(5,5),DCOEF(5,5),
     1ECOEF(5,5),ACOEF(5,5,5),BCOEF(5,5,5),PS2(5),PSD2(5),PSU(5),
     2PSDU(5),TAU,TSTORE,INST,IFIN,TIME(40),TA(40,5),TB(40,5),TSO(40,5),
     3TETA(40,5),TETD(40,5),TEN(40),TPR(40,40)

      DATA HDASH/10H----------/
      WRITE(6,10) COMENT,(HDASH,I=1,13)
   10 FORMAT (1H1/1X,19HNREC PROGRAM NONLIN///30X,18A4/30X,2H--,7A10///
     151X,3A10   /52X,28H TIME-DEPENDENT OUTPUT DATA / 51X,3A10)
      IF (INST.EQ.1) WRITE(6,15)
   15 FORMAT(///47X,37H* INSTABILITY ENCOUNTERED IN SYSTEM *)
      WRITE(6,20) (HDASH,I=1,6)
   20 FORMAT (///40X,5H-----,6A10/54X,37HTRAVELING WAVE, AMPLITUDE OF SI
     1N TERM)
      WRITE(6,30) (HDASH,I=1,6),(HOED(J),J=1,5),(HDASH,K=1,6)
   30 FORMAT (40X,5H-----,6A10/67X,11HMODE NUMBER/30X,4HTIME,2X,
     15A13/30X,4H----,6X,5H-----,6A10)
      DO 40 I=1,ISTORE
      WRITE(6,50) TIME(I),(TA(I,J),J=1,NM)
      IF(I.EQ.5*(I/5)) WRITE(6,60)
   40 CONTINUE
   50 FORMAT (22X,F12.4,6X,5E13.4)
   60 FORMAT(30X)
      WRITE(6,70) (HDASH,I=1,6)
   70 FORMAT(///40X,5H-----,6A10/54X,37HTRAVELING WAVE, AMPLITUDE OF COS
     1 TERM)
      WRITE(6,30) (HDASH,I=1,6),(HOED(J),J=1,5),(HDASH,K=1,6)
      DO 80 I=1,ISTORE
      WRITE(6,50) TIME(I),(TB(I,J),J=1,NM)
      IF(I.EQ.5*(I/5)) WRITE(6,60)
   80 CONTINUE
      WRITE(6,90) (HDASH,I=1,6)
   90 FORMAT (///40X,5H-----,6A10/59X,27HAMPLITUDE OF TRAVELING WAVE)
      WRITE(6,30) (HDASH,I=1,6),(HOED(J),J=1,5),(HDASH,K=1,6)
      DO 100 I=1,ISTORE
      WRITE(6,50) TIME(I),(TSO(I,J),J=1,NM)
      IF(I.EQ.5*(I/5)) WRITE(6,60)
  100 CONTINUE
      WRITE(6,110) (HDASH,I=1,6)
  110 FORMAT (///40X,5H-----,6A10/59X,27HMAGNITUDE OF TRAVELING WAVE)
      WRITE(6,30)  (HDASH,I=1,6),(HOED(J),J=1,5),(HDASH,K=1,6)
      DO 120 I=1,ISTORE
      WRITE(6,50) TIME(I),(TETA(I,J),J=1,NM)
      IF(I.EQ.5*(I/5)) WRITE(6,60)
  120 CONTINUE
      WRITE(6,130) (HDASH,I=1,13),(HOED(J),J=1,5),(HDASH,K=1,7)
  130 FORMAT(///28X,A10,2X,5H-----,6A10/51X,
     143HTIME DERIVATIVE OF TRAVELING WAVE MAGNITUDE/30X,5HTOTAL,5X,
     25H-----,6A10/29X,8HACOUSTIC,30X,11HMODE NUMBER/15X,4HTIME,11X,
     36HENERGY,       5A13/15X,4H----,9X,A10,2X,5H-----,6A10)
      DO 140 I=1,ISTORE
      WRITE(6,150) TIME(I),TEN(I),(TETD(I,J),J=1,NM)
```

```
      IF(I.EQ.5*(I/5)) WRITE(6,60)
  140 CONTINUE
  150 FORMAT( 7X,F12.4,6X,F13.4,2X,5E13.4)
      WRITE(6,160) COMENT,(HDASH,I=1,17)
  160 FORMAT(1H1/1X,19HNREC PROGRAM NONLIN///30X,18A4/30X,2H--,7A10///
     123X,10A10  /50X,46HINSTANTANEOUS NORMALIZED PRESSURE DISTRIBUTION)
      NTAB=(NZSTEP-1)/8+1
      DO 200 M=1,NTAB
      MS=8*(M-1)+1
      ME=8*M
      IF(ME.GT.NZSTEP) ME=NZSTEP
      WRITE(6,170) (HDASH,I=1,10),(J,J=MS,ME)
  170 FORMAT(/  23X,10A10/66X,14HAXIAL LOCATION/15X,4HTIME,12X,I2,7I12)
      WRITE(6,180) (HDASH,I=1,10)
  180 FORMAT (15X,4H----,4X,10A10)
      DO 200 I=1,ISTORE
      WRITE(6,210) TIME(I),(TPR(I,J),J=MS,ME)
      IF(I.EQ.5*(I/5)) WRITE(6,60)
  200 CONTINUE
  210 FORMAT(7X,F12.3,6X,8F12.4)
      IF(IFIN.EQ.1) WRITE(6,250)
  250 FORMAT(///53X,26H* CALCULATIONS COMPLETED *)
      RETURN
      END
```

APPENDIX C

PROGRAM HLMHLT: A USER'S MANUAL

STATEMENT OF THE PROBLEM

Program HLMHLT determines the eigenvalues and eigenfunctions of the Helmholtz equation for an annular duct divided axially into two chambers by a step change in the sonic velocity; boundary surfaces are permitted to be acoustically absorptive, and general continuity conditions can be specified across the sonic velocity discontinuity.

Consider two axially contiguous annular chambers, designated Chambers 1 and 2, with the latter having the larger value of sonic velocity. The specific equations solved by the computer program are as follows:

$$\nabla^2 \eta_1 + k_1^2 \eta_1 = 0 \qquad \text{for } 0 \le \xi_1 \le \ell_1$$
$$\nabla^2 \eta_2 + k_2^2 \eta_2 = 0 \qquad \text{for } 0 \le \xi_2 \le \ell_2 \tag{C1}$$

where k_i is a nondimensional wave number for Chamber i:

$$k_i = \frac{\omega_c R_{oi}}{c_{oi}} \tag{C2}$$

η_i is a nondimensional unsteady pressure function: $(p'/\rho_0$
∇^2 is the Laplacian operator in cylindrical coordinates which are nondimensionalized with respect to the outer radius, R_{o_i}.

The general solution of Equation C1 is obtained via separation of variables:

$$\eta_i = F_\theta F_{r_i} F_{\xi_i} \tag{C3}$$

$$F_\theta = B_\theta e^{i m \theta} + B'_\theta e^{-i m \theta} \tag{C4}$$

$$F_{r_i} = C_{r_i} J_m(\alpha_i r_i) + C'_{r_i} Y_m(\alpha_i r_i) \tag{C5}$$

$$F_{\xi_i} = C_{\xi_i} \cos(n_i \xi_i) + C'_{\xi_i} \sin(n_i \xi_i)/n_i \tag{C6}$$

where m is the tangential wave number (an integer)
α_i is the radial wave number in chamber i
n_i is the axial wave number in chamber i
J_m and Y_m are Bessel functions of the first and second kinds of order m.

The solution of Equation C1 for homogeneous boundary and chamber-to-chamber transition conditions consists of eigenvalues k_i and eigenfunctions (resonant mode shapes) in which the relative magnitudes of the constants of integration in Equations C4, C5, and C6 are specified. The eigenvalue, or combined wave number, is related to the radial and axial wave numbers as follows:

$$k_i^2 = \alpha_i^2 + \eta_i^2 \tag{C7}$$

Since the radial and axial eigenvalue solutions are not unique, it is convenient to introduce a system of indices to distinguish among various solutions:

$$k_{i,l,\kappa} \quad ; \quad \alpha_{i,l,\kappa} \quad ; \quad \eta_{i,l,\kappa}$$

where l is related to the magnitude of the real part of the α solution, and κ, to that of the η solution (hence, l is the radial wave index and κ is the axial wave index). Similar indices must be appended to the constants of integration which determine the mode shape, again to keep track of different resonant modes.

The tangential component of the solution (Equation C4) is arbitrary so long as m is an integer. Accordingly, the computer program requires m to be specified as an input, and the value supplied governs the remainder of the solution (indeed, a tangential wave index, $M = m$, should in principle be appended above, but it has not been because the program is restricted to investigating a single value of m for any one case).

The radial eigenvalue problem consists of the determination of the radial wave numbers, $\alpha_{i,l,\kappa}$, such that Equation C5 satisfies the following boundary conditions:

$$\frac{1}{\eta_{i,l,\kappa}} \frac{\partial \eta_{i,l,\kappa}}{\partial r_i} = jk_{i,l,\kappa} A_a = \bar{A}_{a_{i,l,\kappa}} \qquad \text{at } r_i = 1.0 \text{ (OUTER RADIUS)} \tag{C8}$$

$$\frac{1}{\eta_{i,l,\kappa}} \frac{\partial \eta_{i,l,\kappa}}{\partial r_i} = -j k_{i,l,\kappa} A_b = \bar{A}_{b_{i,l,\kappa}} \qquad \text{at } r_i = b_i \text{ (INNER RADIUS)} \tag{C9}$$

where A_a and A_b are specific acoustic admittance ratios (Ref 9) and are thus, in general, complex numbers. Note that except under extraordinary circumstances α_i must be identical to α_1, so that use of the index i with the radial eigenvalue solution is academic rather than significant.

The axial eigenvalue problem consists of the determination of the axial wave numbers, $\eta_{i,l,\kappa}$, such that the angular frequency ω is the same in both chambers (see Equations C2 and C7) and such that Equation C6 satisfies the following boundary requirements:

$$\frac{1}{\eta_{1,t,\kappa}}\frac{\partial \eta_{1,t,\kappa}}{\partial z_1} = -j k_{1,t,\kappa}\left(A_0 + M_0\frac{\eta_{1,t,\kappa}^2}{k_{1,t,\kappa}^2}\right) = \bar{A}_{0,t,\kappa} \qquad \text{at } z_1 = 0 \text{ (UPSTREAM)} \tag{C10}$$

$$\frac{1}{\eta_{2,t,\kappa}}\frac{\partial \eta_{2,t,\kappa}}{\partial z_2} = j k_{2,t,\kappa}\left(A_2 - M_2\frac{\eta_{2,t,\kappa}^2}{k_{2,t,\kappa}^2}\right) = \bar{A}_{2,t,\kappa} \qquad \text{at } z_2 = \ell_2 \text{ (DOWNSTREAM)} \tag{C11}$$

where again A_0 and A_2 are specific acoustic admittance ratios, and M_0 and M_2 are Mach numbers at the upstream and downstream boundaries, respectively. The remaining conditions required to define the axial eigenvalues pertain to the transition between the two chambers: at $z_1 = \lambda_1$ and $z_2 = \lambda_2$ (the flamefront):

$$\eta_{2,t,\kappa} = f\eta_{1,t,\kappa} + f' u'_{z_1,t,\kappa} \tag{C12}$$

$$u'_{z_2,t,\kappa} = g\eta_{1,t,\kappa} + g' u'_{z_1,t,\kappa} \tag{C13}$$

where the coefficients f, f', g, and g' may be complex, and the unsteady axial velocity, $u'_{z_i,t,\kappa}$, is defined as follows:

$$u'_{z_i} = \frac{c_{0i}}{j k_{i,t,\kappa}\gamma}\frac{\partial \eta_{i,t,\kappa}}{\partial z_i} \tag{C14}$$

Equations C12 and C13 are conveniently rewritten, using Equation C14, to yield the following transition conditions:

$$\eta_{2,t,\kappa} = \bar{f}_{t,\kappa}\eta_{1,t,\kappa} + \bar{f}'_{t,\kappa}\frac{\partial \eta_{1,t,\kappa}}{\partial z_1} \tag{C15}$$

$$\frac{\partial \eta_{2,t,\kappa}}{\partial z_2} = \bar{g}_{t,\kappa}\eta_{1,t,\kappa} + \bar{g}'_{t,\kappa}\frac{\partial \eta_{1,t,\kappa}}{\partial z_1} \tag{C16}$$

Also the option is available to the program user to supply directly input values for $\bar{f}$, $\bar{f}'$, $\bar{g}$, and $\bar{g}'$ when conditions more general than those of Equations C12 and C13 are sought.

The solution developed within Program HLMHLT thus involves principally the determination of the radial, axial, and combined resonant wave numbers: $\alpha_{i,t,\kappa}$; $\eta_{i,t,\kappa}$; $k_{i,t,\kappa}$. In physical terms these wave numbers suffice to determine the acoustic resonant frequencies and energy

decrements for the two-chamber duct, where the decrements are zero unless some of the admittance ratios have nonzero real parts (conductances). In more general terms, the program is capable of defining the acoustic "spectrum" of the two-chamber duct.

STRUCTURE OF THE NUMERICAL SOLUTION

Both the radial and axial eigenvalue problems stated in the preceding paragraphs are unusual mathematically in that the combined wave number, $k_{i,L,K}$, appears as an explicit factor in the boundary and transition equations. The problem here is that the boundary and transition equations in effect cannot be specified until the over-all eigenvalues, k_i, are known. In a standard eigenvalue problem the boundary conditions involve only constants which are independent of the eigenvalues. The present problem, on the other hand, will in general yield nonorthogonal eigenfunction solutions, so that care must be taken both in generating and in using the solutions.

The unusual form of the eigenvalue problem is handled by Program HLMHLT via an iteration technique: in any one iteration all boundary coefficients ($\bar{A}_{a_{i,L,K}}$, etc.) and transition coefficients ($\bar{f}_{L,K}$, etc.) are assumed to be simple constants, and the iteration converges on accurate final values of these coefficients. The technique thus reduces the problem to one of standard form during any one iteration.

The essential calculation steps are as follows:

1) Specify the tangential wave number, m.

2) Estimate the combined wave number, $k_{i,L,K}$ for the L^{th} radial, K^{th} axial mode.

3) Calculate the boundary and transition coefficients, using the current value of $k_{i,L,K}$: $\bar{A}_{a_{i,L,K}}$, $\bar{A}_{b_{i,L,K}}$, $\bar{A}_{o_{L,K}}$; $\bar{A}_{g_{i,L,K}}$, $\bar{f}_{L,K}$, $\bar{f}'_{L,K}$, $\bar{g}_{L,K}$, $\bar{g}'_{L,K}$ (see Equations 44 through 52).

4) Solve the radial and axial eigenvalue problems for $\alpha_{i,L,K}$ and $\eta_{i,L,K}$ assuming that all boundary and transition coefficients are straightforward complex constants.

5) Calculate $k_{i,L,K} = \sqrt{\alpha^2_{i,L,K} + \eta^2_{i,L,K}}$, and return to step 2 unless the iteration on $k_{i,L,K}$ has converged.

The only other oddity of the Program HLMHLT structure is the need to use an elaborate method for solving the standard form radial and axial eigenvalue problems for complex rather than real wave numbers.

CAPABILITIES AND LIMITATIONS

In essence, Program HLMHLT is capable of determining the resonant

acoustic frequencies, energy decrements, and associated three-dimensional mode shapes for annular and cylindrical ducts. There are three important ways in which this capability has been generalized beyond more standard treatments of the problem:

1) The duct is assumed to consist of two axially contiguous chambers, distinguished by a step change in sonic velocity; momentum losses at the interface between the two chambers can be specified in the input (i.e., losses associated with baffles and flame holders).

2) The upstream, downstream, inner, and outer boundaries are all defined numerically by acoustic admittances-- complex numbers, the real part of which define damping at the boundary surfaces, and the imaginary part, flexibility at the surfaces. Thus, the frequencies, decrements, and mode shapes calculated by the program include full recognition of acoustic energy absorption (or amplification) at all the boundary surfaces.

3) At the upstream and downstream boundaries, the steady through-flow interacts with the acoustic oscillations. Program HLMHLT takes into account the distortion of the resonant acoustic mode caused by through-flow at the boundary surfaces (but not the distortion caused by through-flow in the remainder of the duct).

In summary, then, this computer program is capable of determining the basic acoustic characteristics of annular ducts, with recognition of acoustic energy absorption and various other factors which complicate the resonant mode shapes. Thus, the program is by no means restricted to augmentors.

For any single input case, Program HLMHLT requires an initial input specification of the tangential wave number, M; the program can then investigate as many as five distinct values of the radial mode index (L) and, similarly, five distinct values of the axial mode index (K). Thus, the program can investigate as many as 25 distinct resonant acoustic modes at a time. Moreover, the solutions do not have to be restricted to the simplest radial and axial wave distributions: the L and K designations are not rigidly restricted to a single mode, but are used only to distinguish among modes in an orderly fashion during any one case. On this last point, however, there is a major limitation of Program HLMHLT as it now stands: radial eigenvalues, α , with real parts greater than 20 cannot be determined accurately, so that examination of radial modes above the fifth for a cylinder should not be attempted without modification of two subroutines.

One additional capability of Program HLMHLT deserving mention is that it can execute three distinct types of numerical solution (as distinguished by the input indicator, ITYPE):

1) An acoustically ideal solution (ITYPE=-1) in which the boundary surfaces are perfectly reflective, and the acoustic disturbance is continuous across the interface between the two chambers;

also required as input are the ranges of values within which to search for solutions of the radial and axial eigenvalues, respectively.

2) An acoustically general solution (ITYPE=0) in which the boundary and transition coefficients can assume arbitrary complex values; again the input must include the ranges of values within which to search for solutions of the real parts of the radial and axial eigenvalues, respectively; also required are initial estimates of the combined wave numbers, $k_{i,L,K}$, with which to calculate boundary and transition coefficients during the first iteration.

3) An acoustically general solution (ITYPE=1) in which the solution proceeds from estimates of the radial and axial eigenvalues, $\alpha_{i,L,K}$ and $\eta_{i,L,K}$, to accurate values.

If little is known about the acoustics of the duct, the first type of solution will be most useful. To be sure no modes are skipped in the more general case, the second type solution is preferable. Whenever reasonably good estimates of the radial and axial wave numbers are available, the third type of solution is most effective.

INPUT DATA

A precise definition of the input data required to run the computer program is given below. For clarification of the significance of the input the reader is referred to the preceding discussion in this section. For some of the input variables (such as those associated with the boundaries and the transition between chambers) there are no definitive formulas available at this time; recommendations for calculating these terms, based on experience with the program, may be found in Section VI of the report. A few remaining input items are rather artificial (such as the limit on the number of iterations), and suggestions are noted in the text. A sample case which is representative ends this section of the report, and the reader may find it helpful to refer to it when absorbing the description below.

Program HLMHLT involves no essential restriction on input units insofar as the eigenvalue solutions are nondimensionalized with respect to the outer radius and the sonic velocity. However, <u>all input units must be consistent</u> (e.g., ft, sec, ft/sec, etc.). The only input items which are dimensional are RO(I), RI(I), XLD(I), CO(I), UO(I) and possibly QQFP and QQGP.

The following comments pertain to the detailed description of the input. The line number is the same as the card number, and the location number refers to columns of the card. Four formats are used for input. "A" indicates alphanumeric characters. "R" indicates real numbers, which are all placed in fields of twelve locations and should include a decimal point. A "C" indicates a complex number which in input

consists of a pair of "R" type numbers with the first being the real part and the second, the imaginary part. "I" indicates integers, which are all placed in fields of six locations; no decimal point may be used, and the number must be placed in the rightmost locations of the allocated field.

Line	Location	Type	Input Item	Comments
1	1-72	A	TITLE	Title of case
2	1-6	I	M	Tangential wave number, m
	7-12	I	KST	Lowest value of the axial wave index, K, for which the axial wave number in Chamber 2, $\eta_{2,L,K}$, is not zero (usually = 1, occasionally = KSTP+1, never > 5)
	13-18	I	KSTP	Lowest value of the axial wave index, K, for which solutions are sought (invariably = 1, never > 5)
	19-24	I	KXQ	Largest value of the axial wave index, K, for which solutions are sought (never > 5)
	25-30	I	LST	Lowest value of the radial wave index, L, for which the radial wave number, $\alpha_{2,L,K}$, is not zero (usually = 1, occasionally = LSTP+1, never > 5)
	31-36	I	LSTP	Lowest value of the radial wave index, L, for which solutions are sought (invariably = 1, never > 5)
	37-42	I	LRQ	Largest value of the radial wave index, L, for which solutions are sought (never > 5)
	43-48	I	NRQ	Number of Newton-Raphson iterations permitted in the precise wave number solutions (50 is a reasonable number)
	49-54	I	ITER	Number of major boundary coefficient redefinition iterations permitted (30 is a reasonable number)

Line	Location	Type	Input Item	Comments
	55-60	I	ITYPE	= -1 if acoustically ideal = 0 if estimates of $\alpha_{\lambda,L,K}$ and $\gamma_{12,LK}$ are not available = 1 if estimates of $\alpha_{\lambda,L,K}$ and $\gamma_{12,LK}$ are given in input
3	1-12	R	RO(1)	Outer radius of Chamber 1, the chamber with the lesser value of sonic velocity
	13-24	R	RI(1)	Inner radius of Chamber 1
	25-36	R	XLD(1)	Length of Chamber 1
	37-48	R	CO(1)	Speed of sound in Chamber 1
	49-60	R	UO(1)	Through-flow velocity at the inlet of Chamber 1
4	1-12	R	RO(2)	Outer radius of Chamber 2, the chamber with the greater value of sonic velocity
	13-24	R	RI(2)	Inner radius of Chamber 2
	25-36	R	XLD(2)	Length of Chamber 2
	37-48	R	CO(2)	Speed of sound in Chamber 2
	49-60	R	UO(2)	Through-flow velocity at exit of Chamber 2
	61-66	I	INRAD	= 1 except in the extraordinary case in which mathematical consistency is abandoned and the radial eigenvalues in Chambers 1 and 2 are not required to be identical
If ITYPE=-1				
5	1-12	R	ALRAN(1,1)	The lower limit of the range within which solutions of the radial wave number in Chamber 1, $\alpha_{1,L,K}$, are to be searched for in an ordered fashion (typically = 0 for a cylinder and 0.1 for an annulus)
	13-24	R	ALRAN(2,1)	The upper limit of the range within which solutions of the radial wave number in Chamber 1, $\alpha_{1,L,K}$, are to be searched for in an ordered fashion (should not exceed 20.0)

Line	Location	Type	Input Item	Comments
	25-36	R	ALRAN(3,1)	The step size to be used in searching the specified range for solutions of the radial wave number in Chamber 1, $\alpha_{1,L,K}$ (typically = 0.50)
6	1-12	R	ALRAN(1,2)	The lower limit of the range within which solutions of the radial wave number in Chamber 2, $\alpha_{2,L,K}$, are to be searched for should they differ from those in Chamber 1 (see preceding line)
	13-24	R	ALRAN(2,2)	The upper limit of the range within which solutions of the radial wave number in Chamber 2, $\alpha_{2,L,K}$, are to be searched for should they differ from those in Chamber 1 (see preceding line)
	25-36	R	ALRAN(3,2)	The step size to be used in searching the specified range for solutions of the radial wave number in Chamber 2, $\alpha_{2,L,K}$, should they differ from those in Chamber 1 (see preceding line)
	If INRAD=1, line 6 can be left blank.			
7	1-12	R	XNRAN(1,1)	The lower limit of the range within which solutions of the axial wave number in Chamber 2, $\eta_{2,L,K}$, are to be searched for in an ordered fashion (typically = 0)
	13-24	R	XNRAN(2,1)	The upper limit of the range within which solutions of the axial wave number in Chamber 2, $\eta_{2,L,K}$, are to be searched for in an ordered fashion

Line	Location	Type	Input Item	Comments
	25-36	R	XNRAN(3,1)	The step size to be used in searching the specified range for solutions of the axial wave number in Chamber 2, $\tau_{1,2,K}$ (typically = 0.01)

End of Input for ITYPE=-1

If ITYPE = 0

5	1-12 13-24	C	QAO	The acoustic admittance ratio, A_{a}, of the upstream boundary surface
	25-36 37-48	C	QAL	The acoustic admittance ratio, A_{ℓ}, of the downstream boundary surface
6	1-12 13-24	C	QAA(1)	The acoustic admittance ratio, A_{a_1}, of the outer boundary surface in Chamber 1
	25-36 37-48	C	QAB(1)	The acoustic admittance ratio, A_{b_1}, of the inner boundary surface in Chamber 1
7	1-12 13-24	C	QAA(2)	The acoustic admittance ratio, A_{a_2}, of the outer boundary surface in Chamber 2
	25-36 37-48	C	QAB(2)	The acoustic admittance ratio, A_{b_2}, of the inner boundary surface in Chamber 2

If INRAD=1, line 7 can be left blank.

8	1-6	I	IADMIT	Normally = 1, in which case the transition coefficients which follow relate unsteady pressures and velocities at the interface between the two chambers (see Equations C12 and C13); = 0 only if the coefficients relate unsteady pressures and their derivatives (see Equations C15 and C16)

Line	Location	Type	Input Item	Comments
9	1-12 13-24	C	QQFF	Coefficient, f or $\bar{f}$, relating η_1 and η_2 at the interface between chambers (see Equations C12-C16)
	25-36 37-48	C	QQFP	Coefficient, f', relating u_1' and η_2 at the interface between chambers; or coefficient, $\bar{f}'$, relating $\partial\eta_1/\partial z_1$, and η_2 (see Equations C12-C16)
10	1-12 13-24	C	QQGF	Coefficient, g, relating η_1 to u_2' at the interface between chambers; or coefficient, $\bar{g}$, relating η_1 and $\partial\eta_2/\partial z_2$ (see Equations C12-C16)
	25-36 37-48	C	QQGP	Coefficient, g', relating u_1' to u_2' at the interface between chambers; or coefficient, $\bar{g}'$, relating $\partial\eta_1/\partial z_1$ and $\partial\eta_2/\partial z_2$ (see Equations C12-C16)
If ITYPE=0				
11	1-12	R	ALRAN (1,1)	The lower limit of the range within which solutions of the real part of the radial wave number in Chamber 1, $\alpha_{1,1,K}$, are to be searched for in an ordered fashion (typically = 0 for a cylinder and 0.1 for an annulus)
	13-24	R	ALRAN(2,1)	The upper limit of the range within which solutions of the real part of the radial wave number in Chamber 1, $\alpha_{1,1,K}$, are to be searched for in an ordered fashion (should not exceed 20)
	25-36	R	ALRAN(3,1)	The step size to be used in searching the specifid range for solutions of the real part of the radial wave numbers in Chamber 1, $\alpha_{1,1,K}$, (typically = 0.05)

Line	Location	Type	Input Item	Comments
12	1-12	R	ALRAN(2,1)	The lower limit of the range within which solutions of the real part of the radial wave number in Chamber 2, $\alpha_{2,\ell,\kappa}$, are to be searched for should they differ from those in Chamber 1 (see preceding line)
	13-24	R	ALRAN(2,2)	The upper limit of the range within which solutions of the real part of the radial wave number in Chamber 2, $\alpha_{2,\ell,\kappa}$, are to be searched for should they differ from those in Chamber 1 (see preceding line)
	25-36	R	ALRAN(3,2)	The step size to be used in searching the specified range for solutions of the real part of the radial wave number in Chamber 2, $\alpha_{2,\ell,\kappa}$, should they differ from those in Chamber 1 (see preceding line)
	If INRAD=1, line 12 can be left blank.			
13	1-12	R	XNRAN(1,1)	The lower limit of the range within which solutions of the real part of the axial wave number in Chamber 2, $\gamma_{2,\ell,\kappa}$, are to be searched for in an ordered fashion (typically = 0)
	13-24	R	XNRAN(2,1)	The upper limit of the range within which solutions of the real part of the axial wave number in Chamber 2, $\gamma_{2,\ell,\kappa}$, are to be searched for in an ordered fashion
	25-36	R	XNRAN(3,1)	The step size to be used in searching the specified range for solutions of the real part of the axial wave number in Chamber 2, $\gamma_{2,\ell,\kappa}$ (typically = 0.01)

Line	Location	Type	Input Item	Comments
14	1-12 13-24	C	QQKP(LSTP,KSTP,2)	Estimated combined wave number, $k_{2,L',K'}$, for mode LSTP, KSTP in Chamber 2
	25-36 37-48	C	QQKP(LSTP,KSTP+1,2)	Estimated combined wave number, $k_{2,L',K'+1}$, for mode LSTP, KSTP+1 in Chamber 2
	49-60	C	QQKP(LSTP,KSTP+2,2)	Estimated combined wave number, $k_{2,L',K'+2}$, for mode LSTP, KSTP+2 in Chamber 2

etc. until mode LRQ, KXQ has been accounted for.

15 or 16	1-12 13-24	C	QQKP(LSTP+1,KSTP,2)	Estimated combined wave number, $k_{2,L'+1,K'}$, for mode LSTP+1, KSTP in Chamber 2
	25-36 37-48	C	QQKP(LSTP+1,KSTP+1,2)	Estimated combined wave number, $k_{2,L'+1,K'+1}$, for mode LSTP+1, KSTP+1 in Chamber 2

etc. until mode LRQ, KXQ has been accounted for.

End of Input for ITYPE=0

If ITYPE=1

11	1-12 13-24	C	ALP(LSTP,KSTP,1)	Estimated radial wave number, $\alpha_{1,L',K'}$, for mode LSTP, KSTP in Chamber 1
	25-36 37-48	C	ALP(LSTP,KSTP+L,1)	Estimated radial wave number, $\alpha_{1,L',K'+1}$, for mode LSTP, KKSTP+1 in Chamber 1
	49-60 61-72	C	ALP(LSTP,KSTP+2,1)	Estimated radial wave number, $\alpha_{1,L',K'+2}$, for mode LSTP, KSTP+2 in Chamber 1

etc. until mode LSTP, KXQ has been accounted for.

12 or 13	1-12 13-24	C	ALP(LSTP+1,KSTP,1)	Estimated radial wave number, $\alpha_{1,L'+1,K'}$, for mode LSTP+1, KSTP in Chamber 1

Line	Location	Type	Input Item	Comments
	25-36 37-48	C	ALP(LSTP+1,KSTP+1,1)	Estimated radial wave number, $\alpha_{1,L'+1,K'+1}$, for mode LSTP+1, KSTP+1 in Chamber 1

etc. until mode LRQ, KXQ has been accounted for.

10+LRQ or 10+2*LRQ	1-12	C	ALP(LSTP,KSTP,2)	Estimated radial wave number, $\alpha_{2,L',K'}$, for mode LSTP, KSTP in Chamber 2

etc. as above until mode LRQ, KXQ has been accounted for.

10+2*LRQ or 10+4*LRQ	1-12 13-24	C	ANP(LSTP,KSTP,2)	Estimated axial wave number, $\eta_{2,L',K'}$, for mode LSTP, KSTP in Chamber 2
	25-36 37-48	C	QNP(LSTP,KSTP+1,2)	Estimated axial wave number, $\eta_{2,L',K'+1}$, for mode LSTP, KSTP+1 in Chamber 2

etc. until mode LRQ, KXQ has been accounted for as above with the radial wave numbers.

End of Input for ITYPE=1

OUTPUT DATA

The output of Program HLMHLT consists of three principal sections:

1) The input information is restated to the extent of fully defining the acoustic configuration being examined.

2) The wave numbers are output in the form of complex number matrices with L designating the radial mode index and K the axial mode index:

   $\alpha_{L,K}$: the radial wave number (see Equation C5)
   $\eta_{L,K}$: the axial wave number (see Equation C6)
   $k_{L,K}$: the combined wave number (see Equation C7)

   When ITYPE=0, the wave number output is provided for various intermediate iterations to enable evaluation of the convergence characteristics of the solution. Thus, it is important to concentrate on the fully converged wave number output; this is identified by a statement, defining convergence, on the page which follows the output.

3) The mode shape coefficients are output in the form again of matrices with L designating the radial mode index and K, the axial mode index:

$\left\{\frac{C_{R_{i,L,K}}}{C_{R_{1,L,K}}}\right\}$: radial mode shape coefficient (see Equation C5)

$\left\{\frac{C_{\zeta_{i,L,K}}}{C_{\zeta_{1,L,K}}}\right\}$: axial mode shape coefficient (see Equation C6)

$\left\{\frac{C_{\zeta_{2,L,K}}}{C_{\zeta_{1,L,K}}}\right\}$: chamber-to-chamber amplification coefficient (see Equation C6)

The radial mode shape in Chamber 2 is here assumed to be the same as in Chamber 1; for all cylinders, the radial coefficient is simply zero.

The converged solution accordingly supplies as output all the information needed to define the resonant acoustic characteristics of the duct as defined by Equations C3 through C7. Real and imaginary parts of the complex numbers are separated by a comma throughout the output.

The combined wave number, $k_{i,L,K}$, contains the principal information insofar as it is in fact a nondimensionalized angular frequency:

$$\omega_{0,L,K} = \frac{k_{i,L,K}\, C_{0i}}{R_{0i}} \qquad (C17)$$

where the resonant acoustic wave for the L-K mode is defined by the following equation:

$$\tilde{\eta}_{i,L,K} = \eta_{i,L,K}\, e^{-j\omega_0 t} \qquad (C18)$$

The real part of the eigenvalue, ω_0, thus defines the angular frequency of the resonant mode, and the imaginary part defines the acoustic growth

rate or, when negative, the acoustic decay rate. In more usable form, then, the combined wave number, $k_{\alpha,L,K}$, suffices to define the frequency, Ω_α, and the decrement, λ_α, for the resonant mode:

$$\Omega_{\alpha,L,K} = \frac{\{k_{\alpha,L,K}\}_{REAL} C_{0\alpha}}{2\pi R_{0\alpha}} \qquad (C19)$$

$$\lambda_{\alpha,L,K} = -2\pi \frac{\{k_{\alpha,L,K}\}_{IMAG}}{\{k_{\alpha,L,K}\}_{REAL}} \qquad (C20)$$

The decrement indicates the fractional acoustic energy lost per cycle.

A few words of warning must be made concerning the output of Program HLMHLT. As mentioned above, it is quite important to verify that the output wave numbers represent fully converged solutions: this verification is on the page following the output. Also, in working with the output, it is important to keep the various modes straight via the L and K indices: for any one mode there are two radial, two axial, and two combined wave numbers associated with which are four output mode shape coefficients.

The most serious difficulty that can occur with Program HLMHLT involves a failure to keep track of the modes when poor initial estimates of the wave numbers are supplied. This trouble occurs only when ITYPE=0 or ITYPE=1-- that is, in the acoustically general cases. The trouble can appear in two forms:

1. Modes with distinct L-K indices may converge to the same wave numbers, so that apparently distinct resonant modes are in fact but one.

2. Modes with sequential L or K values may not in fact be sequential when the iteration process converges in such a way as to skip a mode entirely.

It is recommended that the basic acoustic properties of the duct be obtained via an ITYPE=-1 solution so that the output in the general case can be evaluated properly. It is also recommended that the output be so evaluated. Finally, when trouble arises, it is best handled by revising the estimated wave numbers in the input to conform more closely with the acoustic spectrum of the duct.

ERROR MESSAGES

The following two error messages can appear:

1) THE NEWTON-RAPHSON ITERATION LIMIT HAS BEEN EXCEEDED. The message also identifies whether the axial or the radial solution is the problem, identifies the mode, and supplies the last pass values of the characteristic function and its derivative.

2) THE SOLUTION HAS FAILED TO CONVERGE. This can occur only when ITYPE $\geq$ 0, and indicates simply that the over-all iteration procedure has, for some mode, failed to produce values of which repeat to the fourth decimal place.

With regard to the Newton-Raphson iteration, the program simply continues the solution by using the last pass values in spite of the fact that they fail to yield adequate values (near zero) of the characteristic function. For this reason, *the Newton-Raphson error message can be ignored unless it occurs on the last iteration in a converged solution*; when it occurs in the last iteration, however, the mode identified in the message has not been determined, and the associated output is not a solution.

MISCELLANEOUS OPERATING INFORMATION

Complex arithmetic with Fortran IV is an essential software requirement for executing cases with Program HLMHLT. On a CDC 6600 computer the program can determine as many as 25 modes in 25 seconds. Consecutive cases can be run back-to-back, and two blank cards at the end of the input suffice for a normal termination of the run. No storage problems should occur with the program on any but the smallest computers with the necessary software capability.

SAMPLE INPUT FOR PROGRAM HLMHLT

A sample case is displayed on the following pages to illustrate not only the format used in Program HLMHLT, but also results which have been used in subsequent analyses. The sample case involves the TF-30 duct burner, which is modeled as a one dimensional (axial) combustion chamber. The solution searches for resonant wave numbers in specified ranges -- that is, the solution is for ITYPE = 0. Chamber dimensions, sound velocities, and admittances which have been used, are consistent with the TF-30 input to Program NØNLIN. It is seen from the output that ten iterations were required to converge on the solution. Further, since the chamber is one dimensional and axial, the radial wave numbers obtained are zero, and the axial and combined wave numbers are identical.

NORTHERN RESEARCH AND ENGINEERING CORPORATION

DATA INPUT SHEET

ENGINEER: J. A. Given PROJECT: Nonlinear Combustion Instability PROJECT NO: 1294

TITLE: Sample to Illustrate Program HLMHLT SHEET: 1 OF 1

LOCATION

1 6	7 12	13 18	19 24	25 30	31 36	37 42	43 48	49 54	55 60	61 66	67 72
ACOUSTICS FOR TF-30 DUCTBURNER											
0	1	1	5	1	1	1	50	30	0		
8.52				8.52		1000.					
5.59				5.59		2700.					
0.		.15		0.0		.25					
0.		0.		0.		0.					
0.		0.		0.		0.					
1											
1.0		0.0		0.0		0.0					
0.		0.		1.0		0.					
0.		10.0		.1							
0.		10.0		.1							
0.		6.0		.005							
.9				1.75				2.5			
3.75				4.75							

AN ACOUSTIC ANALYSIS OF ANNULAR DUCTS WITH AN AXIAL DISCONTINUITY

ACOUSTICS FOR TF-30 DUCTBURNER

DUCT DIMENSIONS

CHAMBER	OUTER RADIUS	INNER RADIUS	AXIAL LENGTH	SPEED O SOUND	END VELOCITY
1	.85200E+01	-0.	.85200E+01	.10000E+04	-0.
2	.55900E+01	-0.	.55900E+01	.27000E+04	-0.

SURFACE ACOUSTIC ADMITTANCE RATIOS

INLET A= 0. , .15000E+00 EXIT A= 0. , .25000E+00

OUTER A= 0. , 0. INNER A= 0. , 0. IN FIRST CHAMBER

OUTER A= 0. , 0. INNER A= 0. , 0. IN SECOND CHAMBER

DISCONTINUITY COEFFICIENTS

COEFFICIENTS FP AND G RELATE PRESSURES AND VELOCITIES AND ARE THUS MODIFIED BY (J*K) FACTORS

F= .10000E+01 , 0. FP= 0. , 0.

G= 0. , 0. GP= .10000E+01 , 0.

EIGENVALUE SOLUTIONS FOR THE 0TH TANGENTIAL MODE ON THE 0TH ITERATION

RADIAL WAVE NUMBERS

IN CHAMBER 1

	K=1		K=2		K=3		K=4		K=5	
L=1	0.0000 ,	-0.0000	0.0000 ,	-0.0000	0.0000 ,	-0.0000	0.0000 ,	-0.0000	0.0000 ,	-0.0000

IN CHAMBER 2

	K=1		K=2		K=3		K=4		K=5	
L=1	0.0000 ,	-0.0000	0.0000 ,	-0.0000	0.0000 ,	-0.0000	0.0000 ,	-0.0000	0.0000 ,	-0.0000

AXIAL WAVE NUMBERS

IN CHAMBER 1

	K=1		K=2		K=3		K=4		K=5	
L=1	1.2674 ,	0.0000	3.0964 ,	0.0000	5.3941 ,	0.0000	8.1672 ,	0.0000	10.9886 ,	0.0000

IN CHAMBER 2

	K=1		K=2		K=3		K=4		K=5	
L=1	.3080 ,	0.0000	.7524 ,	0.0000	1.3108 ,	0.0000	1.9846 ,	-0.0000	2.6702 ,	-0.0000

COMBINED WAVE NUMBERS

IN CHAMBER 1

	K=1		K=2		K=3		K=4		K=5	
L=1	1.2674 ,	0.0000	3.0964 ,	0.0000	5.3941 ,	0.0000	8.1672 ,	0.0000	10.9886 ,	0.0000

IN CHAMBER 2

	K=1	K=2	K=3	K=4	K=5

L=1	.3080	0.0000	.7524	0.0000	1.7108	0.0000	1.9846	0.0000	2.6702	0.0000

EIGENVALUE SOLUTIONS FOR THE 0TH TANGENTIAL MODE ON THE 1TH ITERATION

RADIAL WAVE NUMBERS

IN CHAMBER 1

	K=1		K=2		K=3		K=4		K=5	
L=1	0.0000 ,	-0.0000	0.0000 ,	-0.0000	0.0000 ,	-0.0000	0.0000 ,	-0.0000	0.0000 ,	-0.0000

IN CHAMBER 2

	K=1		K=2		K=3		K=4		K=5	
L=1	0.0000 ,	-0.0000	0.0000 ,	-0.0000	0.0000 ,	-0.0000	0.0000 ,	-0.0000	0.0000 ,	-0.0000

AXIAL WAVE NUMBERS

IN CHAMBER 1

	K=1		K=2		K=3		K=4		K=5	
L=1	.9026 ,	0.0000	2.6920 ,	0.0000	5.1711 ,	0.0000	8.0073 ,	0.0000	10.8273 ,	0.0000

IN CHAMBER 2

	K=1		K=2		K=3		K=4		K=5	
L=1	.2193 ,	0.0000	.6542 ,	0.0000	1.2566 ,	0.0000	1.9458 ,	0.0000	2.6310 ,	0.0000

COMBINED WAVE NUMBERS

IN CHAMBER 1

	K=1		K=2		K=3		K=4		K=5	
L=1	.9026 ,	0.0000	2.6920 ,	0.0000	5.1711 ,	0.0000	8.0073 ,	0.0000	10.8273 ,	0.0000

IN CHAMBER 2

	K=1	K=2	K=3	K=4	K=5

L=1 .2193 • 0.0000 .6542 • 0.0000 1.2566 • 0.0000 1.9458 • 0.0000 2.6310 • 0.0000

ITERATION 2

ITERATION 3

ITERATION 4

ITERATION 5

ITERATION 6

ITERATION 7

ITERATION 8

ITERATION 9

ITERATION 10

EIGENVALUE SOLUTIONS FOR THE 0TH TANGENTIAL MODE ON THE 10TH ITERATION

RADIAL WAVE NUMBERS

IN CHAMBER 1

	K=1		K=2		K=3		K=4		K=5	
L=1	0.0000 ,	-0.0000	0.0000 ,	-0.0000	0.0000 ,	-0.0000	0.0000 ,	-0.0000	0.0000 ,	-0.0000

IN CHAMBER 2

	K=1		K=2		K=3		K=4		K=5	
L=1	0.0000 ,	-0.0000	0.0000 ,	-0.0000	0.0000 ,	-0.0000	0.0000 ,	-0.0000	0.0000 ,	-0.0000

AXIAL WAVE NUMBERS

IN CHAMBER 1

	K=1		K=2		K=3		K=4		K=5	
L=1	.4833 ,	0.0000	2.4950 ,	0.0000	5.0978 ,	0.0000	7.9589 ,	0.0000	10.7779 ,	0.0000

IN CHAMBER 2

	K=1		K=2		K=3		K=4		K=5	
L=1	.1174 ,	0.0000	.6063 ,	0.0000	1.2388 ,	0.0000	1.9340 ,	0.0000	2.6191 ,	0.0000

COMBINED WAVE NUMBERS

IN CHAMBER 1

	K=1		K=2		K=3		K=4		K=5	
L=1	.4833 ,	0.0000	2.4950 ,	0.0000	5.0978 ,	0.0000	7.9589 ,	0.0000	10.7779 ,	0.0000

IN CHAMBER 2

	K=1	K=2	K=3	K=4	K=5

L=1	.1174	0.0000	.6063	0.0000	1.2384	0.0000	1.9340	0.0000	2.6191	0.0000

SOLUTION HAS CONVERGED AFTER 10 ITERATIONS

MODE SHAPE COEFFICIENTS FOR THE 0TH TANGENTIAL MODE

RADIAL COEFFICIENT

IN CHAMBER 1

	K=1	K=2	K=3	K=4	K=5
L=1	0. , 0.	0. , 0.	0. , 0.	0. , 0.	0. , 0.

AXIAL COEFFICIENT

IN CHAMBER 1

	K=1	K=2	K=3	K=4	K=5
L=1	.7260E-01, 0.	.3743E+00, 0.	.7647E+00, 0.	.1194E+01, 0.	.1617E+01, 0.

IN CHAMBER 2

	K=1	K=2	K=3	K=4	K=5
L=1	-.1510E-01, 0.	.2291E+00, 0.	.1903E+01, 0.	-.1628E+02, 0.	-.2527E+01, 0.

CHAMBER TO CHAMBER AMPLIFICATION COEFFICIENT

IN CHAMBER 2

	K=1	K=2	K=3	K=4	K=5
L=1	.9553E+00, 0.	-.7078E+00, 0.	.2370E+00, 0.	.4445E-01, 0.	-.3624E+00, 0.

(AXIAL COEFFICIENT) * (AMPLIFICATION COEFFICIENT)

IN CHAMBER 2

	K=1	K=2	K=3	K=4	K=5
L=1	-.1443E-01, 0.	-.1622E+00, 0.	.4510E+00, 0.	-.7236E+00, 0.	.9157E+00, 0.

LISTING OF PROGRAM HLMHLT

```
      PROGRAM HLMHLT(INPUT,OUTPUT,TAPE5=INPUT,TAPE6=OUTPUT)
      COMPLEX QAO,QAL,QAA(2),QAB(2),QQFF,QQFP,QQGF,QQGP,QQKP(5,5,2)
      COMPLEX XJ
      COMPLEX AO,AL,AA,AB,QFF,QFP,QGF,QGP,ALP,QNP,QKP
      COMPLEX QFL1,QFL2
       COMPLEX FN,FNP,C1Q(5,5,2),C2Q(5,5,2),C3Q(5,5)
      DIMENSION UO(2)
      DIMENSION TITLE(12)
      DIMENSION XLD(2)
      COMMON/DIM/RO(2),RI(2),XL(2),CO(2),INRAD
      COMMON/BOUN/AO(5,5),AL(5,5),AA(5,5,2),AB(5,5,2),QFF(5,5),QFP(5,5),
     1  QGF(5,5),QGP(5,5)
      COMMON/WAVE/M,ALP(5,5,2),QNP(5,5,2),QKP(5,5,2)
      COMMON/RANGE/ALRAN(3,2),XNRAN(3),KST,KXQ,KSTP,LST,LRQ,LSTP,NRQ
   10 DO 100 L=1,5
      DO 100 K=1,5
      DO 100 I=1,2
       ALP(L,K,I)=(0.0,0.0)
      QNP(L,K,I)=(0.0,0.0)
      QKP(L,K,I)=(0.0,0.0)
      QQKP(L,K,I)=(0.0,0.0)
  100 CONTINUE
      READ (5,9000) TITLE
      READ (5,9010) M,KST,KSTP,KXQ,LST,LSTP,LRQ,NRQ,ITER,ITYPE
      IF(KXQ+LRQ+M  .LE.  0) STOP
      WRITE (6,9200) TITLE
      DO 200 I=1,2
      READ (5,9020) RO(I),RI(I),XLD(I),CO(I),UO(I),INRAD
       WRITE (6,9210) I,RO(I),RI(I),XLD(I),CO(I),UO(I)
      UO(I)=UO(I)/CO(I)
      XL(I)=XLD(I)/RO(I)
  200 CONTINUE
      WRITE(6,9220)
      IF(ITYPE .GE. 0) GO TO 250
      WRITE (6,9225)
      QAO=(0.0,0.0)
      QAL=(0.0,0.0)
       DO 220 I=1,2
      QAA(I)=(0.0,0.0)
      QAB(I)=(0.0,0.0)
  220 CONTINUE
      QQFF=(1.0,0.0)
      QQFP=(0.0,0.0)
       QQGF=(0.0,0.0)
      QQGP=(RO(2)/RO(1))*(CO(1)/CO(2))**2
      IADMIT=0
      GO TO 280
  250 READ (5,9030) QAO,QAL
      WRITE (6,9230) QAO,QAL
      READ(5,9030)QAA(1),QAB(1)
      WRITE (6,9240) QAA(1),QAB(1)
      READ(5,9030) QAA(2),QAB(2)
      WRITE (6,9250) QAA(2),QAB(2)
      WRITE (6,9260)
```

```
      READ (5,9010) IADMIT
      IF (IADMIT .GT. 0) WRITE (6,9270)
      READ(5,9030) QQFF,QQFP
      WRITE(6,9280) QQFF,QQFP
      READ(5,9030)QQGF,QQGP
      WRITE (6,9290) QQGF,QQGP
  280 B=(RO(2)*CO(1)/(RO(1)*CO(2)))**2
      BP=SQRT(B)
      IF (ITYPE .LE. 0) GO TO 500
      DO 300 I=1,2
       DO 300 L=LSTP,LRQ
      READ (5,9030)(ALP(L,K,I),K=KSTP,KXQ)
  300 CONTINUE
      DO 350 L=LSTP,LRQ
      READ (5,9030) (QNP(L,K,2),K=KSTP,KXQ)
      DO 350 K=KSTP,KXQ
      QNP(L,K,1)=CSQRT((QNP(L,K,2)**2+ALP(L,K,2)**2)/B-ALP(L,K,1)**2)
  350 CONTINUE
      DO 400 I=1,2
      DO 400 L=LSTP,LRQ
      DO 400 K=KSTP,KXQ
      QQKP(L,K,I)=CSQRT(ALP(L,K,I)**2+QNP(L,K,I)**2)
      QKP(L,K,I)=QQKP(L,K,I)
  400 CONTINUE
      GO TO 650
  500 DO 550 I=1,2
      READ (5,9030) (ALRAN(K,I),K=1,3)
  550 CONTINUE
      READ (5,9030)(XNRAN(K),K=1,3)
      IF (ITYPE .LT. 0) GO TO 650
      DO 600 L=LSTP,LRQ
      READ (5,9030) (QQKP(L,K,2),K=KSTP,KXQ)
      DO 600 K=KSTP,KXQ
      QQKP(L,K,1)=QQKP(L,K,2)/BP
  600 CONTINUE
  650 XJ=CMPLX(0.0,1.0)
      ITERQP=0
  660 DO 700 L=LSTP,LRQ
      DO 700 K=KSTP,KXQ
      IF (ITYPE .GE. 0) GO TO 665
      QFL1=0.0
      QFL2=0.0
      GO TO 668
  665 CONTINUE
      QFL1=QNP(L,K,1)/QQKP(L,K,1)
      QFL2=QNP(L,K,2)/QQKP(L,K,2)
      IF (UO(1) .EQ. 0.0) QFL1=0.0
      IF (UO(2) .EQ. 0.0) QFL2=0.0
  668 CONTINUE
      AO(L,K)=XJ*QQKP(L,K,1)*(-QAO-UO(1)*QFL1**2)
      AL(L,K)=XJ*QQKP(L,K,2)*(QAL-UO(2)*QFL2**2)
      IF (ITYPE .EQ. 0 .AND. ITERQP .EQ. 0)
     1QNP(L,K,2)=CMPLX(0.0,-AIMAG((AO(L,K)+AL(L,K))/10.0)    )
      QFF(L,K)=QQFF
      QFP(L,K)=QQFP
```

```
      QGF(L,K)=QQGF
      QGP(L,K)=QQGP
      IF (IADMIT .LE. 0) GO TO 670
      QFP(L,K)=-QFP(L,K)*XJ*CO(1)/(1.4*QQKP(L,K,1))
      QGF(L,K)=XJ*QQKP(L,K,2)*1.4*QGF(L,K)/CO(2)
      QGP(L,K)=QGP(L,K)*(RO(2)/RO(1))*(CO(1)/CO(2))**2
  670 CONTINUE
      DO 700 I=1,2
      AA(L,K,I)=XJ*QQKP(L,K,I)*QAA(I)
      AB(L,K,I)=-XJ*QQKP(L,K,I)*QAB(I)
      IF (ITYPE .EQ. 0 .AND. ITERQP .EQ. 0)
     1ALP(L,K,I)=CMPLX(0.0,-AIMAG((AA(L,K,I)+AB(L,K,I))/5.)  )
  700 CONTINUE
      IF (ITYPE .GT. 0 .OR. ITERQP .GT. ITER/4) GO TO 2000
 1000 CALL ACUSTK(0,0)
      GO TO 3000
 2000 CALL ACUSTK(1,1)
 3000 DO 3100 I=1,2
      DO 3100 L=LSTP,LRQ
      DO 3100 K=KSTP,KXQ
      QKP(L,K,I)=CSQRT(ALP(L,K,I)**2+QNP(L,K,I)**2)
 3100 CONTINUE
      IF(ITYPE.GT.0.OR.(ITERQP.GT.1.AND.ITERQP.LT.ITER-2))GO TO 3950
 3200 WRITE (6,9300) M,ITERQP
      DO 3300 I=1,2
      WRITE (6,9310) I,(K,K=KSTP,KXQ)
      DO 3300 L=LSTP,LRQ
      WRITE (6,9320) L,(ALP(L,K,I),K=KSTP,KXQ)
 3300 CONTINUE
      WRITE (6,9330)
      DO 3400 I=1,2
      WRITE (6,9310) I,(K,K=KSTP,KXQ)
      DO 3400 L=LSTP,LRQ
      WRITE (6,9320) L,(QNP(L,K,I),K=KSTP,KXQ)
 3400 CONTINUE
      WRITE (6,9340)
      DO 3500 I=1,2
      WRITE (6,9310) I,(K,K=KSTP,KXQ)
      DO 3500 L=LSTP,LRQ
      WRITE (6,9320) L, (QKP(L,K,I),K=KSTP,KXQ)
 3500 CONTINUE
      IF (ITYPE .GE. 0 .AND. ITERQP .LT. ITER) GO TO 4000
      IF (ITYPE .LT. 0) WRITE (6,9350) ITERQP
      IF (ITERQP .GE. ITER) WRITE (6,9360) ITERQP
      GO TO 6000
 3950 IF (ITERQP .EQ. 2) WRITE (6,9380)
      WRITE (6,9370) ITERQP
 4000 ITERQP=ITERQP+1
      IF (ITERQP .GT. ITER) GO TO 3200
      DO 4500 I=1,2
      DO 4500 K=KSTP,KXQ
      DO 4500 L=LSTP,LRQ
      IF (CABS(QQKP(L,K,I)-QKP(L,K,I)).GT. 1.0E-3) GO TO 4600
 4500 CONTINUE
      ITYPE=-1
```

```
      ITERQP=ITERQP-1
      GO TO 3200
 4600 C=ITERQP*5
      DO 4700 I=1,2
      DO 4700 K=KSTP,KXQ
      DO 4700 L=LSTP,LRQ
      QQKP(L,K,I)=QQKP(L,K,I)/C+(C-1.0)*QKP(L,K,I)/C
 4700 CONTINUE
      GO TO 660
 6000 CONTINUE
      WRITE (6,9390) M
      DO 6100 L=LSTP,LRQ
      DO 6100 K=KSTP,KXQ
      IF (RI(1) .LE. 0.0) GO TO 6050
      CALL CJFUN (FN,FNP,ALP(L,K,1),AA(L,K,1),M)
      C1Q(L,K,1)=FN
      CALL CYFUN(FN,FNP,ALP(L,K,1),AA(L,K,1),M)
      IF (CABS(FN) .EQ. 0.0 ) FN=(1.0E-20,0.0)
      C1Q(L,K,1)=-C1Q(L,K,1)/FN
      GO TO 6100
 6050 C1Q(L,K,1)=(0.0,0.0)
 6100 CONTINUE
      I=1
      WRITE(6,9310)I,(K,K=KSTP,KXQ)
      DO 6200 L=LSTP,LRQ
      WRITE (6,9420) L,(C1Q(L,K,1),K=KSTP,KXQ)
 6200 CONTINUE
      WRITE (6,9400)
      DO 6300 L=LSTP,LRQ
      DO 6300 K=KSTP,KXQ
       C2Q(L,K,1)=AO(L,K)
      FN=CCOS(QNP(L,K,2)*XL(2))
      FNP=CSIN(QNP(L,K,2)*XL(2))
      IF (CABS(QNP(L,K,2)).LE. 0.0) GO TO 6230
      FNP=FNP/QNP(L,K,2)
      GO TO 6240
 6230 FNP=(1.0,0.0)
 6240 C2Q(L,K,2)=FN-AL(L,K)*FNP
      IF (CABS(AL(L,K)) .GT. 1.0E5) C2Q(L,K,2)=FN/AL(L,K)-FNP
      IF (CABS(C2Q(L,K,2)).EQ. 0.0) C2Q(L,K,2)=(1.0E-20,0.0)
      IF (CABS(AL(L,K)) .GT. 1.0E5) C2Q(L,K,2)=(QNP(L,K,2)**2*FNP/AL(L,K)
     1  )*FN)/C2Q(L,K,2)
      IF (CABS(AL(L,K)).GT. 1.0E5) GO TO 6300
      C2Q(L,K,2)=(QNP(L,K,2)**2*FNP+AL(L,K)*FN)/C2Q(L,K,2)
 6300 CONTINUE
      DO 6400 I=1,2
      WRITE (6,9310) I,(K,K=KSTP,KXQ)
      DO 6400 L=LSTP,LRQ
      WRITE (6,9420) L,(C2Q(L,K,I),K=KSTP,KXQ)
 6400 CONTINUE
      I=2
      WRITE(6,9410)
      DO 6500 L=LSTP,LRQ
      DO 6500 K=KSTP,KXQ
      FN=CCOS(QNP(L,K,1)*XL(1))
```

```
      FNP=CSIN(QNP(L,K,1)*XL(1))
      IF (CABS(QNP(L,K,1)) .LE. 0.0) GO TO 6430
      FNP=FNP/QNP(L,K,1)
      GO TO 6440
 6430 FNP=(1.0,0.0)
 6440 C3Q(L,K)=FN*(QFF(L,K)*AO(L,K)*QFP(L,K))+FNP*(QFF(L,K)*AO(L,K)-
     1 QFP(L,K)*QNP(L,K,1)**2)
      IF (CABS(AO(L,K)) .GT. 1.0E5) C3Q(L,K)=AO(L,K)*(FN*(QFF(L,K)/
     1  AO(L,K)+QFP(L,K))+FNP*(QFF(L,K)-QFP(L,K)*QNP(L,K,1)**2/AO))
 6500 CONTINUE
      WRITE (6,9310) I,(K,K=KSTP,KXQ)
      DO 6600 L=LSTP,LRQ
      WRITE (6,9420) L, (C3Q(L,K),K=KSTP,KXQ)
 6600 CONTINUE
      DO 6700 L=LSTP,LRQ
      DO 6700 K=KSTP,KXQ
      C3Q(L,K)=C3Q(L,K)*C2Q(L,K,2)
 6700 CONTINUE
      I=2
      WRITE(6,9430)
      WRITE(6,9310) I,(K,K=KSTP,KXQ)
      DO 6800 L=LSTP,LRQ
      WRITE(6,9420)L,(C3Q(L,K),K=KSTP,KXQ)
 6800 CONTINUE
      GO TO 10
 9000 FORMAT(12A6)
 9010 FORMAT(10I6)
 9200 FORMAT(1H1,30X,65HAN ACOUSTIC ANALYSIS OF ANNULAR DUCTS WITH AN AXIAL
     1IAL DISCONTINUITY  , ////,30X,12A6,////////,20X,15HDUCT DIMENSIONS,/
     2 ///,1X,7HCHAMBER,6X,12HOUTER RADIUS,5X,12HINNER RADIUS,5X,12HAXIA
     3L LENGTH,5X,13HSPEED O SOUND,4X,13H END VELOCITY )
 9020 FORMAT (5E12.0,I6)
 9210 FORMAT(/,5X,I1,8X,E12.5,5X,E12.5,5X,E12.5,5X,E12.5,5X,E12.5)
 9220 FORMAT (////,20X,34HSURFACE ACOUSTIC ADMITTANCE RATIOS ,//)
 9030 FORMAT(6E12.0)
 9230 FORMAT(10X,9HINLET A= ,F12.5,3H , ,E12.5,20X,9HEXIT A=  ,E12.5,3H
     1, ,E12.5//)
 9240 FORMAT(10X,9HOUTER A= ,F12.5,3H , ,E12.5,20X,9HINNER A= ,E12.5,
     1 3H , ,E12.5,10X,16HIN FIRST CHAMBER , //)
 9250 FORMAT(10X,9HOUTER A= ,E12.5,3H , ,E12.5, 20X,9HINNER A= ,E12.5,
     1 3H , , E12.5,10X,17HIN SECOND CHAMBER , //)
 9260 FORMAT(////,20X,26HDISCONTINUITY COEFFICIENTS ,  //)
 9270 FORMAT(30X,92HCOEFFICIENTS FP AND G RELATE PRESSURES AND VELOCITIE
     1S AND ARE THUS MODIFIED BY (J*K) FACTORS ,//)
 9280 FORMAT(10X,2HF=,E12.5,3H , ,E12.5,25X,3HFP=,E12.5,3H , ,E12.5,//)
 9290 FORMAT(10X,2HG=,E12.5,3H , ,E12.5,25X,3HGP=,E12.5,3H , ,F12.5,//)
 9300 FORMAT(1H1,30X,29HEIGENVALUE SOLUTIONS FOR THE ,I1,     26HTH TANG
     1ENTIAL MODE ON THE ,I2,12HTH ITERATION,////,20X,19HRADIAL WAVE NUM
     2BERS ,  )
 9310 FORMAT(//50X,11HIN CHAMBER  ,I1,/7X,5(9X,2HK=,I1,13X)//)
 9320 FORMAT(1X,2HL=,I1,3X,5(F9.4,3H , , F9.4,4X)//)
 9330 FORMAT(///,20X,18HAXIAL WAVE NUMBERS ,   )
 9340 FORMAT(///,20X,21HCOMBINED WAVE NUMBERS,   )
 9350 FORMAT(1H1,30X,29HSOLUTION HAS CONVERGED AFTER I2,11H ITERATIONS ,
     1 //)
```

```
9360 FORMAT(1H1,30X,55HITERATION HAS BEEN TERMINATED WITHOUT CONVERGENC
     1E AFTER  ,I2, 11H ITERATIONS, //)
9225 FORMAT(20X,88HBOTH CHAMBERS HAVE ACOUSTICALLY RIGID SURFACES AND T
     1HE FLAME-FRONT IS ACOUSTICALLY IDEAL ,///)
9370 FORMAT (30X,10HITERATION ,I2,//)
9380 FORMAT(1H1)
9390 FORMAT (1H1,30X,32HMODE SHAPE COEFFICIENTS FOR THE ,I1,18HTH TANGE
     1NTIAL MODE  ,////,20X,18HRADIAL COEFFICIENT  ,)
9400 FORMAT(///,20X,17HAXIAL COEFFICIENT  ,)
9410 FORMAT(///,20X,44HCHAMBER TO CHAMBER AMPLIFICATION COEFFICIENT ,)
9420 FORMAT(1X,2HL=,I1,2X,5(F1).4,1H,,E11.4,2X))
9430 FORMAT(///,20X,49H(AXIAL COEFFICIENT) * (AMPLIFICATION COEFFICIENT
     1)   ,)
      END
```

```
      SUBROUTINE ACUSTK(INDIC1,INDIC2)
      COMPLEX AO,AL,AA,AB,QFF,QFP,QGF,QGP,ALP,QNP,QKP,AQ,FN,FNP,
     1    ZDEL, QN1,QN2
      COMPLEX FQN,FQNP,AQP,QNP1,QNP2
      COMMON/DIM/RO(2),RI(2),XL(2),CO(2),INRAD
      COMMON/BOUN/AO(5,5),AL(5,5),AA(5,5,2),AB(5,5,2),QFF(5,5),QFP(5,5),
     1  QGF(5,5),QGP(5,5)
      COMMON/WAVE/M,ALP(5,5,2),QNP(5,5,2),QKP(5,5,2)
      COMMON/RANGE/ALRAN(3,2),XNRAN(3),KST,KXQ,KSTP,LST,LRQ,LSTP,NRQ
      NFRN=NRQ/4
      IF (INDIC1) 3000,1000,2000
 1000 I=1
      IF (LST .GT. LRQ) GO TO 3000
 1050 B=RI(I)/RO(I)
      K=1
 1100 L=LST
 1110 LP=LST
      FNTST=0.0
      AQ=CMPLX(ALRAN(1,I),AIMAG(ALP(L,K,I)))
 1150 CALL ANFUN(FN,FNP,AQ,AA(L,K,I),AB(L,K,I),B,M)
      IF (REAL(FN) .NE. 0.0) GO TO 1170
      FNTST=1.0
      GO TO 1175
 1170 CONTINUE
      IF (FNTST/REAL(FN) .GE. 0.0) GO TO 1200
 1175 CONTINUE
      AQP=AQ+ALRAN(3,I)*REAL(FN)/(FNTST-REAL(FN))
      DO 1185 N=1,NFRN
      CALL ANFUN(FQN,FQNP,AQP,AA(L,K,I),AB(L,K,I),B,M)
      IF(CABS(FQN).LE.1.0E-5)GO TO 1195
      IF(CABS(FQNP).EQ.0.0) GO TO 1200
      XR=REAL(FQN)
      XI=AIMAG(FQN)
      XPR=REAL(FQNP)
      XPI=AIMAG(FQNP)
      ZDEL=CMPLX(-XPI*XI-XPR*XR,XPI*XR-XPR*XI)/(XPR**2+XPI**2)
      IF(CABS(ZDEL).GT.5.*CABS(FQN))ZDEL=ZDEL*CABS(FQN)/(2.*CABS(ZDEL))
      AQP=AQP+ZDEL
      IF(REAL(AQP).LT.0.0)AQP=CMPLX(0.0,AIMAG(AQP))
      IF (CABS(ZDEL) .LE. .01 .OR. CABS(FQN) .LE. .1) GO TO 1195
 1185 CONTINUE
      GO TO 1200
 1195 LP=LP+1
      IF (LP .LE. L) GO TO 1200
      ALP(L,K,I)=AQP
      L=L+1
      IF (L .GT. LRQ)  GO TO 1300
      GO TO 1110
 1200 FNTST=REAL(FN)
      AQ=AQ+ALRAN(3,I)
      IF (REAL(AQ) .LE. ALRAN(2,I)) GO TO 1150
 1300 LRQ=L-1
      IF (LRQ .LE. LSTP)  LRQ=LSTP
      K=K+1
```

```
      IF (K .LE. KXQ) GO TO 1100
      IF (I .GE. 2)  GO TO 2000
      I=2
      IF (INRAD) 1050,1050,1350
1350  DO 1400  L=LST,LRQ
      DO 1400  K=1,KXQ
      ALP(L,K,2)=ALP(L,K,1)
1400  CONTINUE
2000  I=1
         IF (LST .GT. LRQ)  GO TO 3000
2050  B=RI(I)/RO(I)
      K=KSTP
2100  L=LST
2150  AQ=ALP(L,K,I)
      N=1
2200  CALL ANFUN(FN,FNP,AQ,AA(L,K,I),AB(L,K,I),B,M)
      IF (CABS(FN) .LE. 1.0E-5)  GO TO 2300
      IF (CABS(FNP).EQ.0.0) GO TO 2290
      XR=REAL(FN)
      XI=AIMAG(FN)
      XPR=REAL(FNP)
      XPI=AIMAG(FNP)
      ZDEL=CMPLX(-XPI*XI-XPR*XR,XPI*XR-XPR*XI)/(XPR**2+XPI**2)
      IF(CABS(ZDEL).GT.5.*CABS(FN ))ZDEL=ZDEL*CABS(FN )/(2.*CABS(ZDEL))
      AQ=AQ+ZDEL
      IF (CABS(ZDEL) .LE. 1.0E-5 .OR. CABS(FN) .LE. 1.0E-5) GO TO 2300
      N=N+1
      IF (N .LE. NRQ) GO TO 2200
2290  CONTINUE
      WRITE (6,9050) L,K,I,XR,XI,XPR,XPI
2300  ALP(L,K,I)=AQ
      L=L+1
      IF (L .LE. LRQ) GO TO 2150
      K=K+1
      IF (K .LE. KXQ) GO TO 2100
      IF (I .GE. 2) GO TO 3000
      I=2
      IF (INRAD) 2050,2050,2350
2350  DO 2400 L=LST,LRQ
       DO 2400 K=KSTP,KXQ
      ALP(L,K,2)=ALP(L,K,1 )
2400  CONTINUE
3000  IF(INDIC2) 5000,3100,4000
3100  L=1
         IF (KST .GT. KXQ) GO TO 5000
      B=(RO(2)*CO(1)/(RO(1)*CO(2)))**2
3150  K=KST
3160  KP=KST
      FNTST=0.0
      QN2=CMPLX(XNRAN(1),AIMAG(QNP(L,K,2)))
3200  QN1        =CSQRT((QN2        **2+ALP(L,K,2)**2)/B-ALP(L,K,1)**2)
      CALL AXFUN(FN,FNP,QN1,QN2,AO(L,K),AL(L,K),QFF(L,K),QFP(L,K),
     1   QGF(L,K),QGP(L,K),B)
       IF (REAL(FN) .NE. 0.0) GOTO 3240
      FNTST=1.0
```

```
      GO TO 3250
 3240 CONTINUE
      IF (FNTST/REAL(FN) .GE. 0.0) GO TO 3300
 3250 CONTINUE
      QNP2=QN2+XNRAN(3)*REAL(FN)/(FNTST-REAL(FN))
      QNP1=CSQRT((QNP2**2+ALP(L,K,2)**2)/B-ALP(L,K,1)**2)
      DO 3260 N=1,NFRN
      CALL AXFUN(FQN,FQNP,QNP1,QNP2,AO(L,K),AL(L,K),QFF(L,K),QFP(L,K),
     1 QGF(L,K),QGP(L,K),B)
      IF (CABS(FQN).LE.1.0E-5)GO TO 3270
      IF(CABS(FQNP).EQ.0.0)GO TO 3300
      XR=REAL(FQN)
      XI=AIMAG(FQN)
      XPR=REAL(FQNP)
      XPI=AIMAG(FQNP)
      ZDEL=CMPLX(-XPI*XI-XPR*XR,XPI*XR-XPR*XI)/(XPR**2+XPI**2)
      IF(CABS(ZDEL).GT.5.*CABS(FQN))ZDEL=ZDEL*CABS(FQN)/(2.*CABS(ZDEL))
      QNP2=QNP2+ZDEL
      IF(REAL(QNP2).LT.0.0)QNP2=CMPLX(0.0,AIMAG(QNP2))
      IF (CABS(ZDEL).LE. .01 .OR. CABS(FQN) .LE. .1) GO TO 3270
 3260 CONTINUE
      GO TO 3300
 3270 KP=KP+1
      IF (KP .LE. K) GO TO 3300
      QNP(L,K,2)=QNP2
      QNP(L,K,1)=CSQRT((QNP(L,K,2)**2+ALP(L,K,2)**2)/B-ALP(L,K,1)**2)
      K=K+1
      IF (K.GT. KXQ) GO TO 3400
      GO TO 3160
 3300 FNTST=REAL(FN)
      QN2=QN2+XNRAN(3)
      IF (REAL(QN2) .LE. XNRAN(2)) GO TO 3200
 3400 KXQ=K-1
      IF (KXQ .LE. KSTP)  KXQ=KSTP
      L=L+1
      IF (L .LE. LRQ) GO TO 3150
 4000 L=LSTP
      IF (KST .GT. KXQ) GO TO 5000
      B=(RO(2)*CO(1)/(RO(1)*CO(2)))**2
 4100 K=KST
 4200 QN2=QNP(L,K,2)
      N=1
 4300 QN1        =CSQRT((QN2        **2+ALP(L,K,2)**2)/B-ALP(L,K,1)**2)
      CALL AXFUN(FN,FNP,QN1,QN2,AO(L,K),AL(L,K),QFF(L,K),QFP(L,K),
     1  QGF(L,K),QGP(L,K),B)
      IF (CABS(FN) .LE. 1.0E-5)  GO TO 4400
      IF (CABS(FNP).EQ.0.0) GO TO 4390
      XR=REAL(FN)
      XI=AIMAG(FN)
      XPR=REAL(FNP)
      XPI=AIMAG(FNP)
      ZDEL=CMPLX(-XPI*XI-XPR*XR,XPI*XR-XPR*XI)/(XPR**2+XPI**2)
      IF(CABS(ZDEL).GT.5.*CABS(FN ))ZDEL=ZDEL*CABS(FN )/(2.*CABS(ZDEL))
      QN2=QN2+ZDEL
      IF (CABS(ZDEL) .LE. 1.0E-5 .OR. CABS(FN) .LE. 1.0E-5) GO TO 4400
```

```
      N=N+1
      IF (N .LE. NRQ) GO TO 4300
 4390 CONTINUE
      WRITE (6,9060) L,K,XR,XI,XPR,XPI
 4400 QNP(L,K,2)=QN2
      QNP(L,K,1)=CSQRT((QNP(L,K,2)**2+ALP(L,K,2)**2)/B-ALP(L,K,1)**2)
      K=K+1
      IF (K .LE. KXQ) GO TO 4200
      L=L+1
      IF (L .LE. LRQ) GO TO 4100
      IF (KSTP .GE. KST)  GO TO 5000
      KP=KST-1
      DO 4700 K=KSTP,KP
       DO 4700 L=1,LRQ
      QNP(L,K,1)=CSQRT((QNP(L,K,2)**2+ALP(L,K,2)**2)/B-ALP(L,K,1)**2)
 4700 CONTINUE
 5000 RETURN
 9050 FORMAT(3X,59HNEWTON-RAPHSON ITERATION HAS EXCEEDED LIMIT FOR RADIA
     1L MODE  , // 3X,2HL=,I2,5X,2HK=,I2,5X,2HI=,I2,5X,2HF=,E14.5,3H , ,
     2 E14.5,5X,3HFP=,E14.5,3H , ,E14.5,//)
 9060 FORMAT(3X,58HNEWTON-RAPHSON ITERATION HAS EXCEEDED LIMIT FOR AXIAL
     1 MODE, // 3X,2HL=,I2,5X,2HK=,I2,5X,2HF=,E14.5,3H , ,E14.5,5X,3HFP=
     2 ,F14.5,3H , ,F14.5,//)
      END
```

```
      SUBROUTINE ANFUN(FN,FNP,Z,AA,AB,B,M)
      COMPLEX FN,FNP,Z,AA,AB,FQ1,FQP1,FQ2,FQP2,YQ1,YQP1,YQ2,YQP2
      CALL CJFUN(FQ1,FQP1,Z,AA,M)
      IF (B .GT. 0.0) GO TO 50
      FN=FQ1
      FNP=FQP1
      RETURN
   50 CALL CJFUN(FQ2,FQP2,B*Z,B*AB,M)
      CALL CYFUN(YQ1,YQP1,Z,AA,M)
      CALL CYFUN(YQ2,YQP2,B*Z,B*AB,M)
      FN=FQ2*YQ1-FQ1*YQ2
      FNP=FQ2*YQP1+FQP2*YQ1*B-FQP1*YQ2-FQ1*YQP2*B
      RETURN
      END
```

```
      SUBROUTINE CJFUN(FN,FNP,Z,A,M)
      COMPLEX FN,FNP,Z,A,ZD2,ZD2S,S,T,Q1,Q2,Q3
      ZD2=Z/2.0
      ZD2S=ZD2**2
      IF (M .EQ. 0)  GO TO 500
      XM =M
      S=1.0/FACT(M)
      T=ZD2
      IF (CABS(T) .EQ. 0.0) T=(1.0,0.0)
      TST=CABS((A+XM+1.0)/(T**M))
      XK=1.0
      FN=(A-XM)*S
      FNP=FN*(XM/2.0)
100   S=S*ZD2S/(XK*(XK+XM))
      T=ZD2S/((XK+1.0)*(XM+XK+1.0))
      Q3=A-XM-2.0*XK
      Q1=T*(Q3-2.0)
      Q2=Q1*(XK+1.0+XM/2.0)
      Q1=(Q1-Q3)*S
       Q2=(Q2-(XK+XM/2.0)*Q3)*S
      FN=FN+Q1
      FNP=FNP+Q2
      IF (CABS(Q1)/TST .LT. 1.0E-8 .AND. CABS(Q2)/TST .LT. 1.0E-8)
     1  GO TO 200
      XK=XK+2.0
      S=S*T
       GO TO 100
200   FN=FN*ZD2**M
      IF (M .EQ. 1) RETURN
      FNP=FNP*ZD2**(M-1)
      RETURN
500   TST=CABS(A+1.0)
      S=1.0
      XK=1.0
      FNP=2.0*ZD2S
      FN=A+FNP
600   S=S*ZD2S/(XK*XK)
       T=ZD2S/((XK+1.0)*(XK+1.0))
      Q3=2.0*ZD2S+XK*A
       Q2=((Q3+A)*T-Q3)*S
       Q1=(T*(2.0*ZD2S/(XK+2.0)+A)-(2.0*ZD2S/(XK+1.0)+A))*S
      FN=FN+Q1
      FNP=FNP+Q2
      IF (CABS(Q1)/TST .LT. 1.0E-8 .AND. CABS(Q2)/TST .LT. 1.0E-8)
     1  GO TO 700
      XK=XK+2.0
      S=S*T
       GO TO 600
700   IF (CABS(ZD2).EQ. 0.0) GO TO 750
      FNP=FNP/ZD2
750   RETURN
      END
```

```
      SUBROUTINE CYFUN(FN,FNP,Z,A,M)
      COMPLEX FN,FNP,Z,A,ZD2,ZD2S,S,T,Q1,Q2,Q3,Q4,GN,GNP
      IF (CABS(Z).GT. 1.0E-5) GO TO 10
      FN=1.0E30
      FNP=1.0E30
      RETURN
   10 ZD2=Z/2.0
      ZD2S=ZD2**2
      IF (M.EQ.0) GO TO 500
       Q4= CLOG(ZD2)*2.0
       FN=0.0
      FNP=0.0
      XM=M
      S=ZD2**(-M)
      DO 50 L=1,M
       K=L-1
       XK=K
      Q1=2.0*ZD2S*FACT(M-K-2)
      Q2=(A+XM)*FACT(M-K-1)
      Q3=S/FACT(K)
      FN=FN+(Q1-Q2)*Q3
      FNP=FNP+(Q1*(XK+1.0-XM/2.0)-Q2*(XK-XM/2.0))*Q3
      S=S*ZD2S
   50 CONTINUE
      GN=FN
      GNP=FNP/ZD2
      PSI1=-.5772156649
      PSI2=PSI1
      DO 60 L=1,M
      XL=L
      PSI2=PSI2+1.0/XL
   60 CONTINUE
      S=1.0/FACT(M)
      XK=1.0
      TST=CABS((A+XM+1.0)/(ZD2)**M)
      Q4=Q4-PSI1-PSI2
      FNP=(A-XM)*Q4
      FN=(FNP-2.0)*S
      FNP=(FNP*XM/2.0+A-2.0*XM)*S
  100 Q4=Q4-(1.0/XK+1.0/(XK+XM))
      T=ZD2S/((XK+1.)*(XM+XK+1.))
      S=S*ZD2S/(XK*(XK+XM))
      PSI1=(1.0/(XM+XK+1.)+1./(XK+1.))
      Q3=A-XM-2.0*XK
      Q1=(Q4*(T*(Q3-2.0)-Q3)+2.0*(1.0-T)-(Q3-2.0)*T*PSI1)*S
      Q2=(Q4*(((Q3-2.0)*(XK+XM/2.+1.)*T)-Q3*(XK+XM/2.))-PSI1*((Q3-2.)*
     1     (XK+XM/2.+1.)*T)+(2.*Q3-A)*(T-1.)-4.*T)*S
      FN=FN+Q1
      FNP=FNP+Q2
      IF (CABS(Q1)/TST .LT. 1.0E-8 .AND. CABS(Q2)/TST .LT. 1.0E-8)
     1  GO TO 200
      Q4=Q4-PSI1
      S=S*T
      XK=XK+2.
```

```
      GO TO 100
  200 FN=(FN*ZD2**M+GN)/3.14159265
      FNP=(FNP*ZD2**(M-1)+GNP)/3.14159265
      RETURN
  500 TST=CABS(A+1.)
      S=1.
      Q4=CLOG(ZD2)+.5772156649
      XK=1.
      FN=(A+2.*ZD2S)
      FNP=A/2.0+Q4*ZD2S*2.0
      FN=FN*Q4    -ZD2S
  600 Q4=Q4-1./XK
      T=ZD2S/((XK+1.)**2)
      S=S*ZD2S/(XK*XK)
      PSI1=1./(XK+1.)
      Q3=2.*ZD2S
      Q1=(Q4*(A*(T-1.)+Q3*(T/(XK+2.)-PSI1))-PSI1*T*(A+Q3/(XK+2.))+
     1    ZD2S*(PSI1**2-T/((XK+2.)**2)))*S
      Q2=(A*(T-1.)/2.                          +Q4*((T-1.)*(Q3+XK*A)+T*A)-
     1       T*PSI1*(Q3+(XK*A)+A))*S
      FN=FN+Q1
      FNP=FNP+Q2
      IF (CABS(Q1)/TST .LT. 1.0E-8 .AND. CABS(Q2)/TST .LT. 1.0E-8)
     1  GO TO 700
      XK=XK+2.
      S=S*T
      Q4=Q4-PSI1
      GO TO 600
  700 FN=(FN-1.)/1.57079632
      FNP=(FNP/ZD2)/1.57079632
      RETURN
      END
```

```
      FUNCTION FACT(N)
       DIMENSION G(20)
      DATA (G(I),I=1,20)/1.,2.,6.,24.,120.,720.,5040.,40320.,362880.,
     1    3628800.,3.99168E7,4.790016E8,6.2270208E9,8.71782912E10,
     2     1.30767437E12,2.09227899E13,3.55687428E14,6.4023737E15,
     3      1.216451E17,2.432902E18/
       IF (N) 10,20,30
   10 FACT=0.0
      RETURN
   20 FACT=1.
      RETURN
   30 IF (N .GT. 20) GO TO 40
      FACT=G(N)
      RETURN
   40 X=N
      FACT=SQRT(6.2831853*X)*(X/2.71828)**N
      RETURN
      END
```

```
      SUBROUTINE AXFUN(FN,FNP,QN1,QN2,A0,AL,QFF,QFP,QGF,QGP,H)
      COMPLEX FN,FNP,QN1,QN2,A0,AL,QFF,QFP,QGF,QGP,XJ,Q1,F1,Q2,F2,DN,
     1  F1,F2,G1,G2,F1P,F2P,G1P,G2P
      COMMON/DIM/R0(2),RI(2),XL(2),C0(2),INHAD
      COMPLEX F1P,F2P
      DATA XJ/(0.0,1.0)/
      Q1=CCOS(QN1*XL(1))
      Q2=CCOS(QN2*XL(2))
      IF (CABS(QN1)) 20,20,30
   20 F1=XL(1)
      F1P=0.0
      DN=1.0E20
      GO TO 40
   30 F1=CSIN(QN1*XL(1))/QN1
      F1P=(XL(1)*Q1-F1)/QN1
      DN=QN2/(R*QN1)
   40 CONTINUE
      IF (CABS(QN2)) 50,50,60
   50 F2=XL(2)
      F2P=0.0
      GO TO 70
   60 F2=CSIN(QN2*XL(2))/QN2
      F2P=(XL(2)*Q2-F2)/QN2
   70 CONTINUE
      F1=(QFF+A0*QFP)*Q1+(A0*QFF-QFP*QN1**2)*F1
      G1=(QGF+A0*QGP)*Q1+(A0*QGF-QGP*QN1**2)*F1
      F2=F2*QN2**2+Q2*AL
      G2=Q2-AL*F2
      F1P=F1*QN1*(-XL(1)*QFF-(XL(1)*A0+2.0)*QFP)+(QFF*A0-QFP*QN1**2)*F1P
      G1P=F1*QN1*(-XL(1)*QGF-(XL(1)*A0+2.0)*QGP)+(QGF*A0-QGP*QN1**2)*F1P
      F2P=QN2*(F2*(1.0-XL(2)*AL)+XL(2)*Q2)
      G2P=-QN2*XL(2)*F2-AL*F2P
       IF (CABS(A0) .LE. 1.0E5) GO TO 80
      F1=(QFF/A0+QFP)*Q1+(QFF-QFP*QN1**2/A0)*F1
      G1=(QGF/A0+QGP)*Q1+(QGF-QGP*QN1**2/A0)*F1
      F1P=F1*QN1*(-XL(1)*QFF/A0-(XL(1)+2.0/A0)*QFP)+(QFF-QFP*QN1**2/A0)
     1  *F1P
      G1P=F1*QN1*(-XL(1)*QGF/A0-(XL(1)+2.0/A0)*QGP)+(QGF-QGP*QN1**2/A0)
     1  *F1P
   80 CONTINUE
      IF (CABS(AL) .LE. 1.0E5) GO TO 90
      F2=F2*QN2**2/AL+Q2
      G2=Q2/AL-F2
      F2P=QN2*(F2*(1.0/AL-XL(2))+XL(2)*Q2/AL)
      G2P=-QN2*XL(2)*F2/AL-F2P
   90 CONTINUE
      FN=F1*F2-G1*G2
      FNP=F2*F1P*DN+F2P*F1-G1P*G2*DN-G1*G2P
      RETURN
      END
```

REFERENCES

1) Smith, G.E. and Bastress, E.K., Propulsion System Flow Stability Program (Dynamic), Part X - Combustion Instability Model Program User's Manual (AFAPL-TR-69-113), Air Force Aero Propulsion Laboratory, Air Force Systems Command, Wright-Patterson Air Force Base, Ohio, February, 1970.

2) Investigation of Combustion Instability in a Turbofan Mixed-Flow Augmentor (NREC Report No. 1161-1), Northern Research and Engineering Corporation, Cambridge, Massachusetts, April, 1972.

3) Culick, F.E.C., Nonlinear Behavior of Acoustic Waves in Combustion Chambers, California Institute of Technology, Daniel and Florence Guggenheim Jet Propulsion Center, Pasadena, California, April, 1975.

4) Romanelli, M.J., "Runge-Kutta Methods for the Solution of Ordinary Differential Equations", Mathematical Methods for Digital Computers, 1960, pp. 110-120.

5) Sansom, Frederick J., et al, MIMIC Programming Manual (SEG-TR-67-31), Systems Engineering Group, Aeronautical Systems Division, Air Force Systems Command, Wright-Patterson Air Force Base, Ohio, July, 1967.

6) Chandrasekhar, S., Hydrodynamic and Hydromagnetic Stability, Clarendon Press, 1961.

7) Unpublished data on TF-30 afterburner tests conducted at NASA, Lewis Research Center, Cleveland, Ohio.

8) Lewis, J.S., The Effect of Local Fuel Concentration on Reheat Jet Pipe Vibrations. Presented at the International Symposium on Combustion in Advanced Gas Turbine Systems, The College of Aeronautics, Cranfield, England, April 4-6, 1967.

9) Morse, P.M. and Ingard, K. Uno, Theoretical Acoustics, McGraw-Hill.

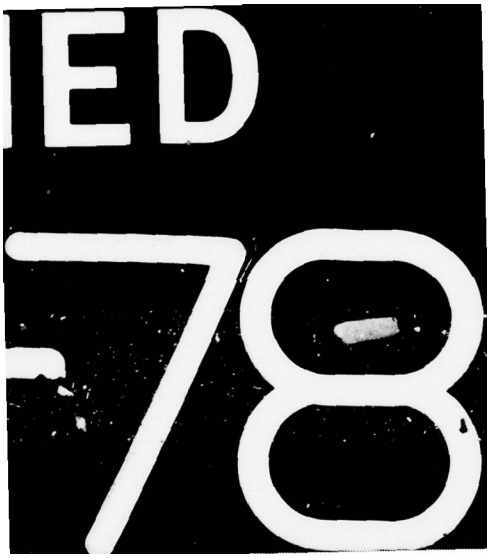
ED
78